



**UNIVERSITÀ DEGLI STUDI DI PISA**

Scuola di Ingegneria

Corso di Laurea Magistrale in

**INGEGNERIA EDILE E DELLE COSTRUZIONI CIVILI**

**TESI DI LAUREA MAGISTRALE**

*Seismic Performance Assessment of a multi-depth Automated Rack-Supported Warehouses via detailed and reduced-order models*

**STUDENTE: Giuseppe DEFINA**

**a.a. 2018/2019**

***RELATORI:***

Prof. Ing. Walter **SALVATORE**

Ing. Francesco **MORELLI**

Prof. Ing. Dimitrios **VAMVATSIKOS** (*National Technical University of Athens*)

PhD student: Dimitrios **TSARPALIS** (*National Technical University of Athens*)

# ***Seismic Performance Assessment of a multi-depth Automated Rack-Supported Warehouse via detailed and reduced-order models***

## Table of contents

ABSTRACT .....	3
SOMMARIO .....	4
ACKNOWLEDGMENT.....	5
1 INTRODUCTION.....	6
1.1 TRADITIONAL STEEL RACKS.....	6
1.2 AUTOMATED RACK SUPPORTED WAREHOUSES .....	9
1.3 PURPOSE OF THE THESIS .....	11
1.4 THESIS STRUCTURE.....	13
1.5 TERMS AND DEFINITIONS.....	13
2 ARSW DESIGN CHARACTERISTICS.....	16
2.1 DESIGN STANDARDS AND STATE OF THE ART.....	16
2.2 DESCRIPTION OF THE CASE STUDY .....	17
2.2.1 Definition of the geometry.....	17
2.2.2 Material properties .....	20
2.2.3 Section properties .....	22
2.2.4 Mechanical properties of frame elements.....	24
2.2.4.1 Upright frame shear stiffness .....	24
2.2.4.2 Pallet and bracing beam end connectors.....	24
2.2.4.3 Floor-upright connection.....	25
2.2.5 Definition of loads .....	25
2.2.6 Definition of mass source and filling grade reduction factor .....	28
3 DETAILED MODEL.....	29
3.1 FINITE ELEMENT MODELLING.....	29
3.1.1 Evaluation of the eccentricity.....	29
3.1.2 Definition of load and load case.....	30
3.2 FINITE ELEMENT ANALYSIS .....	32
3.2.1 Modal Analysis.....	32
3.2.2 Lumped-plasticity element properties .....	34
3.2.3 Evaluation of $N_{b,Rd}$ considering the buckling phenomena.....	37
3.2.4 Push-over Analysis.....	44

3.2.5	Discussion of the results .....	44
4	REDUCED-ORDER MODEL.....	49
4.1	REMINDERS ABOUT TIMOSHENKO BEAM ELEMENT'S PROPERTIES AND MATRICES .....	50
4.1.1	Stiffness Matrices of Euler-Bernoulli Beam Element.....	51
4.1.2	Stiffness Matrices of Timoshenko Beam Elements.....	52
4.2	PROPERTIES OF EQUIVALENT BEAMS.....	53
4.2.1	Material properties .....	55
4.2.2	Frame length.....	55
4.2.3	Cross-section Area.....	56
4.2.4	Moment of Inertia.....	56
4.2.5	Shear Area.....	57
4.3	2D MODEL FINITE ELEMENT ANALYSIS .....	59
4.3.1	Modal Analysis.....	62
4.3.2	Reliability of the Reduced-order model .....	64
4.3.3	Push-over Analysis.....	72
5	CONSIDERATION ABOUT THE 3D REDUCED-ORDER MODEL .....	76
5.1.1	Modal Analysis.....	77
6	CONCLUSION AND FUTURE WORK.....	81
7	REFERENCES.....	82

## ***Abstract***

The present thesis is part of a research activity carried out principally at the National Technical University of Athens in the context of the Erasmus European exchange programme and concluded at the University of Pisa. The main objective of this thesis was the assessment of the seismic performance of an Automated Rack-Supported Warehouses, in particular one of the case studies to be examined in the European research project “STEELWARE”.

ARSWs represent the evolution of the traditional racking system. The purpose of designing such structures arises from the necessity to store a huge amount of goods, improving the efficiency in storing and therefore, providing substantial savings in terms of cost. ARSWs, despite their lightness, can reach considerable heights bearing very high loads, larger than their dead load and opposite to what happens in usual civil engineering structures. Furthermore, they are also designed to support the weight of all the non-structural elements (clad, roof, technological facilities, ...). Thus, standard design approaches are not applicable to this type of structures, especially when we consider seismic and wind actions. Moreover, due to their structural configuration (cold formed profile, open sections, non-linear behaviour of the main connections,...), and also to the fact that highly sophisticated machines need to run along loading-unloading aisles to store and retrieve goods in a completely automatic way, the design of the ARSWs no margin of mistake is allowed. By examining all of those problems and considering that the ARSWs consist of hundreds or thousands of steel members and nodes connected to each other, it has become clear that the finite element analysis for these structures is a demanding work; the problem arises considering nonlinear phenomena, that may lead to prohibitive analysis costs in terms of time and CPU or even convergence and stability problems [1].

The purpose of this thesis was to develop a computationally simpler model called reduced-order model, in terms of less degrees of freedom, in order to check their nonlinear behaviour under seismic actions but checking to reach a balance between costs and accuracy. The reduced-order model was developed by substituting the upright frames and the roof truss of the detailed model with simpler beams. Assigning to the beams the same properties of the detailed model, it must be considered the shear deformation of the uprights in contrast to what happens in typical columns; the Euler-Bernoulli beam theory cannot be used and the Timoshenko beam theory must be considered, determining suitably linear properties ( $A$ ,  $I$ ,  $A_{eff}$ ) depending on the different type of the bracing elements configuration. Apart from the modelling, first of all, a modal analysis has been performed for both models and the reliability of the reduced-order model in the elastic region was assessed; using the results of the modal analysis, the stresses on all the elements of each upright frame have been estimated. Examining the results above, it is clear that the reduced-order model can ensure a good accuracy.

## **Sommario**

Il presente lavoro di tesi è stato svolto inizialmente presso la National Technical University of Athens nell'ambito del programma di scambio europeo "Erasmus" e si è concluso presso l'Università di Pisa. Il fine della tesi è stato la valutazione delle prestazioni di un magazzino automatico verticale (MAV) autoportante in acciaio sotto un'azione sismica di medio/alto livello, che è uno dei casi studio del progetto di ricerca europeo "STEELWARE".

Gli ARSW rappresentano la naturale evoluzione in altezza e larghezza, del tradizionale sistema di scaffalature. La richiesta di realizzare tali strutture nasce dalla necessità di immagazzinare una sempre maggiore quantità di merci, in strutture più efficienti nell'abito della distribuzione e in termini di sicurezza. Gli ARSW, nonostante la loro leggerezza, possono raggiungere notevoli altezze portando carichi molto elevati, più grandi del carico proprio al contrario di quanto accade nelle normali strutture civili. Inoltre, a loro è demandato anche il compito di sostenere il peso di tutti gli elementi non strutturali (rivestimenti, struttura di copertura, impianti tecnologici, ...). nonché di resistere all'azione sismiche e al vento. Tuttavia, a causa delle loro caratteristiche strutturali (profili sagomati freddo, sezioni aperte, comportamento non lineare dei collegamenti, ...), e per il fatto che i sistemi di carico e scarico merci sono completamente automatizzati, non è consentito nella progettazione alcun margine di errore. Considerando tutti questi problemi e il fatto che gli ARSW sono costituiti da centinaia o migliaia di elementi e nodi collegati tra loro, diventa chiaro che un'analisi agli elementi finiti per questo tipo di strutture è molto complessa; il problema si amplifica nel considerare le non linearità, che possono portare ad analisi proibitive in termini di tempo e di CPU o anche a problemi di convergenza e stabilità [1]. Lo scopo della tesi è stato dunque quello di elaborare un modello più semplice dal punto di vista computazionale detto modello ridotto, in termini di riduzione del numero di gradi di libertà, verificandone il comportamento in ambito lineare e non lineare, al fine di raggiungere un equilibrio tra costi e accuratezza. Il modello ridotto è stato sviluppato sostituendo gli "upright frames" e la struttura reticolare della copertura con elementi monodimensionali. Nel determinare le corrispondenti proprietà ( $A$ ,  $I$ ,  $A_{eff}$ ), degli elementi equivalenti è necessario tenere in considerazione la deformabilità a taglio degli "upright frames", contrariamente a ciò che accade nelle travi per cui vale la teoria di Eulero-Bernoulli. A conclusione del presente lavoro, è stata eseguita inizialmente un'analisi modale per entrambi i modelli, completo e ridotto, valutando l'affidabilità del modello ridotto in ambito elastico, e per terminare si è operato un confronto anche in ambito non lineare. Utilizzando poi i risultati dell'analisi modale, sono state stimate le sollecitazioni degli elementi del modello completo a partire dal modello ridotto. Esaminando i risultati di cui sopra, è chiaro che il modello ridotto è in grado di garantire una buona affidabilità.

## ***Acknowledgment***

The research activity, that was the topic of my master thesis, was monitored and organized by the members of the National Technical University of Athens under the coordination of Professor Dimitrios Vamvatsikos and the supervision of Ing. Francesco Morelli from the University of Pisa. I would like to thank firstly Francesco Morelli and the Professor Walter Salvatore for the opportunity they have given me to have the best professional experience of my university career at the NTUA; in particular Ing. Morelli for the well-grounded advice he gave me to carry out my research activity under the supervision of the precious scientific guide of Professor Vamvatsikos.

I feel the need to express my gratitude also to Professor Ioannis Vayas for the ospitality and Professor Vamvatsikos who makes me feel part of his professional team, who works inside the steel structure institute at NTUA; I really enjoyed their company. Akrivi (“precious” guide in Athens, and happiness spreader with her butterfly effect entrance), Konstantinos B., Konstantinos V., Dimitrios B., Panagiotis T., Zaxarias F., and all the team of the laboratory of steel structures as well (the best chef ever and his wingman); thank you for making me feel part of this big family for all six months. A speech deserves the valuable support and collaboration of the PhD student Dimitrios Tsarpalis during all these months both at the NTUA and after my return at the University of Pisa, thank you for your unlimited availability.

During my research, the information that the industrial partners provided us, were essential to work on the case study; the design was contributed by the Industrial partners above involved in the European research project “STEELWARE: Advanced structural solutions for automated STEEL rack supported WARhouses”, thanks to the support of the European Commission through the Research Fund for Coal and Steel (RFSR-CT-2011-00031), Grant agreement N. 754102, 2017-2021. The results of some experimental tests provided by the industrial partners, were essential for the definition of the elements properties of the structural elements of the case study as well. In addition, the master thesis titled “*Analysis of pallet racking systems with equivalent beam elements*” of the PhD student Dimitrios Tsarpalis, was useful to implement the reduced-order model. The valuable comments and supervision of Prof. Vamvatsikos, who helped me improve the quality of my Master thesis, were deeply appreciated, and the suggestion Ing. Morelli gave me were important as well to conclude my work.

I feel the need to thank Prof. Vamvatsikos again, who gave me the opportunity to take part to the STEELWARE meeting in Arnhem, encouraging me to believe in my potential and throw myself into this new experience, and Akrivi supporting me as well.

Last but not least, I would like to express my deep gratitude towards my parents and all my friends I met during the university and the Erasmus experience as well.

# **1 Introduction**

## **1.1 Traditional Steel Racks**

The traditional steel racks (SR) concern structures that aim to store goods inside warehouses before being distributed. The goods stored in pallets or box-containers, are handled or using forklift trucks in multi-level horizontal rows where their distribution depends on logistic strategies. These structures are usually made out of cold formed profiles, that are supposed to bear their self-weight, the loads related to the goods stored in them as well as the seismic action. In order to prevent the instability of upright frames, in the transversal direction (cross-aisle) diagonal elements are always placed. In the longitudinal direction (down-aisle), rack designers usually prefer avoiding bracings to make the shelves accessible on both sides, allowing an efficient loading and unloading of goods in service. Therefore, in these kinds of structures usually the beam-to-uprights connections aims to prevent the horizontal actions. However, in high seismic regions, this configuration is usually not adequate to resist strong horizontal loads because of insufficient flexural stiffness of the beam-to-upright connections and efficient bracing systems are requested [2]. Under seismic action, the sliding of the pallet needs to also be considered in order to prevent damages to people and the structure itself due to the movement and the consequent falling of stored goods between beams or outside the track in the aisle. Therefore, the importance to design efficient racking system structures is also due to the really high economic and social impact that these structures have. Racks are widely used in warehouses where tons of more or less valuable goods are stored and where their loss could have a very large economic impact as well as in terms of loss of life (see Figure 1-1). Regarding these structures, plenty of research studies have been conducted, whose positive outcomes have resulted in the latest EN16681 standards dealing with the seismic design of pallet racking systems.



**Figure 1-1:** Collapse of storage racks due to Emilia earthquake, 2012

There are several kinds of pallet racking systems related to their functionality including:

- 1) Gravity systems: are characterized by their slightly inclined flat surface, that slide through channels on wheels or rollers, making it possible to slide load units without automation, relying uniquely on the force of gravity. This system operates according to the FIFO principle (First In First Out) where the items are loaded at the higher end and removed at the lower end level (Figure 1-2). It is also available in the LIFO version (Last In First Out), where storage and picking of the load units occur on the same side<sup>1</sup>.
- 2) Drive-in and Drive-through racks: is the solution for stocking merchandise according to the LIFO system. The access is either only one-sided or from both sides. Differently from pallet racks, in drive-in systems the rail beams supporting pallet units run along the rack depth, allowing a very high storage space utilization at the cost of a reduced accessibility [3] (Figure 1-3).

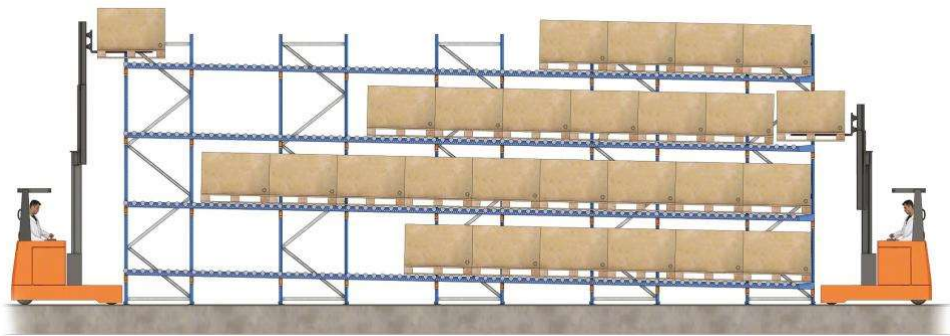


**Figure 1-2:** Example of FIFO system in a Flow rack<sup>2</sup>



**Figure 1-3:** Drive-in/ Drive-through pallet racks<sup>2</sup>

<sup>1</sup> <http://www.sacmaspa.com/sacma.php?s=95>

<sup>2</sup> <https://www.mecalux.com/pallet-racks/>

- 3) Push Back Racking Systems: this system adopts the LIFO (Last In First Out) principle, where storage and picking of the load occur on the same side but are separate increasing the productivity. When a pallet is loaded onto the system, it pushes the next pallet back and when a pallet is unloaded, it is pushed to the front of the system relying uniquely on the force of gravity (Figure 1-4 a).
- 4) Mobile pallet racks: The shelving units are installed over guided mobile bases that slide laterally, thus eliminating the need for aisles. The operator gives the order to automatically open the unit, either by remote control or manually by flicking a switch (Figure 1-4 b).
- 5) Automated racking systems: are organized to store and retrieve load units in a completely automated way thanks to the use of computerized S/R cranes. The automated system can be either simple, double or with multi-depths (see Figure 1-5):

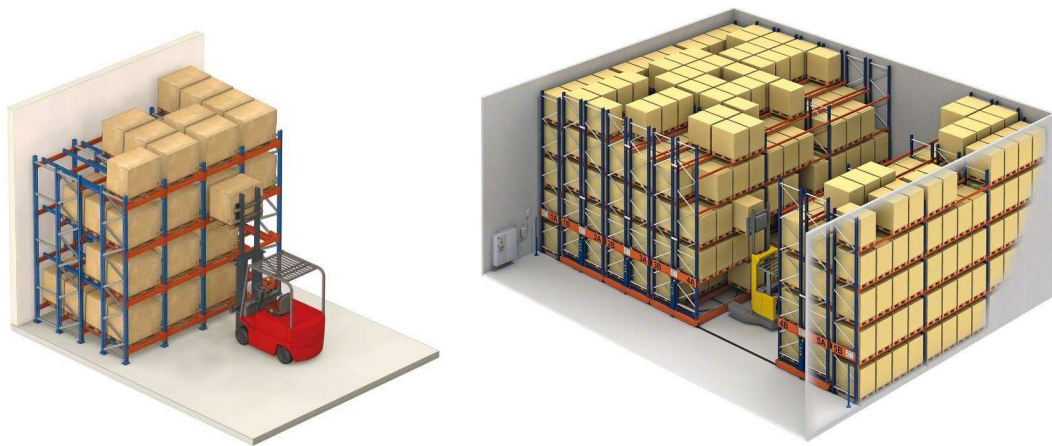


**Figure 1-4: a) Push back racking system<sup>2</sup>, b) Mobile pallet racks**

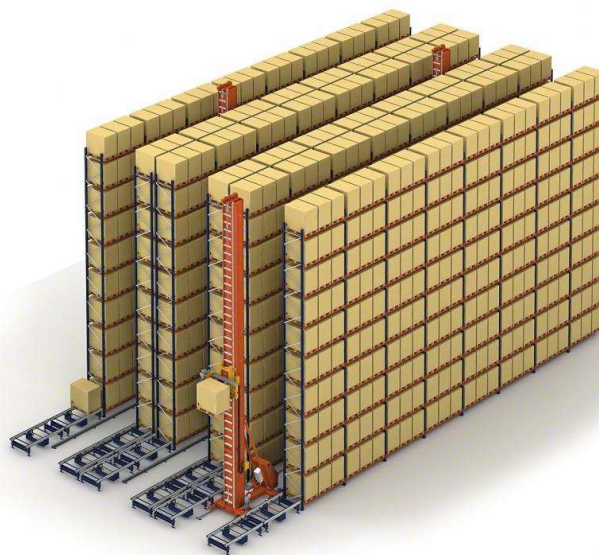


**Figure 1-5: Automated pallet rack<sup>2</sup>**

a) Automated double depth cranes: this solution belongs to direct-access systems and provides a great accessibility to the unit loads, stored with a maximum number of two units for each row in cross aisle direction, but decreases the use of the available surface of the warehouse.

b) Automated multi depth shuttle: this solution belongs to compact systems and provides greater surface occupation and therefore maximum storage density, while losing accessibility to the pallets that are stored in long storage tunnels and handled by a particular equipment called “shuttle”.

Classical types of storage racks are also well described also by Pekoz et al. [4].

## **1.2 Automated Rack Supported Warehouses**

With the increasing demand from customers, the necessity of retail giants like Amazon, e-bay, ecc., for bigger and optimized spaces where goods can be stored as well as more functional racking systems in terms of ergonomics and structural capacity also against the horizontal forces, has rapidly increased. The modern storage racking systems are structures that satisfy exactly these needs due to the reduced weight, the increased strength and the possibility to store a huge quantity of goods in really high structure having reduced inter-storey heights, that allow a full and optimized exploitation of the available spaces. These characteristics combined with the fact to be standardized and adaptive structures, significantly increase the economy and the structural efficiency of the whole structure compared to the traditional warehouses.

The Automated Rack Supported Warehouses (ARSW) or clad rack warehouses are the most recent racking system structures made of huge “forests of steel” [5], where highly sophisticated machines run along loading-unloading aisles to store and retrieve goods in a totally automated way. Using high-specialized robotic equipment for handling pallets, significantly increases the efficiency in the logistics industry, making the operations of handling goods faster, often imposed by logistic strategies, and reducing or eliminating the human error. Statistical analyses highlighted that the pallets, in fully loaded conditions, cover about 54% of the plan surface and 40% of the volume [6]. In addition, these structures, which can be more than 40 m tall, 100 m wide and 150 m long [1], not only support really heavy loads more than their dead load but also the weight of all building elements (clads, roof, technological facilities...) and all the environmental actions (wind, snow, seismic action...) that act on them, representing the basic distinction between SR and ARSW. In Figure 1-6, a difference between the two racking systems is shown; storage warehouses can reach up to 12-15 meters [7].



**Figure 1-6:** Examples of existing storage warehouses: **a)** Traditional pallet racking system, height 8 m; **b)** ARSW, height 35<sup>3</sup>

On the other hand, being the storage/retrieval system (AS/RS) totally automated, high expectations have to be guaranteed. Therefore, no margin of mistake can be accepted in positioning the profiles, so the absolute verticality of the uprights is requested in order to allow the correct functioning of forklift moving into the loading-unloading aisles. Moreover, the construction phase could be very critical and needs to be taken into account, especially concerning the wind action. In the Figure 1-7 a partial collapse of an ARSW during its construction phase is shown.



**Figure 1-7:** Premature collapse of an ARSW during construction phase<sup>3</sup>

---

<sup>3</sup> See reference [1]

Moreover, these structures are made of thin cold-formed profiles with non-bisymmetric cross-section, reaching considerable heights and bearing very high loads, larger than their dead load and opposite to what happens in usual civil engineering structures. The choice of using thin cold-formed profiles, allows for the best possible performance while minimizing weight, making the storage and transportation easier as well, and achieving a very low cost for the skeleton frames [3]. On the other hand, the behaviour of these structures is affected by the geometry of their sections, the high slenderness, the perforation along the profiles as well as the behaviour of their joints (beam-to-upright and base-plate connection). Open cross-section members are, in fact, prone to three buckling modes which, in order of wavelength are: local, distortional and lateral torsional buckling [8]. These structures are affected also by non-linear behaviour due to the connections that make their modelling difficult. As a result, finite elements simulation and experimental method could be necessary. Overall, these problems are amplified when the structures are placed in a seismic area where they have to withstand horizontal dynamic forces.

All of these reasons highlight the immediate need to give appropriate instruments to the designers in order to ensure the ARSW safety, in particular under the effects of horizontal actions, representing ARSWs collapse a high economic and social impact.

By the way, many advantages are offered by ARSW:

- Significant cost saving in construction;
- Short construction periods;
- Roof and cladding are directly fixed to the rack structure;
- Storage in height: maximum use of available surface area for a high storage density;
- ARSW system is adjustable and eventually demountable;
- They can be fully automated which increases the efficiency of storage and logistics;
- Reduced responsibility for the owner of storage system as the system is assembled as a whole (building + storage).
- Energy efficiency, less carbon foot-print (less heating);
- No interference of rack with the building columns or the building vertical bracing system. Especially in high seismic zones this eliminates the need for seismic separation detailing between building and rack structure;
- Reduction of workers needed inside the warehouse.

### **1.3 Purpose of the Thesis**

The clad rack warehouses are an improvement of the storage racking system concept, due mainly to the weight of all building elements (clads, roof, technological facilities...) and all the

external actions (wind, snow, seismic...) these structures are interested by in addition to the stored goods they have to bear as well as the traditional racks. In the world (not only in Europe), the lack of official design rules and procedures for this new kind of structures, force designers to adopt rules conceived for steel building. In particular, designers must refer to the actual design practise, that however concerns storage rack systems much smaller than automated warehouses [9] e [10]. The lack of a specific knowledge of the ARSW's behaviour and the huge economic impact in terms of loss of the big amounts of goods and, despite the limited number of workers required in automated warehouses, in terms also of the risk of the employer's life, raise the demand for further researches. In this context, take place the purpose of the STEELWARE European project, where my thesis will fit to give a contribution.

By examining the finite element model of an ARSW, made of thousands of elements, it's clear that a non-linear analysis of the whole structure is really computationally hard to be solved. For example, the case study examined, consists of 110.000 nodes connected by 200.000 elements, with 650.000 number of free DOFs to be solved (see Figure 1-8). The purpose of the thesis was to develop a reduced-order model in order to check the ARSW's behaviour in the elastic and inelastic region in two dimensions, working on a model computationally simpler than the detailed one by ensuring the reliability of the reduced-order model. A significant reduction of 55% in terms of number of DOFs has been gained making easier doing non-linear analyses for such structures.

At the end, some considerations about the reduced-order model in three dimensions have been done comparing the results of the modal analysis with the ones of the detailed model. The results of the 3D model show the possibility to extend all the findings to three dimensions that is a desirable future work.

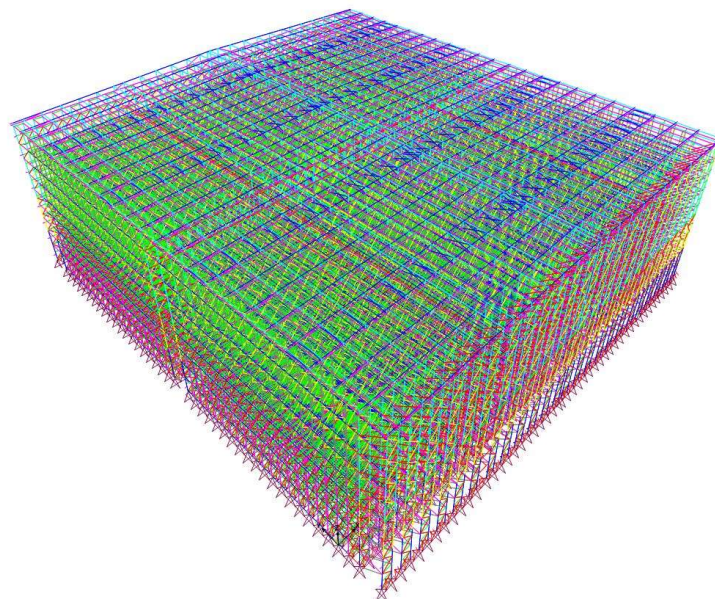


**Figure 1-8:** Numerical 3D model of the ARSW case study

## 1.4 Thesis structure

After an introduction on the pallet racking system, exposing the structural issues and the state of the art concerning the regulation which today are driving the design of such structures, a multi-depth ARSW has been analysed.

The thesis is divided in three main parts:

- the design characteristics of the ARSW case study;
- analysis of the Detailed model;
- analysis of the Reduced-order model.

Chapter 2 starts illustrating the currently practise and regulation for the design of an ARSW. In the further paragraphs all the properties of the case study, like the geometry, sections, materials and structural properties given by the industrial partners, are included.

Chapter 3 discusses the finite element analyses of the case study in two dimensions. Modal and Push-over analyses were executed for the detailed model and the results have been discussed.

Chapter 4 introduces the reduced-order model, first of all discussing the linear properties of the equivalent beams. In particular cross-section area, moment of inertia and effective shear area have been calculated. Later, finite element analyses have been executed. A modal analysis first, comparing the results with the detailed model and checking the reliability of the reduced-order model. At the end also a push-over analysis has been executed comparing the results with the detailed model also in the inelastic region.

Chapter 5 presents some considerations about the Reduced-order model in three dimensions showing the significant gain in terms of free DOFs.

Although each of the chapters ends with the concluding comments, Chapter 6 draws main conclusions, providing also recommendations for the future work.

## 1.5 Terms and definitions

In order to make easier the comprehension of the present work, the following terms and definitions are given:

- Uprights: Cold formed perforated columns with mono-symmetric open section, mostly prone to compression and to three buckling modes which, in order of wavelength are: local, distortional and lateral torsional buckling;
- Upright frames: two upright linked together by a system of bracing members;

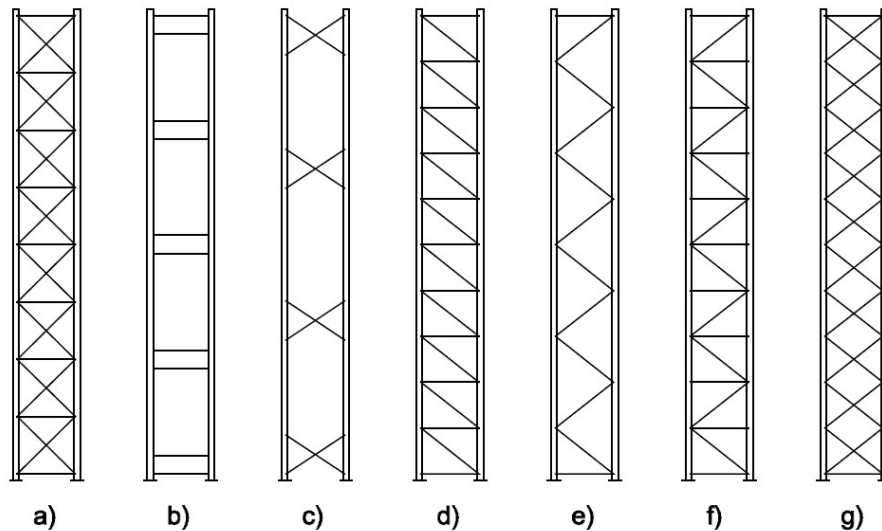


**Figure 1-9:** Typical frame bracing configurations (EN 16681 - §8.3): (a) X-braced frame with horizontal elements; (b) battened frame; (c) partially braced frame; (d) Z-braced frame; (e) D-braced frame; (f) K-braced frame; (g) X-braced frame

- Bracing members: horizontal and diagonal (diagonal bracings) truss members bolted to the upright providing to the stability in Cross-aisle direction;
- Bracing tower: upright frames connected by x-shaped concentric spine bracings absorbing the horizontal forces;
- Spine bracings: diagonals and horizontal beams (bracing beams) linking adjacent frames in the vertical plane, parallel to down-aisle direction, limiting the horizontal displacement;
- Pallet beams: horizontal members, hooked to the uprights, which bear the z-pallet profile where the loads are applied;
- Supporting shuttle beams: I section members where the shuttle beams are anchored;
- Shuttle beams: R section rails where the shuttle runs inside aisle;
- Beam end connectors: angular connectors welded to the beams, having hooks which engage in slots in the uprights;

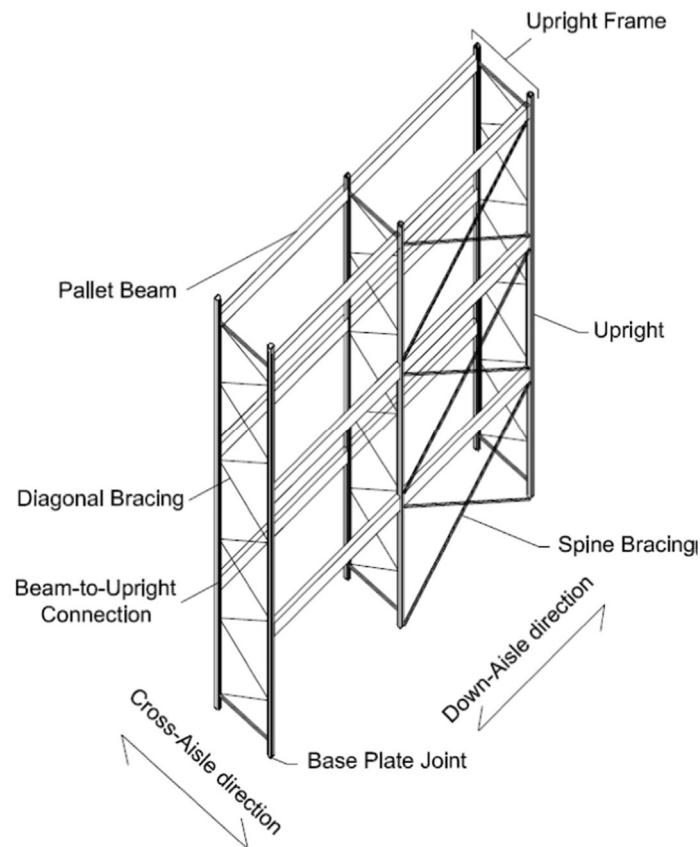


**Figure 1-10:** Typical braced pallet rack configuration<sup>4</sup>

- Aisle: storage channel for loading-unloading the pallet;
- Bay: the space between two upright frames in the down-aisle direction;
- Storage cell: channel along the z-pallet profile where the pallets are placed;
- Cross-aisle direction: the transversal direction of a racking system;
- Down-aisle direction: the longitudinal direction of a racking system;
- Unit load: is the load referred to a single pallet or box-container which weight for the case study is defined in the Table 2-9.

<sup>4</sup> Kanyilmaz A., Brambilla G., Chiarelli G., Castiglioni C., 2016, "Assessment of the seismic behaviour of braced steel storage racking systems by means of full scale pushover tests", *Thin-Walled Structures*.

## **2 ARSW Design characteristics**

### **2.1 Design standards and state of the art**

ARSWs are complex structures, different from ordinary buildings and from traditional steel racks (SR) mostly in terms of environmental loads, which the ARSWs are dedicated to supporting, besides their self-weight and the weight of the stored goods, and no official codified standards concerned them are available. Their proper characteristics significantly influence the response of the structure under seismic action and no “general design rules” are properly suitable. As a result, the lack at both European and worldwide levels of official specific standards forced designers to work without commonly accepted references following their personal experience, supported by experimental evidence and theoretical studies as well as industrial requirements. Currently, for the design of ARSWs, we must refer to the state of the art of storage racking system, even if there are considerable differences between both structures. A lot of researches concerning SR, considering the performances of these structures under seismic action, brittle failures, ecc., has lead to codified standards for the design of SR. The results came out from the two projects titled “SEISRACKS: Storage RACKS in SEISmic Area” [9] and “SEISRACKS2: SEISmic Behavior of Steel Storage Pallet RACKing Systems” [10], they were the baselines for the EN16681:2016, currently used for the design under seismic forces of steel storage systems. If recent specific design rules exist for SR, less prescriptions raise about ARSWs. In Europe, the references for the design of ARSWs are now “building code” (like Eurocode, which, however, do not take into account particularities of self-supporting warehouse structures) and recommendations for steel storage racks like the EN15512 [8] and the EN16681 [11] (referred to the design of SR in seismic area), which are, however, quite different from ARSWs. These codes represent the evolution of FEM 10.2.08 [12], published by the technical committee Working Group 2 of the “Federation Europeenne de la Manutention” (FEM). In the United States (US), the design of industrial steel storage racks is carried out according to the Rack Manufacturers Institute (RMI) specification “Specification for the Design, Testing and Utilization of Industrial Steel Storage Racks” [13], which is tied closely to the AISI specification [14] for the cold-formed steel design (North American specification for the design of cold-formed steel structural member).

The SEISRACKS project is an important input to the “STEELWAR: Advanced structural solutions for automated STEEL rack supported WARhouses”, which is the first research project concerning the study of ARSWs. The partners and experts involved in this project aim to build codified standards for the design of such structures considering, for example, the wind actions in construction phases, the efficient distributions of storage goods due to the logistic load

strategies for different ARSWs typologies as well as their behaviour under seismic actions proposing new approaches aiming at increasing ARSW safety, reliability and economy.

The references used for the design of the case study are mentioned below:

- EN15512:2009, “Steel static storage systems - Adjustable pallet racking systems - Principles for structural design”;
- EN16681:2016, “Steel static storage systems - Adjustable pallet racking systems - Principles for seismic design”;
- EN1993-1-3:2006, “Design of steel structures - Part 1-3: General rules - Supplementary rules for cold-formed members and sheeting”;
- EN1993-1-8:2005 (for base plates design), “Design of steel structures - Part 1-8: Design of joints”;
- ETAG 001 series (relative to anchor bolts), Guideline for European technical approval of metal anchors for use in concrete;
- FEMA 460 - Seismic Considerations for Steel Storage racks Located in Areas Accessible to the Public [15];
- NTC18 – Norme tecniche per le costruzioni.

## **2.2 Description of the case study**

The case study was extrapolated from the STEELWARE project where five industrial partners were requested to design two different typologies of ARSW (double and multi-depth), simulating the request of a potential customer and considering three levels of seismic action (i.e. 30 case studies = 5 designers x 3 levels of seismic action x 2 main typologies of ARSW). The specific drawings, like the exact dimensions of the structure and of each section, and the results of the specific tests as well, will not be mentioned because of a non-disclosure agreement between the industrial partners involved. According to these would-be requests, the case study is a multi-depth warehouse, to be built-up in Van (Turkey), for pallets storage, designed for a moderate/high seismicity level ( $0.25 \div 0.30$  g) of seismic hazard. All structural profiles and connections were chosen among ones that are of common use in design practice. However, all the information about the case study, provided by the industrial partners and detailed in the following paragraphs, were useful for modelling the structure on a finite element software (SAP2000, CSI).

### **2.2.1 Definition of the geometry**

The multi-depth warehouse of the present case study is made of thin cold-formed profiles with non-bisymmetric and open cross-sections. The transversal direction (cross-aisle), consists

of build-up columns, the upright frames, that consist of two columns of mono-symmetric thin cold formed profiles linked together by bracing members, a system of diagonal and horizontal trusses with a “K-braced frame” configuration (Figure 1-9 f). These elements, which connect the single uprights, ensuring the stability in the cross-aisle direction, can work both in compression and tension. The case study is around 70 m long in both directions and more than 20 meters high. The exact measures cannot be given, so all the dimensions given, are related to one specific dimension, as detailed below (Figure 2-1).

Therefore, the structure consist of two consecutive multi-depth blocks of racks interspaced of  $W_D$ ; each of them include twelve upright frames for each block, where  $W_T$  represents the total length along the cross-aisle direction, about  $48W_A$ , and two loading-unloading aisles ( $W_C$ ), placed in the middle of each block, run along the down-aisle direction. All the uprights are perforated in order to allow an easy connection of the bracing profiles to the uprights, with circular holes to bolt the bracing members and oblique slots for the engaging of the beams (see Figure 2-2), which run along the down-aisle direction. Both the beams and the bracing members, have regular spacing from the floor to the top. The upright frames are simply connected on the top with the roof. The roof, modelled like a truss, consists of continue chords on the top and on the bottom, truss vertical framing profiles, and diagonals, both bolted to the chords.

In the longitudinal direction (down-aisle), three bracing towers with X-shaped concentric braces (simply connected to the uprights) are used to prevent the horizontal forces, two at both ends of the rack and one in the middle. Between the two bracing towers, palled beams are placed (hooked to the uprights) to support the load units by means of semi-rigid beam-to-column joints.

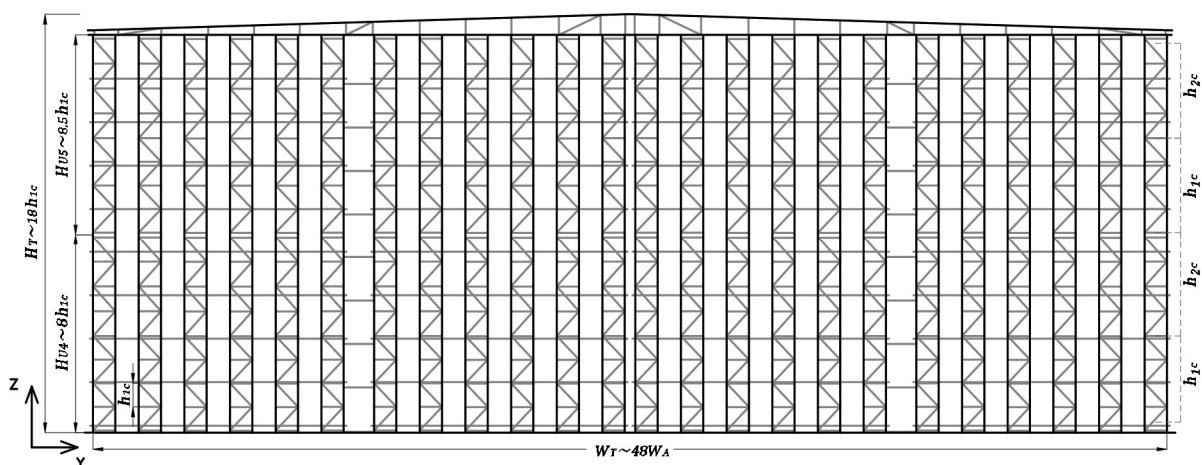


**Figure 2-1:** Geometric properties of the Cross-aisle section



**Figure 2-2: (a)** Beam connection detail<sup>5</sup>; **(b)** Distribution of pallets along the bays<sup>6</sup>

Overall, the ARSW is composed of 40 bays for an entire length of  $L_T$  with 9 pallet-loading levels and a total height of about  $H_T = 8h_{1D}$  (Figure 2-3). Every storage cell has a capacity of 13 unit loads (inside each bay) for each envelope of rack block (it means  $13 \times 4 = 52$  pallets along the entire cross-aisle direction) and they are placed on Z-section profiles, simply connected (bolted) to the pallet beams, like detailed in the paragraph 2.2.5 . The bracing beams and the pallet beams are linked to the uprights with hooking connectors at their end joints, performed with angles welded to the beam ends, which are engaged in the inclined holes of the uprights and locked with a bolt to prevent the connector from disengaging when subjected to a vertical load (Figure 2-2 a). This kind of connection needs to be modelled considering its particular behaviour as detailed in the paragraph 2.2.4.2. Regarding the base-plates, they are welded to the uprights and bolted to the concrete floor. On the top, the upright frames are connected with  $\Omega$ -section profiles (R5 section), simply connected at both ends.

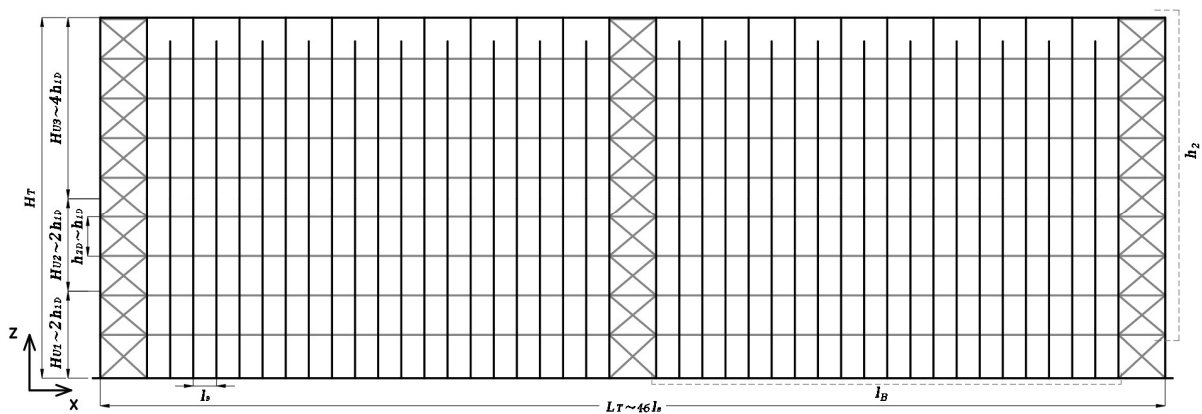


**Figure 2-3:** Geometric properties of sections in the down-aisle direction

<sup>5</sup> <https://www.wiremeshpartitionpanels.com>

<sup>6</sup> <https://www.mecalux.com>

### 2.2.2 Material properties

Warehouses are structures made of steel elements; in the case study three different grades of steel have been adopted and the relative properties are detailed and summarised in Table 2.4:

- S275JR
- S350GD
- S355JR

According to the § 8.1.4 of the EN15512 [8], the mechanical properties of basic materials shall be measured from tensile tests in order to:

- a) determine the minimum guaranteed mechanical properties for the steel used in production;
- b) justify the use in design of a yield stress higher than the guaranteed value;
- c) demonstrate adequate ductility.

Thanks to the industrial partners, a series of tensile tests on several steel members has been performed, in order to evaluate the mechanical properties for such steels; for those materials the results of the experimental tests were not given, the same properties have been determined by the author according to various research from the literature.

#### **Evaluation of mechanical properties from “OPUS” research:**

The mechanical properties of the structural steels S275JR and S355JR, have been evaluated according to the research “OPUS” [16]. The aim of the European Commission research was the assessment of the influence of material properties’ scattering on the final performance of structures, working under seismic actions. A large amount of quality control of steel production on different steel products, was made in the research; all of this data was statically analysed and the correspondence with literature probabilistic models was checked. The following mechanical properties have been taken into consideration (Table 2-1, 2-2, 2-3):

- Yielding strength ( $f_y$ );
- Ultimate tensile strength ( $f_t$ );
- Ultimate elongation ( $\epsilon_u$ ).

**Table 2-1: Yielding stress ( $f_y$ ) for structural steel profiles**

Steel Quality	Producer	Thickness		Mean value	Standard Deviation	5% percentile	95% percentile	Curotsi	Skewness	Co.V.	Samples	Production Standard
		Min	Max									
		[mm]	[mm]									
S235J0JR (+M) <sup>(*)</sup>	AM	3	16	328.8	15.87	306	357.45	-0.138	0.337	0.048	312	EN10025-2
S355J0 (+M)	AM	3	16	414.09	21.62	379.65	449	-0.144	0.108	0.052	314	EN10025-2
S460M	AM	3	16	495.26	17.19	469.6	525	0.043	0.517	0.035	113	EN10025-4
S235J0JR (+M)	AM	16	40	327.68	22.77	294.65	369	0.0668	0.35	0.039	294	EN10025-2
S275J0JR (+M)	AM	16	40	349.3	33.05	303	414	0.572	0.803	0.095	915	EN10025-2
S355J2K2 (+M)	AM	16	40	454.9	27.6	407	497	-0.324	-0.191	0.061	8207	EN10025-2
S460M	AM	16	40	521.1	26.75	474	566	0.027	-0.023	0.051	778	EN10025-4
S275M	RIVA	3	16	361.77	22.91	326.42	403	-0.14	0.03	0.063	2125	EN10025-4
S355M	RIVA	3	16	396.5	11.84	375.36	413	-0.67	-0.23	0.03	61	EN10025-4
S355J0JR	Corus	16	40	395.56	16.18	-	-	-	-	0.041	9127	EN10025-2

**Table 2-2: Tensile strength ( $f_t$ ) for structural steel profiles**

Steel Quality	Producer	Thickness		Mean value	Standard Deviation	5% percentile	95% percentile	Curotsi	Skewness	Co.V.	Samples	Production Standard
		Min	Max									
		[mm]	[mm]									
S235J0JR (+M) <sup>(*)</sup>	AM	3	16	435.41	11.17	417.55	453.45	0.993	0.586	0.026	312	EN10025-2
S355J0 (+M)	AM	3	16	546.16	18.43	517	577.35	0.491	-0.243	0.034	314	EN10025-2
S460M	AM	3	16	620.98	16.16	596	648	-0.306	-0.152	0.026	113	EN10025-4
S235J0JR (+M)	AM	16	40	436.34	13.74	413	459.35	1.01	-0.27	0.031	294	EN10025-2
S275J0JR (+M)	AM	16	40	471.9	18.3	444	504	1.536	0.581	0.039	915	EN10025-2
S355J2K2 (+M)	AM	16	40	546.84	24.45	507	585	-0.579	-0.065	0.045	8207	EN10025-2
S460M	AM	16	40	614.95	30.45	562.85	664.3	-0.076	-0.002	0.05	778	EN10025-4
S275M	RIVA	3	16	479.44	12.77	460.3	503.3	0.07	0.46	0.063	2125	EN10025-4
S355M	RIVA	3	16	574.34	11.92	551.68	590.6	1.03	-0.78	0.021	61	EN10025-4
S355J0JR	Corus	16	40	525.29	15.12	-	-	-	-	0.029	9127	EN10025-2

**Table 2-3: Elongation at fracture ( $\epsilon_u$ ) for structural steel profiles**

Steel Quality	Producer	Thickness		Mean value	Standard Deviation	5% percentile	95% percentile	Curotsi	Skewness	Co.V.	Samples	Production Standard
		Min	Max									
		[mm]	[mm]									
S235J0JR (+M) <sup>(*)</sup>	AM	3	16	35.03	1.58	31.88	37.38	0.573	-0.487	0.045	312	EN10025-2
S355J0 (+M)	AM	3	16	27.34	1.60	24.33	29.61	1.068	-0.632	0.058	314	EN10025-2
S460M	AM	3	16	24.76	1.27	22.49	26.57	1.607	-0.929	0.051	113	EN10025-4
S235J0JR (+M)	AM	16	40	32.15	1.6	29.49	34.33	0.826	-0.592	0.05	294	EN10025-2
S275J0JR (+M)	AM	16	40	29.67	2.08	26.24	33.14	0.12	-0.155	0.07	915	EN10025-2
S355J2K2 (+M)	AM	16	40	25.93	1.82	23.32	29.42	0.293	0.632	0.07	8207	EN10025-2
S460M	AM	16	40	23.4	1.63	20.68	25.9	0.51	0.049	0.07	778	EN10025-4
S275M	RIVA	3	16	33.86	1.74	30.61	36.28	0.92	-0.62	0.051	2125	EN10025-4
S355M	RIVA	3	16	27.75	1.83	24.94	30.67	-0.04	0.5	0.066	61	EN10025-4
S355J0JR	Corus	16	40	28.3	2.061	-	-	-	-	0.073	9127	EN10025-2

**Table 2-4: Mechanical properties for the steel grades used for the case study**

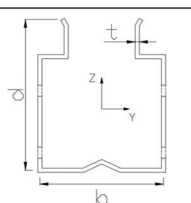
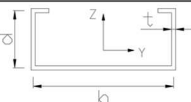
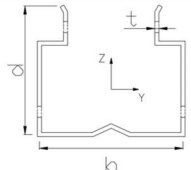
Mean value			
MPa	S350GD	S355JR	S275JR
$f_y$	380	396	349
$f_t$	449	525	472
$\epsilon_u$ (%)	29%	28,30%	29,67%

In Table 2-4 the mechanical properties of the three steel grades mentioned and used in the case study has been summarised.

### 2.2.3 Section properties

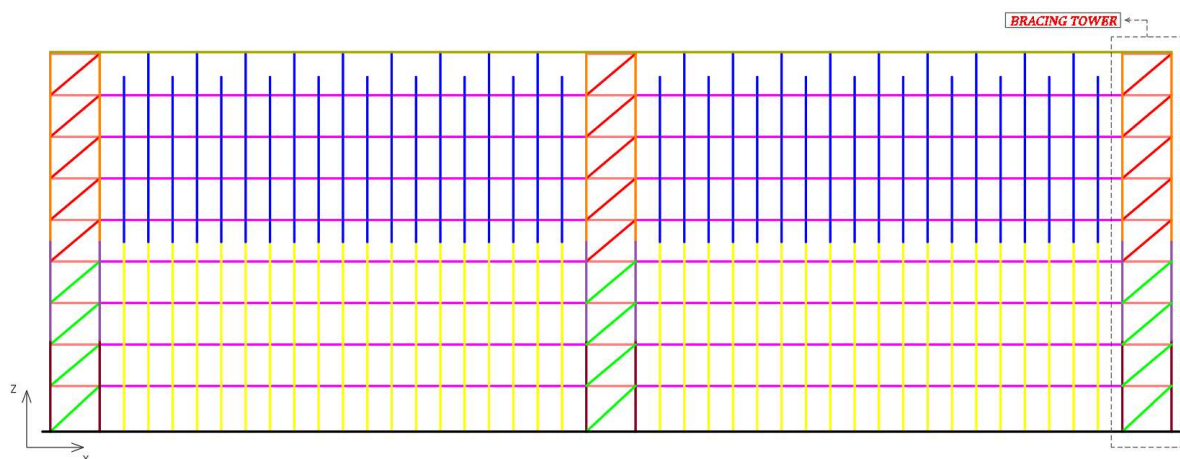
According to common use in design practice of such kinds of structures, various sections are used for different elements of warehouses, related to their proper function. All of the sections used for the case study and relative geometrical properties are summarised in the tables below:

**Table 2-5 (a):** Section properties in the down-aisle direction (cold formed profiles)

Down-aisle_Cold formed profiles						
Geometry Section	Section	Profile description	$A_g$ [mm <sup>2</sup> ]	$I_y$ [mm <sup>4</sup> ]	$I_z$ [mm <sup>4</sup> ]	Material Steel grade
	U 1	Lower bracing uprights Reinforced	3443	6,77E+06	9,03E+06	S350GD
	U 2	Lower bracing uprights	1720	3,85E+06	3,93E+06	S350GD
	U 3	Upper bracing uprights	1070	2,40E+06	2,49E+06	S350GD
	U 4	Lower pallet uprights	1290	2,89E+06	2,98E+06	S350GD
	U 5	Upper pallet uprights	860	1,93E+06	2,01E+06	S350GD
	BP 1	Pallet beams	541	7,95E+05	9,79E+04	S355JR
L section	D 1	Upper vertical bracings	276	1,23E+05	2,14E+04	S355JR
	R 5	Top end upright connections	538	3,79E+05	4,47E+05	S350GD

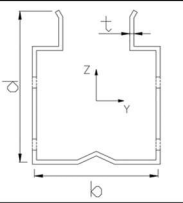
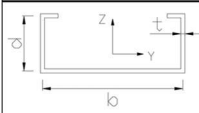
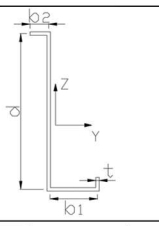
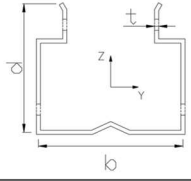
**(b):** Section properties in the down-aisle direction (hot rolled profiles)

Down-aisle_Hot rolled profiles						
Geometry Section	Section	Profile description	$A_g$ [mm <sup>2</sup> ]	$I_y$ [mm <sup>4</sup> ]	$I_z$ [mm <sup>4</sup> ]	Material Steel grade
H section	BB 1	Bracing beams - Wall and Cladding purlin	2124	3,49E+06	1,34E+06	S275JR
L section	D 2	Lower vertical bracings	568	7,12E+04	2,01E+05	S355JR



**Figure 2-4:** Location of each member in the down-aisle direction (the colours are related to the ones used for the sections mentioned in Table 2-5)

**Table 2-6 (a):** Section properties of sections in the cross-aisle direction (cold formed profiles)

Cross-aisle_Cold formed profiles						
Geometry Section	Section	Profile description	$A_g$ [mm <sup>2</sup> ]	$I_y$ [mm <sup>4</sup> ]	$I_z$ [mm <sup>4</sup> ]	Material Steel grade
	U 4	Lower pallet uprights	1290	2,89E+06	2,98E+06	S350GD
	U 5	Upper pallet uprights	860	1,93E+06	2,01E+06	S350GD
	H 1	Upright horizontals	249	8,34E+04	1,77E+05	S350GD
	D 1	Lower upright diagonals	498	1,54E+05	3,35E+05	S350GD
	D 2	Upper upright diagonals - Roof truss verticals and diagonals	332	1,08E+05	2,31E+05	S350GD
	Z 1	Z pallet profiles	818	5,35E+06	3,22E+05	S350GD
	R 1	Roof truss upper chords	680	6,07E+05	1,38E+06	S350GD

**(b):** Section Properties of sections in the cross-aisle direction (hot rolled profiles)

Cross-aisle_Hot rolled profiles						
Geometry Section	Section	Profile description	$A_g$ [mm <sup>2</sup> ]	$I_y$ [mm <sup>4</sup> ]	$I_z$ [mm <sup>4</sup> ]	Material Steel grade
I section	R 2	Roof truss lower chords	1640	5,41E+06	4,49E+05	S275JR
I section	S 1	Supporting Shuttle beams	1030	1,71E+06	1,59E+05	S275JR
H section	W 1	Wall purlins	2124	3,49E+06	1,34E+06	S275JR

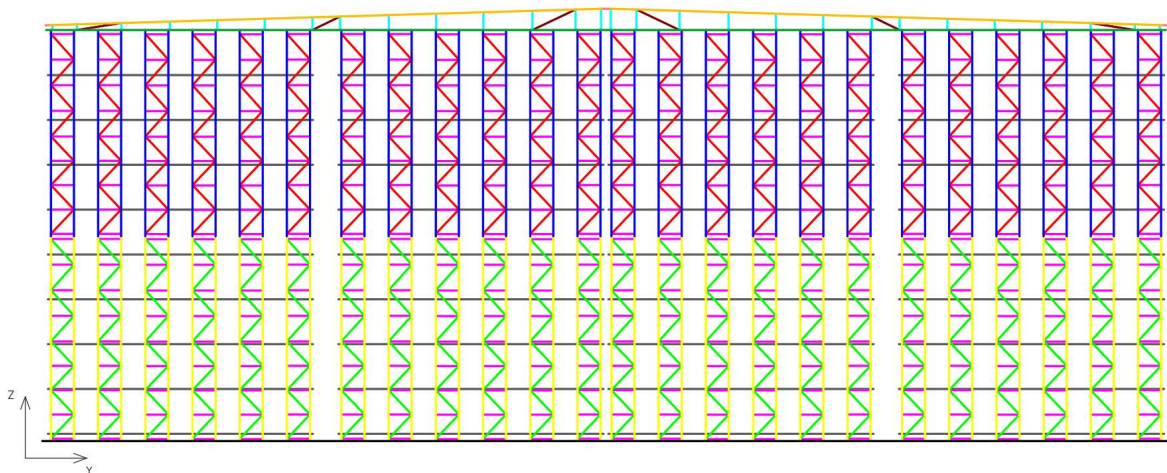


**Figure 2-5:** Location of each section in the cross-aisle direction (the colours are related to the ones used for the sections mentioned in Table 2-6)

## **2.2.4 Mechanical properties of frame elements**

The performance of the pallet racking system strongly depends on the efficiency of their elements and relative connections. For example, the connection between a column and a beam can be classified as fixed, pinned or semi-rigid, affecting the buckling load of a column [17]. According to the European Standards EN15512 and EN16681, to observe the influence of such connections and of other factors, such as perforations, local and distortional buckling effects, or for the assessment of the shear stiffness of upright frames, specific tests should be performed, in order to properly simulate their nonlinear behaviour. The value adopted in the case study in order to take into account these effects, has been derived from some experimental tests performed by the industrial partner involved in the design of the case study. Where the tests concerning the behaviour of some members were missing, the finite element analysis on Abaqus was performed or some results from literature was checked. The specific results for the three particular connections, are reported in detail in the following paragraphs.

### **2.2.4.1 Upright frame shear stiffness**

The purpose of the test is to determine the transverse shear stiffness per unit length of the upright frame in order to assess its stability and its shear strength (see annex A.2.8 of EN15512). The load deflection curve obtained from this test shows a nonlinear behaviour, so the stiffness may be defined as the slope of the best straight line that fits the curve over its full range. The value determined from the test, may be used to derive a reduced bracing area or a spring constant for the bracing connection. In this case study, an axial spring has been applied to the diagonal and the value of the stiffness is the following:  $K_{ax} = 3516 \text{ N/mm}$  for the diagonals on the lower part (D1) and  $K_{ax} = 3642 \text{ N/mm}$  for the diagonals on the upper part (D2).

### **2.2.4.2 Pallet and bracing beam end connectors**

All the beam end connectors are filled with beam connector locks, which prevent the connectors from disengaging when subjected to vertical loads (see Figure 2.2). Such boltless semi-rigid connections consist of angled end plates welded to each end of beams with interlocking arrangements to join with perforated uprights. The beam end connectors provide to the beams and unbraced racks were the only source of stiffness required for down-aisle stability, when, for practical reason, the pallet racks were not braced in the down-aisle direction [17]. In order to simulate this kind of connection, a rotational spring has been assigned to the end of the pallet beams and of the bracing beams to take into account the stiffness and the bending strength of the beam end connector. The method used to evaluate the rotational spring from the tests is detailed in the annex A.2.4 of the EN15512-2009. The resulting values summarized in Table 2-8 have been applied at the end of the relative beams.

**Table 2-7:** Stiffness end connectors

Stiffness end connectors		
kNm/rad	Rotation about Y in down aisle plan	Rotation about vertical axes Z
<b>Pallet beam end connector</b>	42,7	1
<b>Bracing beam end connector</b>	58	1

### 2.2.4.3 Floor-upright connection

The upright base-plate is connected to the floor with 2 post-installed chemical anchor bolts M20 (8.8), while the bracing base-plate (referred to the bracing tower) is connected with 4 threaded bars M20 (8.8). According to the requirements of the annex A.2.7 of the EN5512, the test has been performed to measure the moment rotation characteristics of the floor-upright connection. Due to its nonlinear behaviour, a rotational spring has been used to represent the stiffness of such connections in the down-aisle direction, and the value assigned for the stiffness of the base plate connection, around Y axis, for both kind of connections is  $K_y = 1016$  kNm/rad.

### 2.2.5 Definition of loads

The ARSWs are “light” structures due to the reduced weight of their elements. Despite their lightness, they are used to bear a very high load of the pallet stored in addition to the weight of all the non-structural elements i.e. clad, roof, etc., as well as all the environmental actions that act on them. Apart from the dead load referred to the weight of all the steel members, the following loads must be taken into account:

#### 1) Pallet loads:

The geometrical characteristics of ARSWs and the automated handling of pallets allows the full exploitation of the available space. The pallet loads represent the main load for the pallet racking system in general and in particular for the ARSWs, more than 95% of the total mass consists of stored goods. The distribution of pallets depends on logistic strategies, affecting the behaviour of ARSWs during seismic events. Even though in serviceability condition not all the shelves are full, in the case study a “full load” condition has been considered in order to consider the worst possible scenario under the horizontal seismic action. Pallets are placed on the Z-section profiles that run in the down-aisle direction, and the way the values are distributed on them along the storage cell, decreasing from the bottom to the top, is schematically shown in Figure 2-6. The unit load, of each single pallet, and the maximum number of UL able to fit per storage cell, are detailed in Table 2-8.

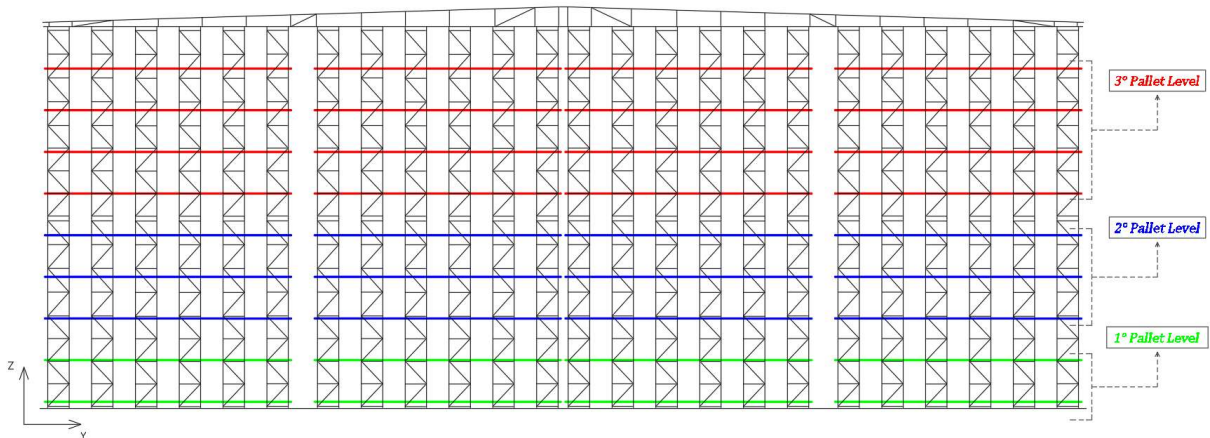


**Figure 2-6:** Distribution of the pallet loads

**Table 2-8:** Unit pallet loads values

Unit Pallet loads		
Levels	$Q_{UL,max}$ [kN]	Number of UL per storage cell
1 to 2	10	13
3 to 5	8	13
6 to 9	6	13

The exact position of the pallets on the pallet beams shall be considered, but according to the prescription of the paragraph 7.5.8 of EN16681, for the purpose of global analysis, the difference between the height of the centre of gravity of the unit loads and the pallet beams where the loads are applied, for multiple bay racks, has been neglected.

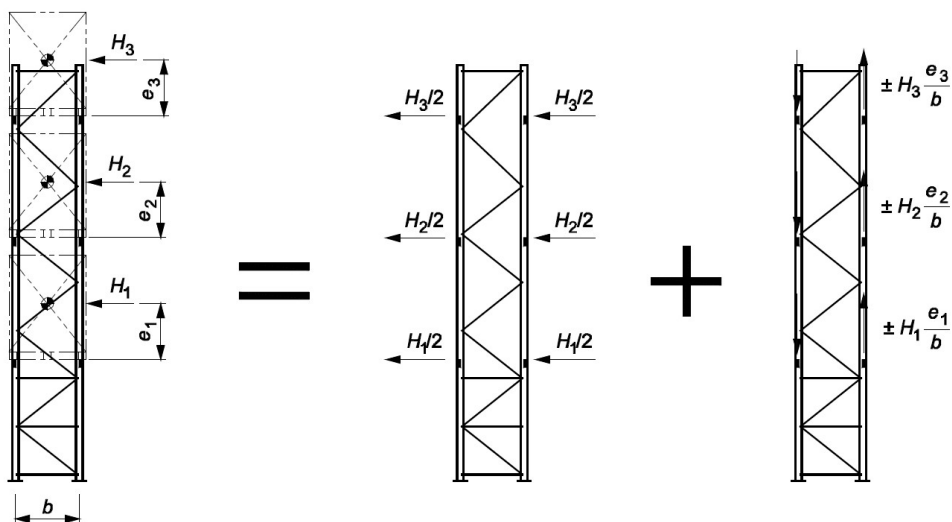


**Figure 2-7:** Effect of the vertical eccentricity of the centre of gravity of the unit load, neglected for the case study<sup>7</sup>

<sup>7</sup> Figure 3, §7.5.8, see [11]

## 2) Additional masses (G2):

The additional masses, in particular, consist of the weight of all the non-structural elements (clad, roof, technological facilities...) that the ARSWs are designed to support; the value and the way the load have been applied are detailed in the paragraph 3.1.2.

## 3) Environmental loads:

Due to their particular configuration, these structures are designed to also support all the environmental actions i.e. snow, wind and seismic action that act on them, representing the basic distinction between SR and ARSW. The contribution of each action is detailed below:

- a) **Snow load:** considered not relevant related to the other loads and for this reason it hasn't been taken into account;
- b) **Wind load:** in the area where the case study is placed, the wind has a "basic speed", and for this reason considered not relevant to take into account in the analysis;
- c) **Seismic load:** the case study has been designed considering a moderate/high seismicity level of the seismic action. The parameter for the definition of the seismic load are resumed in Table 2-9

**Table 2-9:** Parameters for the definition of the seismic load

Design life	$V_R$	50 years
Importance class		I
Importance factor	$\gamma_I$	0.8
Peak ground acceleration	PGA	0.3 g
Ground class		C
Design spectrum type		From National standard $T_R = 475$
UL to beam friction coefficient	$\mu_s$	0.37
Behaviour factor both direction	$q$	1.5
Design spectrum modification factor	$K_D$	0.8

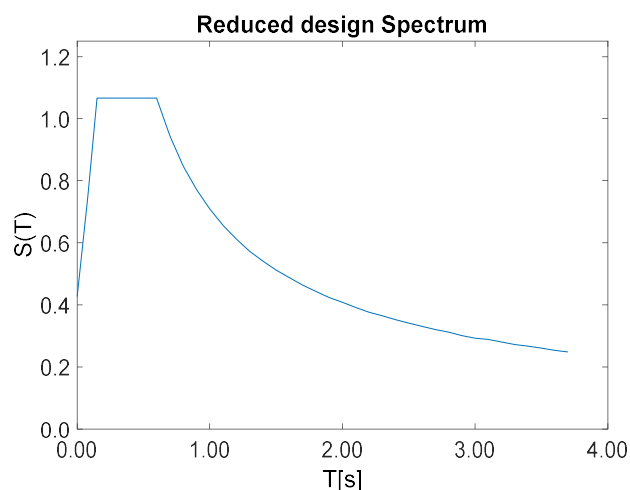


**Figure 2-8:** Design spectrum ( $q=1,5$ )

### 2.2.6 Definition of mass source and filling grade reduction factor

Considering that the distribution of pallets is strongly related to the industrial logistic strategies, and that in serviceability condition not all the shelves could be filled, the design weight of unit loads to be considered in the evaluation of the horizontal seismic action, must to be determined as follows (see paragraph 7.5.4 EN16681):

$$W_{E,UL} = R_F \cdot E_{D2} \cdot Q_{P,rated}$$

where:

- $R_F$  is the rack filling grade reduction factor, related to the occupancy of stored goods that can be assumed during a seismic event.

For the analysis,  $R_F = 0,8$  has been assumed in the cross and the down-aisle direction;

- $E_{D2}$  is the unit load weight modification factor depending on the type of unit load, in order to consider the relative damping effect<sup>8</sup>.

The value of 1 has been assumed;

- $Q_{P,rated}$  represents the value of the weight of unit loads reported in the previous paragraph.

Consequently, a multiplier of 0,8 has been used for the definition of the mass source.

---

<sup>8</sup> Table 5, §7.5.5, see [11]

### **3 Detailed Model**

The objective of this chapter was the simulation of the case study through a finite element software (Sap 2000, CSI) in order to evaluate the structure behaviour in the elastic and inelastic regions. The detailed drawings, useful to implement the model, have been provided by the industrial partner, however, additional information prescribed by the standards and by the experience of the author were considered to model the case study as well. In the next paragraphs the procedure followed for the definition of the model and how the analyses were performed are well detailed.

#### **3.1 Finite Element Modelling**

All of the members drawn using the FEA software have been modelled as mono-dimensional beams or truss elements, and the specific information was given to the software for the simulation of the various connections (bracing members, beam to column, base plate, ...) as derived from the relative tests and as well as mentioned in the previous chapter; releases have been assigned to the ends of all of the members simply connected (modelled as pinned joints) and axial or rotational springs, to all the connections, which, examining the relative tests, showed a nonlinear behaviour, according to what was previously mentioned in paragraph 2.2.4. Modelling all the elements on the FEA software we should be aware of the tolerances and the eccentricities related to the “as-built” situation of the structure; the assessment of eccentricity has been detailed in the following paragraph. In addition, as usual, only the contribution of the spine bracings in tension has been taken into account, considering, for safety reasons, the bracing in compression failed. Furthermore, all of the properties regarding the materials as well as the sections used were well detailed in the previous paragraphs.

##### **3.1.1 Evaluation of the eccentricity**

The evaluation of the eccentricities, denoted by “e”, have been considered according to paragraph 8.6 of EN15512. In the global analysis, the effects of bracing eccentricity, could be neglected under some conditions (see Figure 3-1). Specifically, in the case study, no resulting secondary moments have been considered in the global analysis because the eccentricity limit, as shown in figure 3-1 (a) and (b), has been respected. Also, the eccentricity between beams and uprights (see the Figure 3-1 c), concerning the distance between the centroidal axis of the beam and the centroidal axis of the upright, has been neglected in global analyses because its value is less than  $0,25 d_u$ , where  $d_u$  is the dimension of the section of the upright.

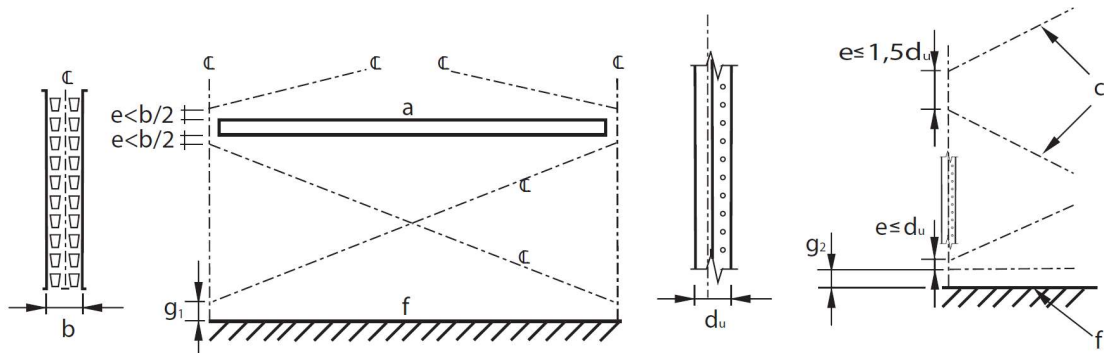
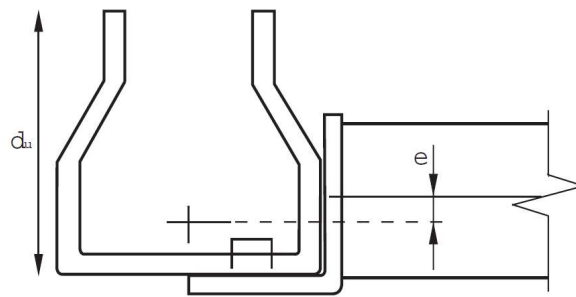


**Figure 3-1:** (a) Eccentricities in spine bracing, (b) Eccentricities in frame bracing



(c) Eccentricity in cross-aisle direction

### 3.1.2 Definition of load and load case

The loads to be considered in the model, as detailed in the previous paragraphs, are given with their relative value and in the way they are considered in the model in the following points:

- 1) **Dead loads:** the dead loads, make sure that the weight of each element is automatically calculated by the FEA software (SAP2000, CSI);
- 2) **Pallet loads:** the Z-pallet profiles, where the pallets are placed, are performed like beams along the cross-aisle direction, and the pallet loads, have been uniformly distributed on the Z-pallet profiles (see Figure 3-2) considering the max number of UL that can fit in each storage cell (13 UL, see §2.2.7); i.e. in the first three levels, a uniformly distributed load of  $\frac{13 \times 1 \text{ kN}}{L_Z}$  has been applied, where  $L_Z$  is the length of the Z-pallet profile in each storage cell;
- 3) **Additional masses (G2):** in the cross-aisle direction an uniformly distributed load of 0,3 kN/m has been applied (on the top chords of the roof as shown in Figure 3-3) and in the down-aisle direction as well (applied on the  $\Omega$ -section profiles, R5, because the roof has not been modelled as shown in Figure 3-4), in order to consider the weight of the roof cladding. In addition, point loads have been applied on the “wall purlins” (W1 section) in order to consider the weight of the wall cladding.

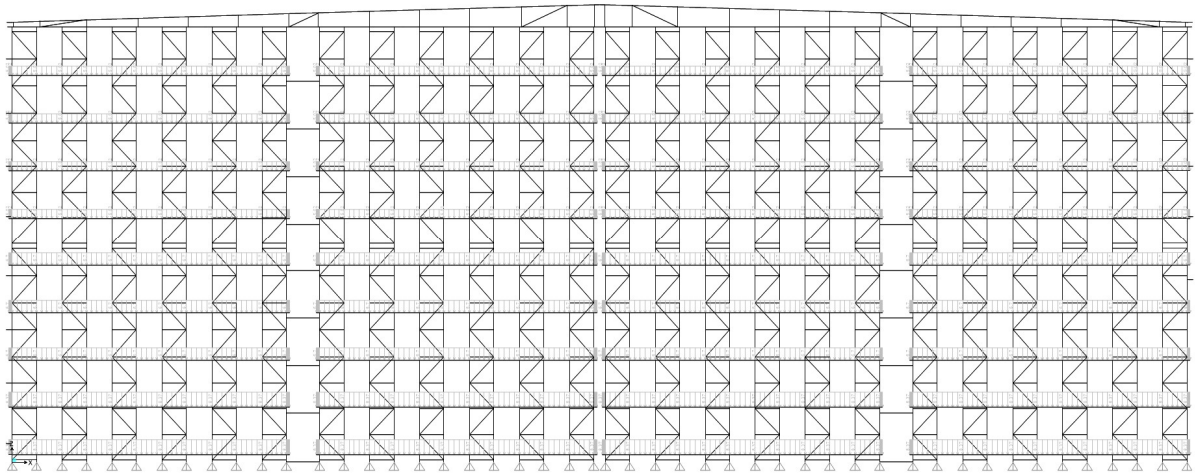


**Figure 3-2:** Pallet loads distribution

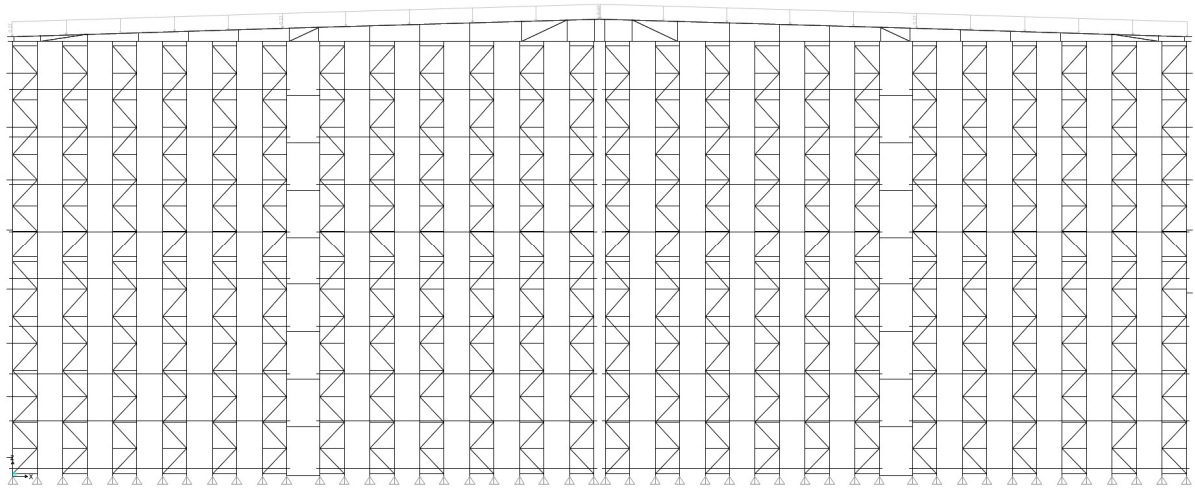


**Figure 3-3:** Additional masses (G2) in the cross-aisle direction

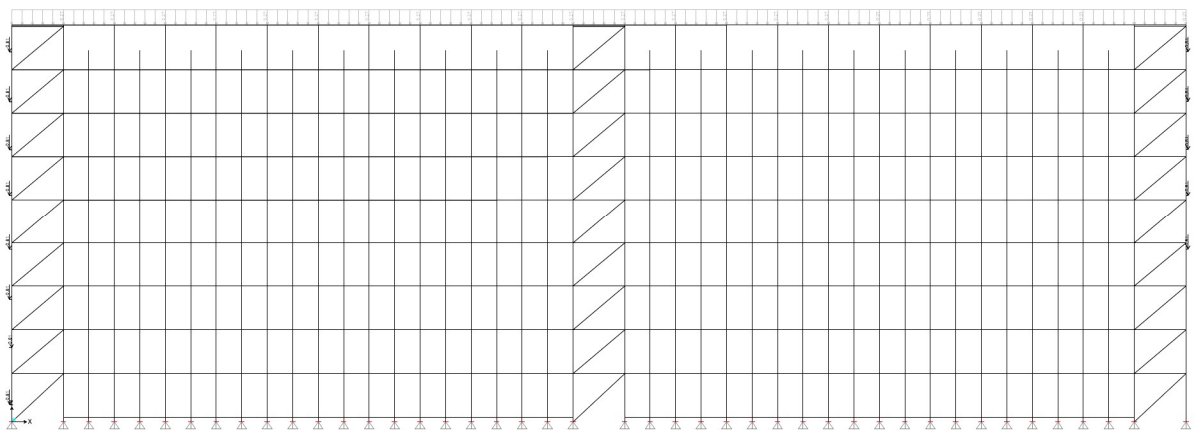


**Figure 3-4:** Additional masses (G2) in the down-aisle direction

## 3.2 Finite Element Analysis

After giving all the information about the design characteristics of the structure and the information to implement the model on SAP2000 as well, we need to evaluate the behaviour of the structure in the elastic and inelastic regions, as detailed below.

### 3.2.1 Modal Analysis

A linear dynamic analysis has first been executed on the 2D detailed model both in the cross-aisle and in the down-aisle direction; later on, a modal analysis in three dimensions has been performed as well, and the eigenmodes between both the 2D models and 3D model have been compared.

The analysis starts from an unstressed condition, a maximum and minimum number of vibration modes equal to 12 has been taken into account by default. The mass for the evaluation of the inertia to be considered in the modal analysis, has been evaluated using the combination of actions reported in paragraph 9.2.1.1 of EN16681 for the design action, taking into account the following loads:

- Dead load;
- G2;
- Pallet loads.

A multiplier of 0,8 has been assigned to the pallet loads in order to consider the possibility that in serviceability condition not all of the shelves would be filled. In Table 3-1, the results about the periods of the first 12 eigenmodes are listed. The free vibration modes shown below, are only related to the first 5 periods, those are the eigenmodes considered adequate to compare the results with the reduced-order model in the next chapter.

**Table 3-1:** Modal periods and mass participation factor in cross and down-aisle section

Modal analysis Cross-aisle direction			Modal analysis Down-aisle direction		
Mode	T [s]	M [%]	Mode	T [s]	M [%]
1	1,703	67,65%	1	1,405	56,35%
2	0,843	67,65%	2	0,483	77,95%
3	0,565	83,23%	3	0,271	82,72%
4	0,409	83,23%	4	0,246	82,72%
5	0,304	87,77%	5	0,212	83,11%
6	0,263	87,77%	6	0,211	85,56%
7	0,215	89,66%	7	0,179	85,56%
8	0,194	89,66%	8	0,170	86,45%
9	0,160	90,57%	9	0,160	86,45%
10	0,152	90,57%	10	0,147	86,85%
11	0,145	90,57%	11	0,143	86,85%
12	0,145	90,57%	12	0,131	86,89%

Later, a modal analysis has also been performed on the 3D model, and only the results of the first eigenmodes have been compared, and considered satisfying for the scope; the 3D model has many more elements than the one in two dimensions, and most of the eigenmodes after the second (related to a short mass participation factor), refer to these single elements. For this reason, no comparison between the further eigenmodes has been done. In Table 3-2 the difference in percentage between the two models have been reported. The results are satisfying, even considering the difference of 10% between the first eigenmodes, due to the huge difference in terms of the number of DOFs between the 2D and the 3D model. More eigenmodes about the 2D models are shown in the next chapter comparing the results with the reduced-order model.

**Table 3-2:** Comparison between 2D and 3D detailed models

Modal Analysis_2D vs 3D model						Modal Analysis_2D vs 3D model					
Mode	2D_Cross-aisle		3D		Differences %	Mode	2D_Down-aisle		3D		Differences %
	T [s]	M [%]	T [s]	M [%]	T [s]		T [s]	M [%]	T [s]	M [%]	T [s]
1	1,703	67,65%	1,526	69,32%	10%	1	1,405	56,35%	1,329	56,14%	5%
2	0,565	15,58%	0,540	11,40%	4%	2	0,483	21,60%	0,458	21,25%	5%

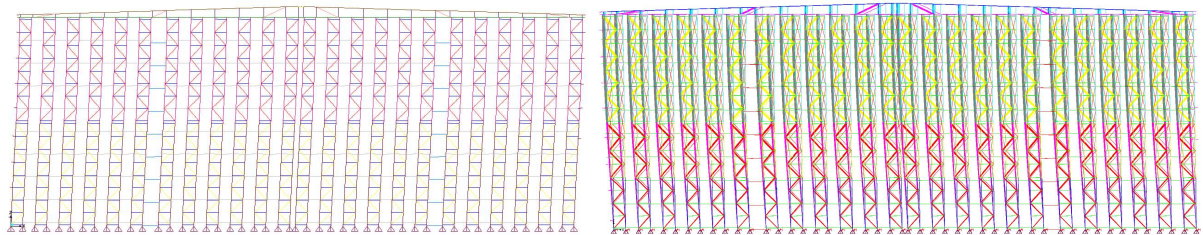
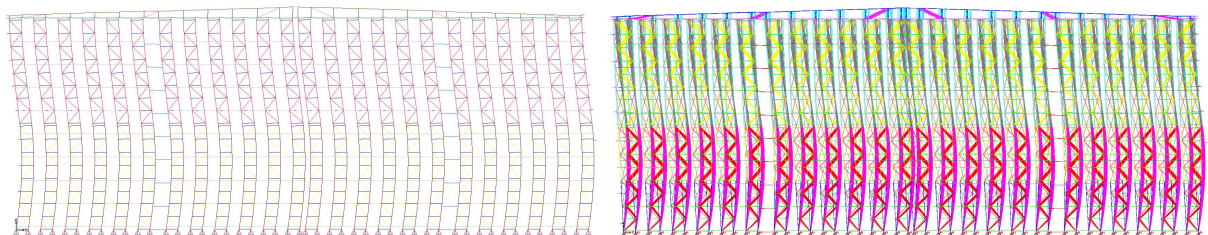


**Figure 3-5 (a):** 1<sup>st</sup> eigenmode of 2D model ( $T_{1,2D}=1.703$  sec) and 3D model ( $T_{1,3D}=1.526$  sec). Translational mode in cross-aisle direction



**(b):** 2<sup>nd</sup> vibration mode of 2D model ( $T_{2,2D}=0.565$  sec) and 3D model ( $T_{2,3D}=0.540$  sec). Sine shape in cross-aisle direction

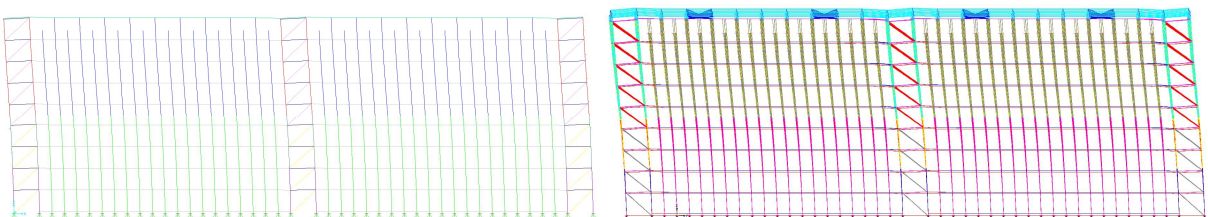
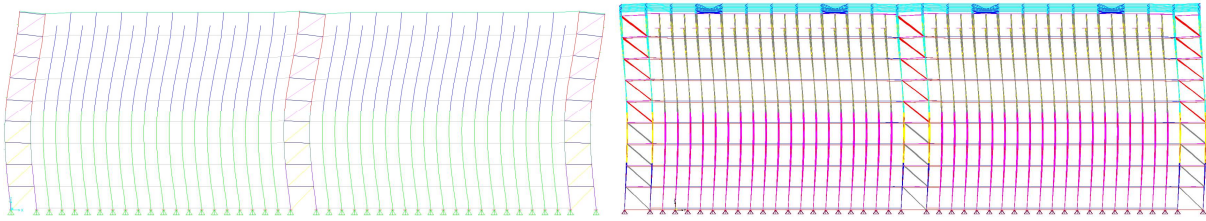


**Figure 3-6:** 1<sup>st</sup> vibration mode of 2D model ( $T_{1,2D}=1.405$  sec) and 3D model ( $T_{1,3D}=1.329$  sec). Translational mode in down-aisle direction



(b): 2<sup>nd</sup> vibration mode of 2D model ( $T_{2,2D}=0.483$  sec) and 3D model ( $T_{2,3D}=0.458$  sec). Sine shape in down-aisle direction

### 3.2.2 Lumped-plasticity element properties

Many problems arise in the prediction of the structural behaviour for the ARSW depending on the geometry of their structural components (high slenderness elements, open-section profiles hence prone to buckling effects, ecc.), as well as the nonlinear behaviour of their joints (i.e. beam end connections and floor-upright connections). For this reason, before “starting” the push-over analysis it’s important to mention the procedure used for the definition of the plastic hinges applied to the frames in order to take into account such effects. Several studies [9] [10] [17], supported by various experimental tests as well, were carried out to examine the nonlinear behaviour of these elements and of their end connections. The results show that the failure occurs mainly in the following elements [18]:

- Base plate connections;
- Uprights at the lowest level: thus forming a “soft-floor” mechanism;
- Beam-to-upright connections: collapse with further increase of transversal displacement;
- Diagonals: buckling of the bracings starting from the lowest level and moving upwards.

Considering that, the plastic hinges were applied to such an element.

For the definition of the hinge properties, a force-displacement or moment-rotation relationship, depending on the kind of failure attended for each member, has been defined. Plastic hinges applied in the case study are mostly “axial” type hinges with a non-symmetrical behaviour in tension and compression; that kind of hinges have been considered for the uprights and the bracings because they are mostly susceptible to axial forces. “Moment” type hinges have been used only for the beams due to their behaviour that shows a bending failure. Therefore, an elastic-plastic behaviour with strain hardening, has been adopted for the “axial hinge” in tension while a brittle behaviour in compression to consider the buckling effects, and elastic perfectly plastic behaviour for the “moment hinges”, symmetric in tension and compression. Different names, colours and symbols, are associated to the achievement of different limit states represented in the diagram: the yielding point (represented by a magenta square), C that is the ultimate capacity (represented by a yellow circle), the orange circle that represent the residual strength for the push-over analysis and the red circle that represent the total failure; and other

three points are also used to define the acceptance criteria of the hinges: the immediate occupancy – IO, the life safety – LS, and the collapse prevention – CP (see Figures 3-7 and 3-8).

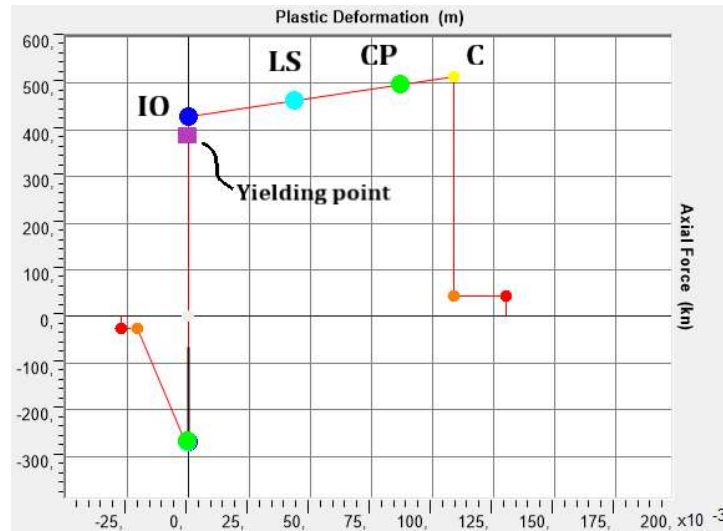


**Figure 3-7:** Force-displacement behaviour of an “axial hinge” and characteristic points

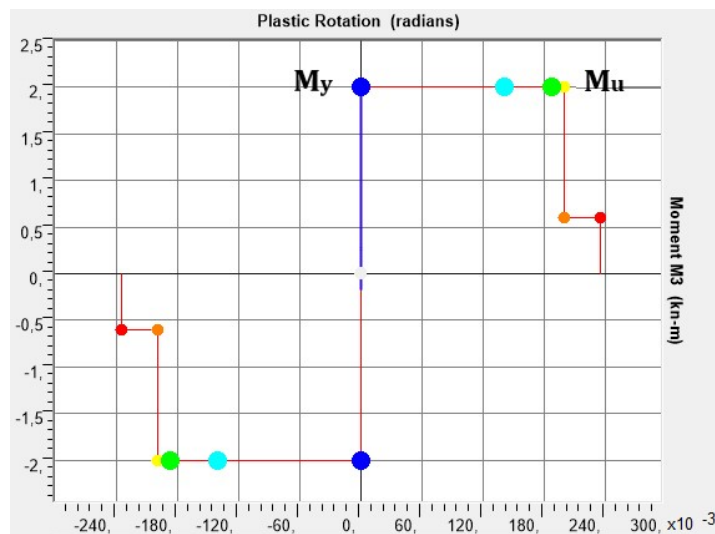


**Figure 3-8:** Moment-rotation behaviour of a “moment hinge” and characteristic points

Therefore, for the definition of the hinge diagram, in both tension and compression, the following characteristic points need to be evaluated:

### **Axial Hinge Properties:**

For some of the elements susceptible to axial forces as uprights, bracing members and spine bracing as well, cross-section profiles of Class 4 are used, and the buckling phenomena must be considered. For this reason, a “brittle” behaviour has been used for the definition of the force/displacement curve under compression, considering the instability phenomena which such elements are prone to and that the buckling effect occurs before the characteristic resistance; the curve is considered to drop when the members reach the ultimate value of the resistance under compression  $N_{b,Rd}$ , where:

- $N_{b,Rd}$ : is the limit in compression considering the buckling effects;
- $\delta_u$ : the ultimate displacement.

A speech deserves the assessment of resistance in compression of the members prone to the buckling phenomena. For some elements, the results of experimental tests, performed by the industrial partners, have been given, but for the members the experimental tests were missing, some evaluations by the author have been done and finite element analysis on Abaqus<sup>9</sup> were performed at the NTUA, thanks to the PhD student Dimitrios Tsarpalis, in order to evaluate  $N_{b,Rd}$ ; in the next paragraph all of the details regarding the procedure followed to evaluate  $N_{b,Rd}$  are given.

Regarding the evaluation of the axial behaviour in tension, the following parameters must be defined:

- $F_y$ : is the resistance to the yield point;
- $\delta_y$ : is the relative displacement to the yield point;
- $F_t$ : is the ultimate resistance;
- $\delta_u$ : is the relative displacement corresponding to the ultimate resistance.

It's important to note that the values of  $f_y$  and  $f_t$  for the evaluation of  $F_y$  and  $F_t$  have been already defined in paragraph 2.1.2.

### **Moment Hinge Properties:**

For the definition of the “moment hinges” curve, a symmetrical behaviour has been considered in tension and compression. The following parameters need to be evaluated:

- $M_y$ : is the moment to the yield point;
- $\theta_y$ : is the relative rotation to the yield point;
- $M_u$ : is the ultimate moment;
- $\theta_u$ : is the relative rotation to the ultimate moment.

---

<sup>9</sup> <https://www.3ds.com/products-services/simulia/products/abaqus/>

The results of the experimental tests performed by the industrial partner are not mentioned due to the non-disclosure agreement between the industrial partners involved; however, all of the values adopted for each parameter, that are the results of experimental tests, evaluation from literature and numerical analysis in Abaqus (to evaluate  $N_{b,Rd}$ ), are included in Table 3.3.

### **3.2.3 Evaluation of $N_{b,Rd}$ considering the buckling phenomena**

The experimental data was not available for all the members of the structure, for this reason, in order to evaluate the reduced resistance in compression  $N_{b,Rd}$ , due to the buckling effects, other evaluations needed to be considered. In particular, finite element analyses on Abaqus were performed on such uprights in order to consider the distortional buckling effect; more details about such analyses are given below. For the same uprights,  $N_{b,Rd}$  has been evaluated according to the European design approach concerning class 4 columns in traditional steel frames [19] as well as for rack uprights [8]. The minimum value, considering different buckling modes, has been considered. In particular, considering the European design approach, the following conditions have been taken into account:

- The effective length of the upright between the beams has been taken into account, considering, for safety reasons, the connection of the beams to the uprights as pinned;
- assuming the ratio between  $f_y$  and  $f_u$  is equal to 1 in order to not consider any increments of strength;
- assuming a safety coefficient is equal to 1;
- assuming the value of  $f_y$  and  $f_u$  is defined in the paragraph 2.1.2.

It's important to note that all the evaluations and different approaches mentioned have been used applying the same conditions in either analysis or testing (loads and boundary conditions). In Table 3.3 (a) and (b), the values assumed for the definition of the hinge properties are listed.

**Table 3-3 (a):** Axial hinge properties in tension and compression

Axial Hinge properties			
Section	Compression	Tension	
	$N_{b,Rd,min}$ [kN]	$F_y$ [kN]	$F_u$ [kN]
U 1	651,10	1159,74	1372,53
U 2	348,91	587,08	694,80
U 3	205,49	355,44	420,66
U 4	268,67	428,73	507,40
U 5	155,51	285,95	338,41
H 1	48,00	79,75	94,38
D 1	60,08	159,49	188,76
D 2	40,32	106,37	125,88
D 1	3,00	177,21	235,33
D 2	7,54	93,75	124,49

**(b):** moment hinge properties (symmetrical behaviour in tension and compression)

Moment Hinge properties				
Section	$M_y$ [kNm]	$\theta_y$ [mrad]	$M_u$ [kNm]	$\theta_y$ [mrad]
BP 1	2,00	46,90	2,01	200,00
BB 1	3,96	38,23	3,96	131,48

### Abaqus analysis:

The numerical analysis on Abaqus has been performed on three different profiles considering various lengths, as required according the European Standard EN 15512, and equally to the experiment tests performed on some uprights. In Figures 3-9, 3-10, 3-11, an example of the tests performed on Abaqus, regarding the profile with cross-section U2, is shown. In particular, the following properties have been adopted for the analysis on Abaqus:

#### Element properties:

- 4 node shell elements with reduced integration;
- Material: S350GD, Elastic perfectly plastic behaviour, Yield stress ( $f_y$ ) = 350 MPa. Fracture stress ( $f_t$ ) = 420 MPa.

#### Boundary conditions:

- Zero displacements and rotations on bottom end;
- Zero horizontal displacements and rotations on top end. Vertical displacement is released.

#### Imperfections:

- According to 1<sup>st</sup> buckling mode obtained by the linear buckling analysis (LBA) analysis, the max imperfection is 2,5 mm

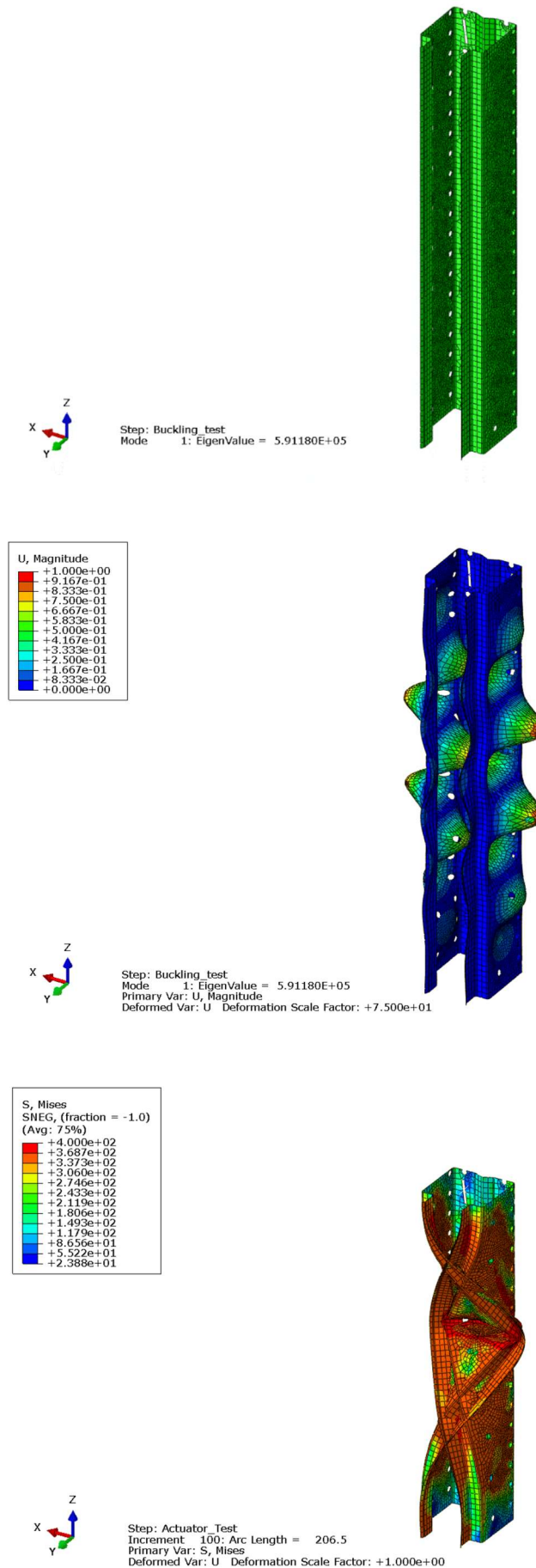


**Figure 3-9:** Buckling analysis with increasing magnitude. Geometrical and material nonlinearity. L=750 mm

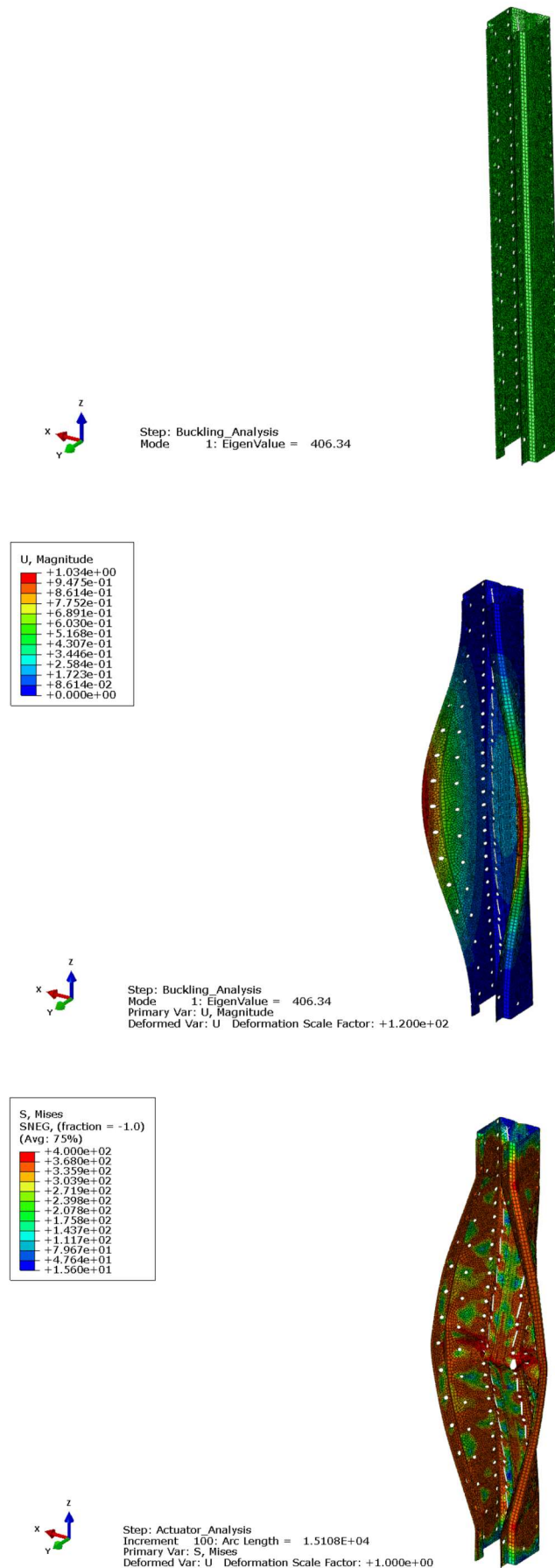


**Figure 3-10:** Buckling analysis with increasing magnitude. Geometrical and material nonlinearity. L=1200 mm

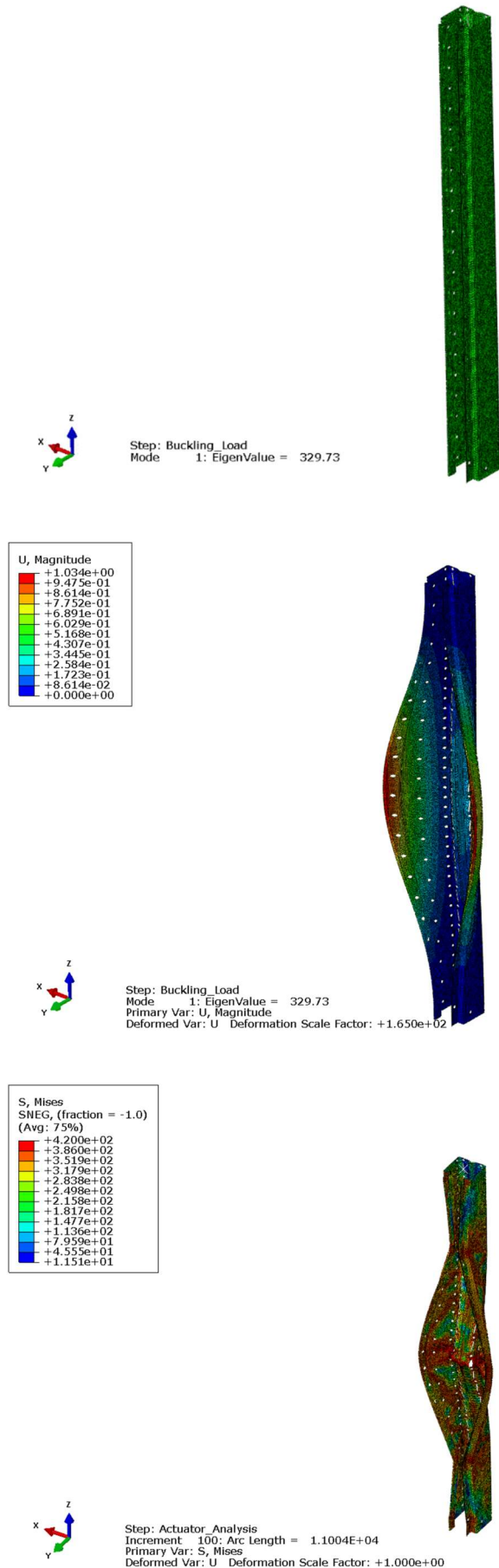


**Figure 3-11:** Buckling analysis with increasing magnitude. Geometrical and material nonlinearity. L=1650 mm

In the following diagrams (Figure 3-12), one for each upright (U2, U3, U4 and U5), the results of the numerical analysis on Abaqus are shown, comparing the response for different lengths; the upright U1, stronger than the others uprights, doesn't show any failure before the failure occur on uprights U2, U3, U4 and U5.

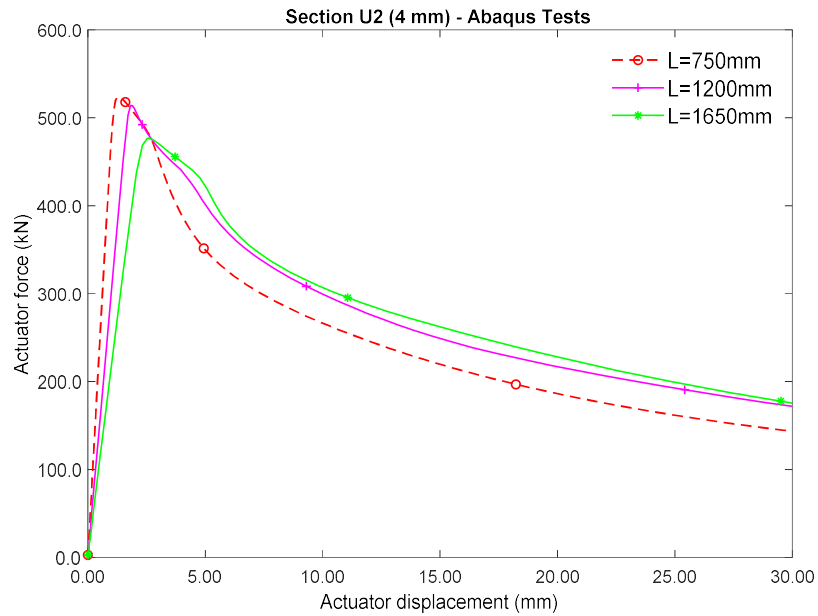
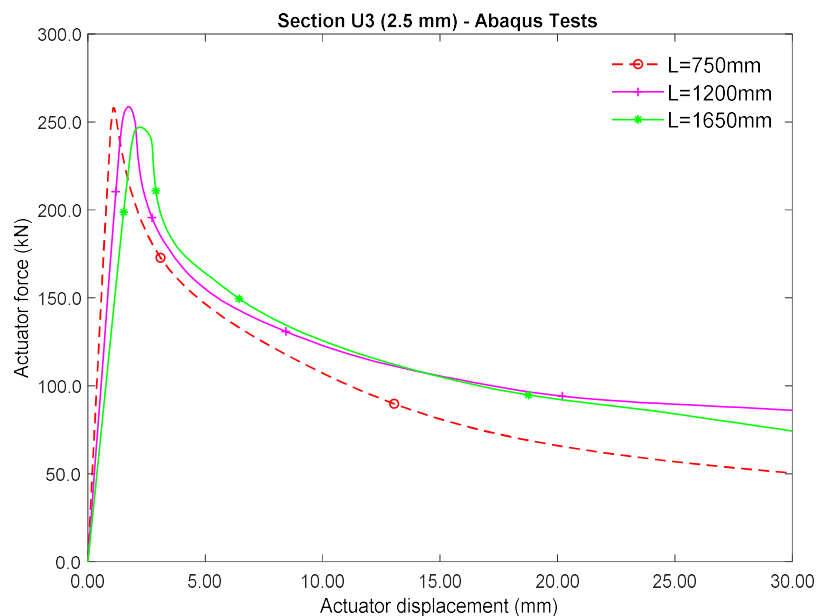
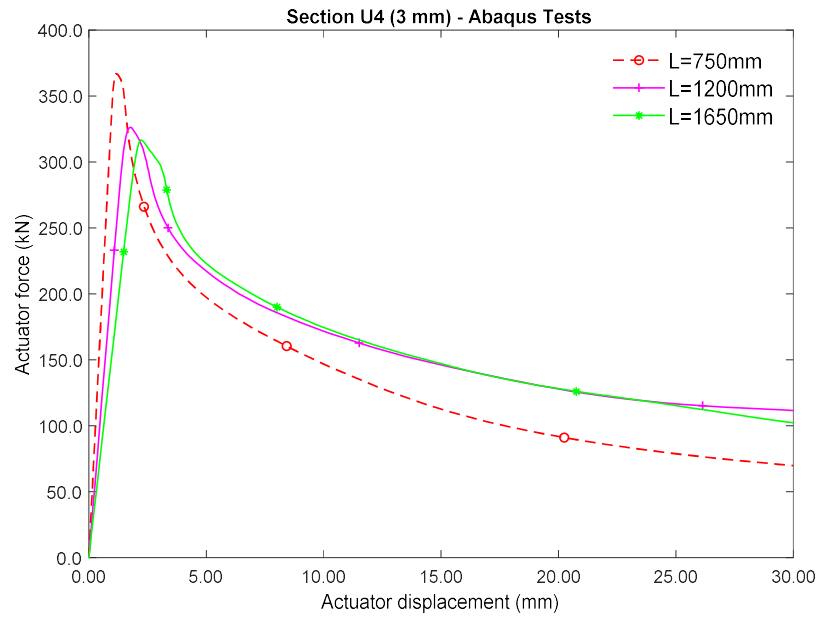


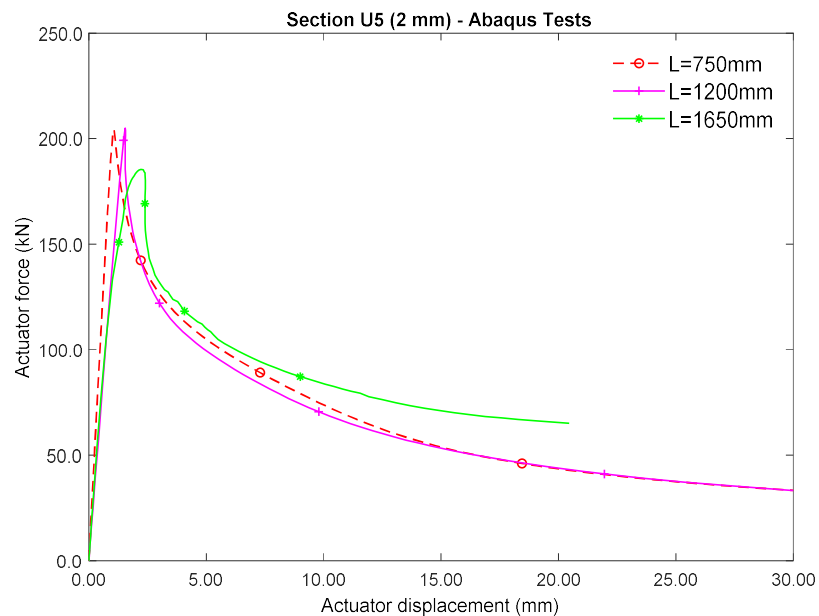
**Figure 3-12 (a):** Results of the buckling analysis on Abaqus for the upright U2 compared for three different lengths



**(b):** Results of the buckling analysis on Abaqus for the upright U3 compared for three different lengths



**(c):** Results of the buckling analysis on Abaqus for the upright U4 compared for three different lengths



**(d):** Results of the buckling analysis on Abaqus for the upright U5 compared for three different lengths

From the finite element analysis on Abaqus it emerged that distortional buckling occurs in every test performed for the uprights. Considering that, these values have been compared with the results of the European approach and the minimum value between them (included in Table 3-3 a) has been used for the definition of the hinge diagram concerning the uprights.

### **3.2.4 Push-over Analysis**

After the definition of the hinge properties, detailed in the previous paragraph, in order to take into account the nonlinear behaviour of some elements of the structure and their connections, we can focus our attention on the incremental nonlinear static analysis carried out for the case study, in both directions. In order to evaluate the structural performance under seismic action, where and when the plastic hinges are, the kind of failure, deformation's capacity of the structure and its ductility, in short, the capacity curve of the structure. The following parameters have been considered for the analysis. In the numerical model, the push-over analysis starts from the end of a nonlinear static condition in order to achieve a real loading situation where the horizontal loads coexist with vertical loads (the gravity loads). In the analysis, both kind of nonlinearity, in geometrical and material terms, have been considered; the material nonlinearity is defined applying plastic hinges to the elements which show a nonlinear behaviour, while the geometric nonlinearity has been considered taking into account P-  $\Delta$  effects. The distribution of the horizontal loading considered is proportional to the product of specified modal shapes. The "displacement control method" was used monitoring a specified node at the top of the structure, basically the highest point of the structure. The "axial hinges" have been applied on all the uprights, bracing members and spine bracings as well, while "moment hinges" on all the pallet and bracing beams susceptible to the bending force.

The output of the push-over analysis is a plot, the push-over curve, where the shear at the base of the structure and the relative displacement of the monitored node are shown, describing the capacity of the structure under the horizontal action considered. The push-over curve is plotted until the last step, when the structure reaches the failure, or if convergence problems occur, or dropped in case a much bigger reduction of the resistance occurs.

### **3.2.5 Discussion of the results**

In the cross-aisle direction, the model responds linearly and elastic until a top displacement approximately equal to 27 cm (yielding point, represented by a magenta square), corresponding to a shear at the base of the structure of about 500 kN when the first upright in the lower part achieves its resistance in compression. After this "limit state" is exceeded, the behaviour is nonlinear, and the push-over curve's slope decreases until a global collapse mechanism has occurred, this is referred to as a "soft-floor" mechanism. The push-over curve drops one of the uprights until it reaches the collapse, while all of the other elements (uprights in the higher part of the structure and bracing members) remain elastic, having reached a global mechanism. The achievement of different limit states in correspondence of the last step, and the capacity curve of the structure obtained applying the above distribution of forces, are shown in Figure 3-13 and 3-14.

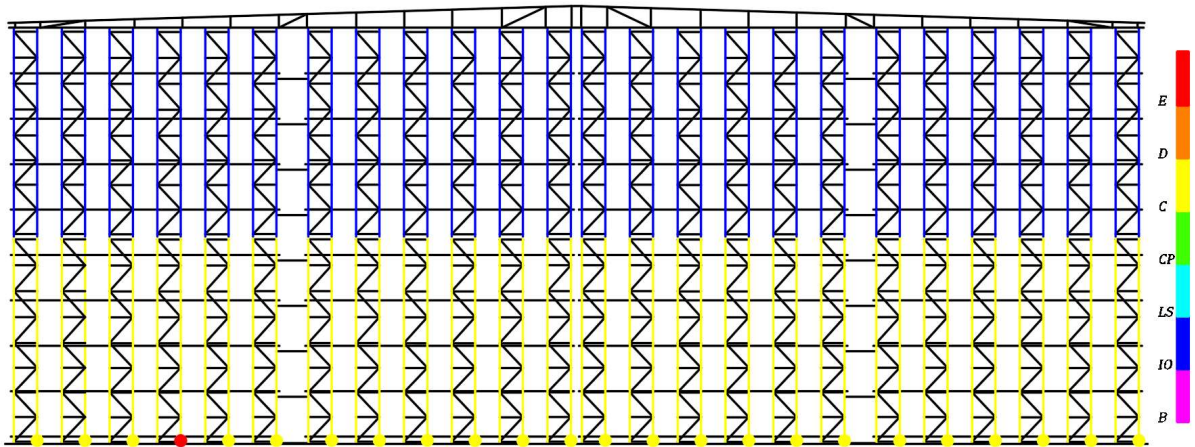


**Figure 3-13:** Achievement of different limit states in correspondence of the last step of the push-over analysis in the cross-aisle direction (about 42 cm of displacement)

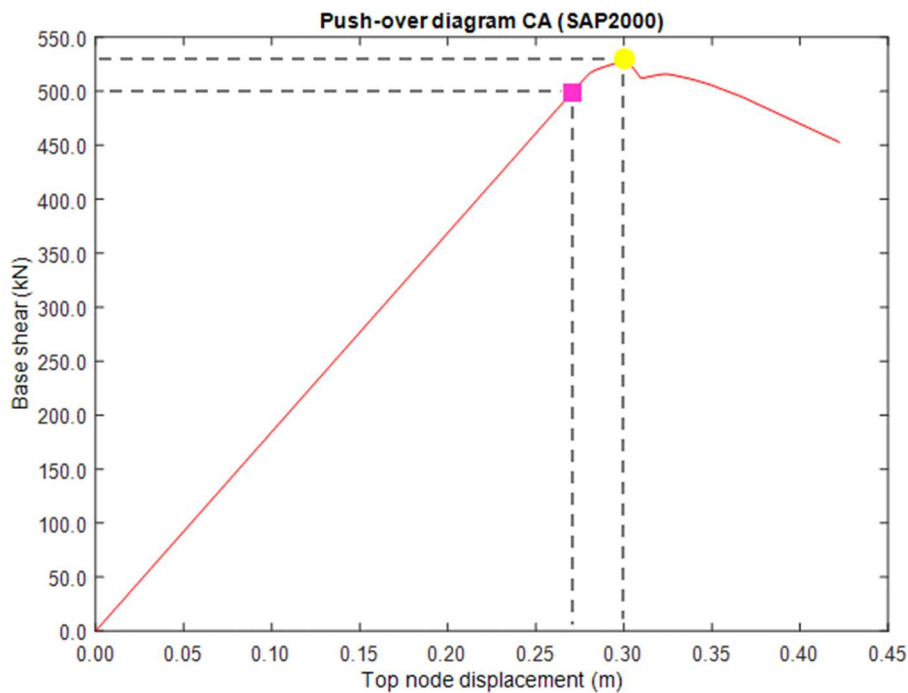


**Figure 3-14:** Push-over curve in the cross-aisle direction

In the down-aisle direction, the failure starts from one upright in the bracing tower, when it reaches the compression resistance, until also the other uprights reach the failure. The failure occurs in the uprights U2, being the uprights in the lower part over-strengthened compared to those that fail. The structure reaches the collapse before the contribution of the other elements (spine bracings and beams). After this “limit state” is exceeded, some elements (pallet beams and a spine bracing in tension) start cooperating while the push-over curve’s slope decreases until the curve has been stopped by the author when a consistent reduction of the resistance occur. The achievement of different limit states in correspondence of the last step, and the

capacity curve of the structure obtained applying the above distribution of forces, are shown in Figure 3-16 and 3-17.

It's important to note that most of the members belong to class 4, which means that they fail before showing their plastic behaviour due to the local buckling effect. Therefore, plasticity does not really exist for class 4 sections. In addition, the shape of the moment-rotation curves are similar for all classes, and so mentioning plastic hinges we referred to an inelastic behaviour [18].

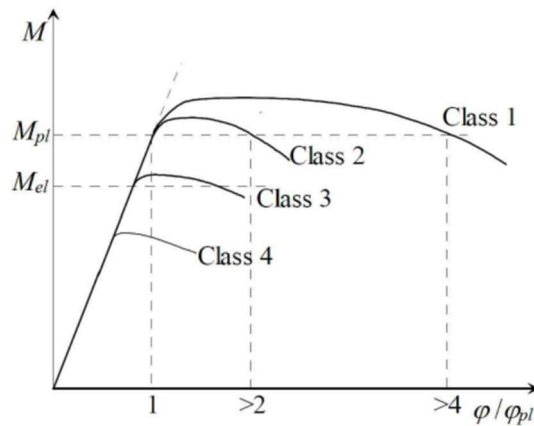


**Figure 3-15:** Moment-rotation curves for different classes of sections<sup>10</sup>

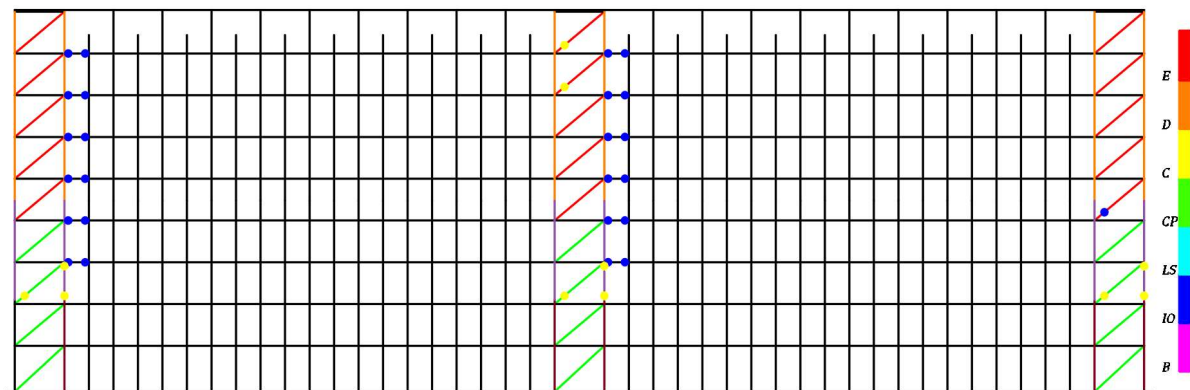


**Figure 3-16:** Achievement of different limit states in correspondence of the push-over analysis in the down-aisle direction (about 25 cm of displacement, when the push-over curve is stopped by the author)

<sup>10</sup> <https://www.researchgate.net>

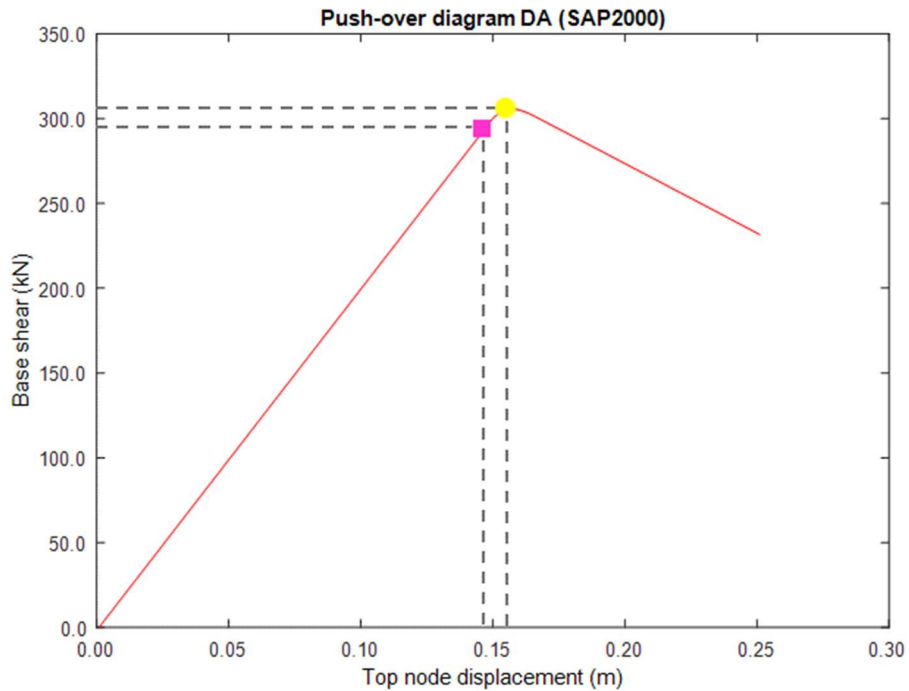


**Figure 3-17:** Push-over curve in the down-aisle direction

According to the results of the push-over analyses, the failure of the structure, in both directions, occurs before the elements designed to bear the horizontal action (i.e. bracing members in the cross-aisle direction and spine bracing in the down-aisle direction), can take it. In order to see the capacity that the other elements have to take the horizontal action, another push-over analysis in the down-aisle direction has been performed using stronger uprights, belonging to class 1; the results are showed in the following Figures. It can be noted that using stronger uprights, allows the pallet beams and spine bracings, to contribute bearing the horizontal actions as well (Figure 3-16), preventing an early fracture and showing a much bigger ductility of the structure (Figure 3-17). According to the capacity design method, this approach may be a solution to exploit the plastic reserves of the structure.

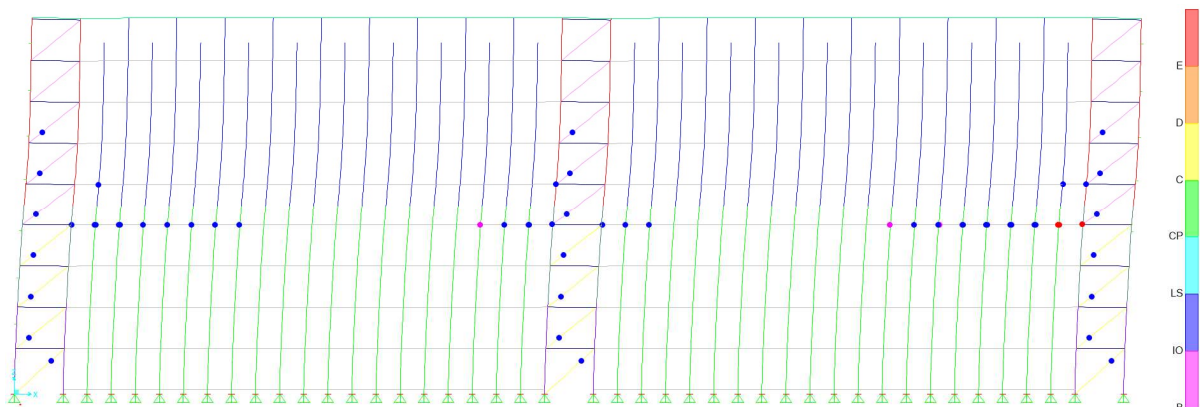


**Figure 3-18:** Achievement of different limit states in correspondence of the push-over analysis in the down-aisle direction using stronger uprights (about 56 cm of displacement)

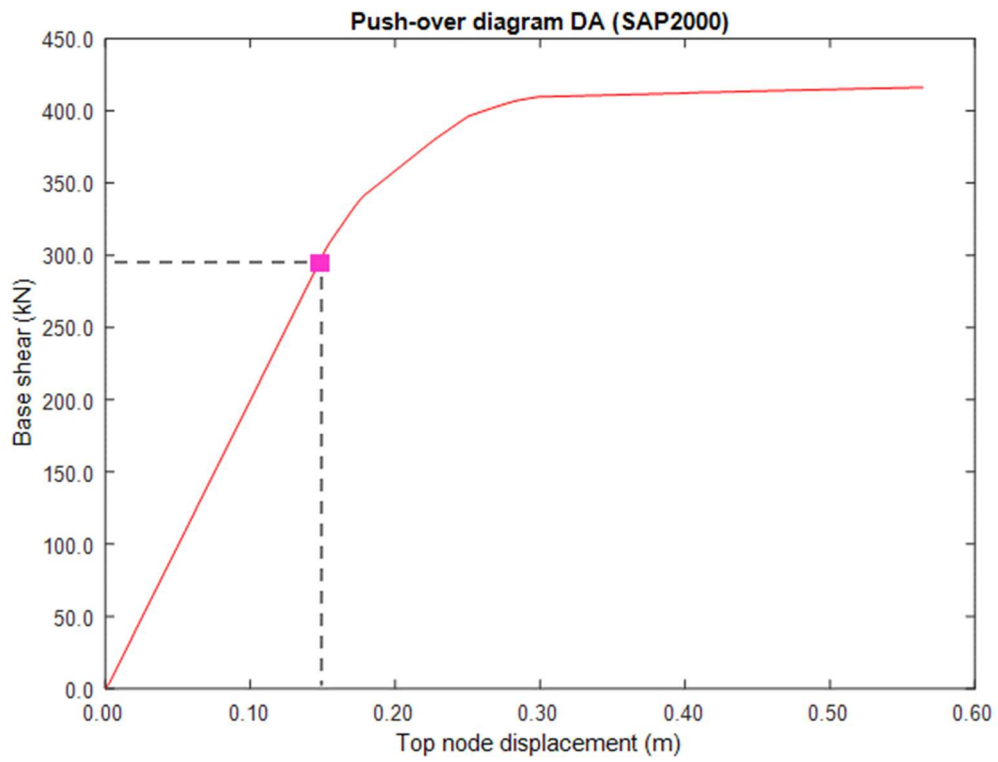


**Figure 3-19:** Push-over curve in the down-aisle direction using stronger uprights

## **4 Reduced-order Model**

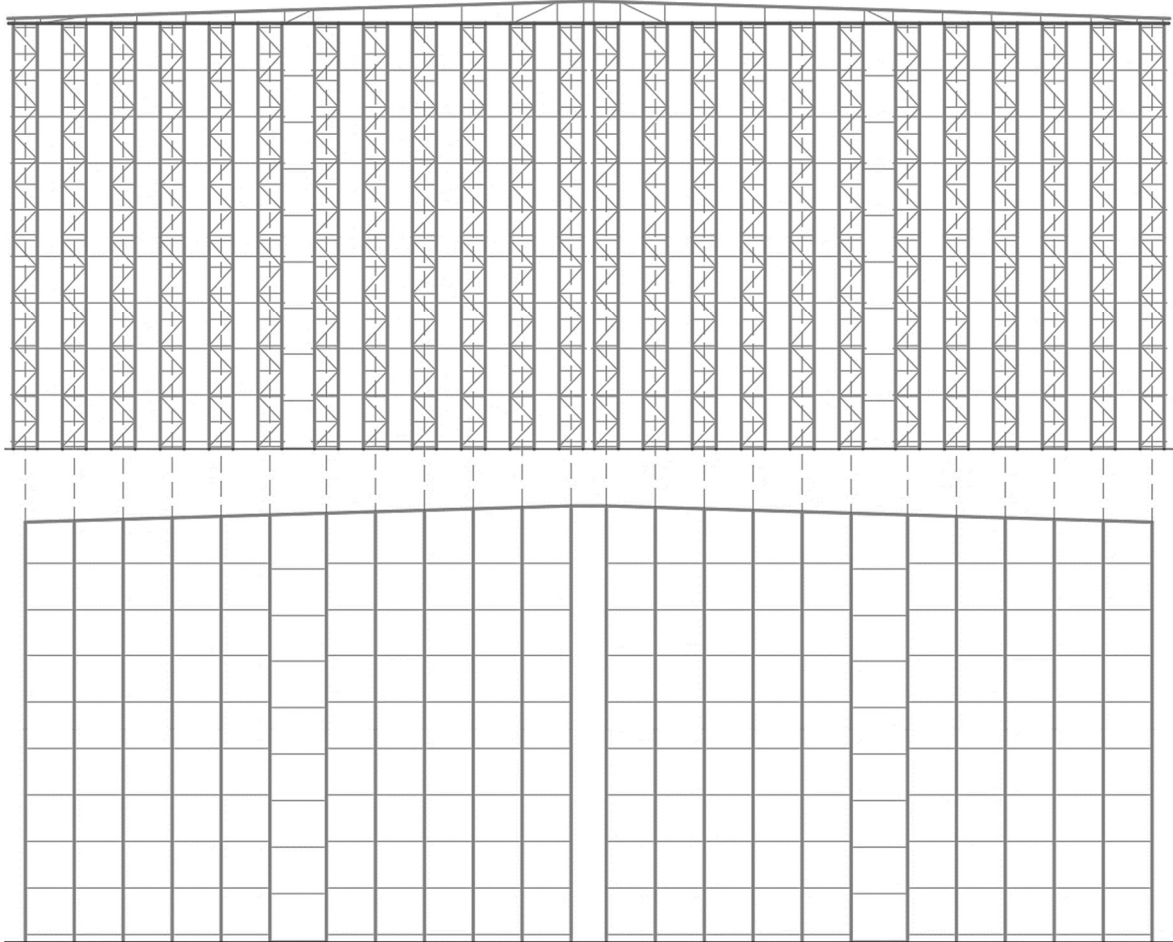


**Figure 4-1:** Scheme of the reduced model

The whole structure needs hundreds of thousands of elements and nodes to be modelled, and finite element analysis would be too computationally hard to be solved; the problems arises considering the nonlinear phenomena i.e. material and geometric nonlinearity, that may lead to prohibitive analysis costs in terms of time and CPU or even convergence and stability problems [1]. This chapter regards the development and the analysis of an “equivalent” model computationally simpler than the “detailed” one where the corresponding behaviour must fit the behaviour of the detailed model. The idea was to reduce the number of elements of the detailed model by substituting the complex elements with simple beams, schematically shown in Figure 4-1, obviously translating the element’s properties of the detailed model reaching a considerable reduction in terms of degrees of freedom; that is the meaning of the name reduced-order model. The best reduction can be achieved in the cross-aisle direction, substituting the upright frames and the roof truss with equivalent beams, where it’s important to take into account the contribution of the bracing members in order to consider the shear deformation of the braced

uprights. For this reason, before performing the analyses of the reduced-order model in the finite element software Sap2000, some notes about the Bernoulli and Timoshenko beam theory have been done and the research studies of the PhD student Dimitrios Tsarpalis within his Master Thesis "*Analysis of pallet racking systems with equivalent beam elements*" [1] was useful for the scope.

#### **4.1 Reminders about Timoshenko beam element's properties and matrices**

To assess the behaviour of a structure, it may be necessary to solve higher-order mathematical models that include more complex effects leading to an increasingly more costly solution. Even so, we cannot expect any more information in the prediction of the physical phenomena than the information contained in the mathematical model [20]. However, a structure made of simpler beams can give satisfying results with less computational costs if it is well modelled. Considering that, a beam structure, may be analysed using the Bernoulli beam theory and the Timoshenko beam theory as well in order to take into account the shear deformation of the beams, and in each case nonlinear effects may be included.

The finite element method is used to approximate a continuum as an assemblage of discrete elements, beam and truss elements, that are interconnected at  $N$  structural joints named nodes and pertaining to the elements. Depending on the dimensions of the problem (1D, 2D, 3D) and the assumptions made for the displacements (rotations, large displacements, plane strain etc.), and therefore, on the number of degrees of freedom of the system, the deformed shape of the body may differ a lot from the initial configuration and thus equilibrium must be established using higher order theories. However, in many practical problems of civil engineering the displacements are infinitesimally small and the equilibrium of the body can be established with respect to its unloaded configuration [20]. That is why the strains corresponding to the "theory of small displacements" are often called "engineering strains". In contrast to the engineering strains, Green-Lagrange strains are used when the effects of large displacements are examined. Solving the differential equations of equilibrium, when appropriate boundary conditions are defined, the three requirements, namely the stress equilibrium, the compatibility, and the constitutive requirements, are evocated to evaluate the element displacements, the element stresses, and the stiffness matrices. For the derivation of these matrices some references used by the author are suggested to take into account for greater details (see references [20], [21], [22], [23], [24], [25]).

### 4.1.1 Stiffness Matrices of Euler-Bernoulli Beam Element

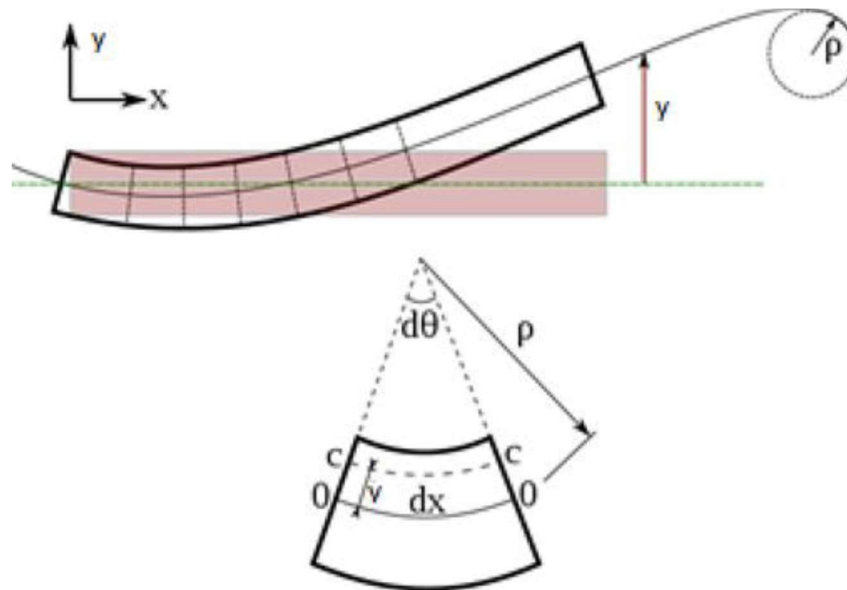


**Figure 4-2:** In the Euler-Bernoulli theory the cross section remain perpendicular to the neutral axis

For the derivation of the stress-strain relation for the Euler-Bernoulli beam element we assume that each cross-section of the beam remains plane and normal to the neutral axis (Figure 4-2); in such beams the effects of shear deformation can be neglected.

Using Green-Lagrange strains instead of “engineering strains”, we can get the following expression for the full elastic stiffness matrix of the Euler-Bernoulli beam elements that takes into account these geometric effects:

$$\overline{\mathbf{K}}_{tot} = \overline{\mathbf{K}}_e + \frac{N}{L} \overline{\mathbf{K}}_g \quad \text{Eq. (4.1)}$$

where:

$\overline{\mathbf{K}}_e$  is the elastic stiffness matrix;

$\overline{\mathbf{K}}_g$  is the geometric matrix;

$\overline{\mathbf{K}}_{tot}$  is the total stiffness matrix [24];

and N is the axial force.

For prismatic homogeneous isotropic beams in three dimensions (6 degrees of freedom at each node), the element stiffness matrices are:

$$\overline{K}_e = \begin{bmatrix} \frac{EA}{L} & 0 & 0 & -\frac{EA}{L} & 0 & 0 \\ 0 & \frac{12EI}{L^3} & \frac{6EI}{L^2} & 0 & -\frac{12EI}{L^3} & \frac{6EI}{L^2} \\ 0 & \frac{6EI}{L^2} & \frac{4EI}{L} & 0 & -\frac{6EI}{L^2} & \frac{2EI}{L} \\ -\frac{EA}{L} & 0 & 0 & \frac{EA}{L} & 0 & 0 \\ 0 & -\frac{12EI}{L^3} & -\frac{6EI}{L^2} & 0 & \frac{12EI}{L^3} & -\frac{6EI}{L^2} \\ 0 & \frac{6EI}{L^2} & \frac{2EI}{L} & 0 & -\frac{6EI}{L^2} & \frac{4EI}{L} \end{bmatrix} \quad \text{Eq. (4.2)}$$

$$\overline{K}_g = \begin{bmatrix} 0 & 0 & 0 & 0 & 0 & 0 \\ 0 & \frac{6}{5} & \frac{L}{10} & 0 & -\frac{6}{5} & \frac{L}{10} \\ 0 & \frac{L}{10} & \frac{2L^2}{15} & 0 & -\frac{L}{10} & -\frac{L^2}{30} \\ 0 & 0 & 0 & 0 & 0 & 0 \\ 0 & -\frac{6}{5} & -\frac{L}{10} & 0 & \frac{6}{5} & -\frac{L}{10} \\ 0 & \frac{L}{10} & -\frac{L^2}{30} & 0 & -\frac{L}{10} & -\frac{2L^2}{15} \end{bmatrix} \quad \text{Eq. (4.3)}$$

#### 4.1.2 Stiffness Matrices of Timoshenko Beam Elements

In contrast to the Euler-Bernoulli beam theory, the Timoshenko beam theory includes shear deformation. Therefore, considering again the geometry of a deformed beam, cross-sections may not remain perpendicular to the neutral axis after deformation. The transverse deformation of a beam with shear and bending strains may be separated into a portion related to shear deformation and a portion related to bending deformation as showed in Figure 4-3.

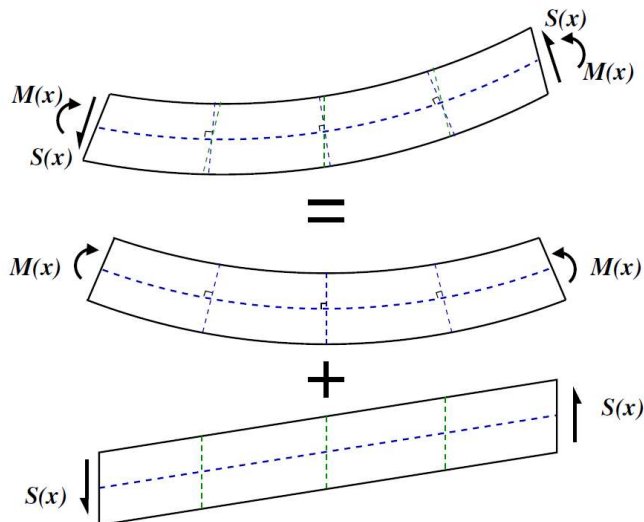


**Figure 4-3:** Rotation of cross-sections in a Timoshenko beam element. The bending and shear deformations are related to bending moments and shear forces, respectively

For prismatic homogeneous isotropic beams in three dimensions (6 degrees of freedom at each node), the element stiffness matrices are:

$$\overline{\mathbf{K}}_e = \begin{bmatrix} \frac{EA}{L} & 0 & 0 & -\frac{EA}{L} & 0 & 0 \\ 0 & \frac{12 EI}{1+\Phi L^3} & \frac{6 EI}{1+\Phi L^2} & 0 & -\frac{12 EI}{1+\Phi L^3} & \frac{6 EI}{1+\Phi L^2} \\ 0 & \frac{6 EI}{1+\Phi L^2} & \frac{4+\Phi EI}{1+\Phi L} & 0 & -\frac{6 EI}{1+\Phi L^2} & \frac{2-\Phi EI}{1+\Phi L} \\ -\frac{EA}{L} & 0 & 0 & \frac{EA}{L} & 0 & 0 \\ 0 & -\frac{12 EI}{1+\Phi L^3} & -\frac{6 EI}{1+\Phi L^2} & 0 & \frac{12 EI}{1+\Phi L^3} & -\frac{6 EI}{1+\Phi L^2} \\ 0 & \frac{6 EI}{1+\Phi L^2} & \frac{2-\Phi EI}{1+\Phi L} & 0 & -\frac{6 EI}{1+\Phi L^2} & \frac{4+\Phi EI}{1+\Phi L} \end{bmatrix} \quad \text{Eq. (4.4)}$$

$$\overline{\mathbf{K}}_g = \begin{bmatrix} 0 & 0 & 0 & 0 & 0 & 0 \\ 0 & \frac{6/5+2\Phi+\Phi^2}{(1+\Phi)^2} & \frac{L/10}{(1+\Phi)^2} & 0 & \frac{-6/5-2\Phi-\Phi^2}{(1+\Phi)^2} & \frac{L/10}{(1+\Phi)^2} \\ 0 & \frac{L/10}{(1+\Phi)^2} & \frac{2L^2/15+L^2\Phi/6+L^2\Phi^2/12}{(1+\Phi)^2} & 0 & -\frac{L/10}{(1+\Phi)^2} & \frac{-L^2/30-L^2\Phi/6-L^2\Phi^2/12}{(1+\Phi)^2} \\ 0 & 0 & 0 & 0 & 0 & 0 \\ 0 & \frac{-6/5-2\Phi-\Phi^2}{(1+\Phi)^2} & -\frac{L/10}{(1+\Phi)^2} & 0 & \frac{6/5+2\Phi+\Phi^2}{(1+\Phi)^2} & -\frac{L/10}{(1+\Phi)^2} \\ 0 & \frac{L/10}{(1+\Phi)^2} & \frac{-L^2/30-L^2\Phi/6-L^2\Phi^2/12}{(1+\Phi)^2} & 0 & -\frac{L/10}{(1+\Phi)^2} & \frac{2L^2/15+L^2\Phi/6+L^2\Phi^2/12}{(1+\Phi)^2} \end{bmatrix} \quad \text{Eq. (4.5)}$$

The term  $\Phi$  is the ratio between the bending stiffness and the shear stiffness and gives the relative importance of the shear deformations to the bending deformations:

$$\Phi = \frac{12EI}{GA_{eff}L^2} \quad \text{Eq. (4.6)}$$

where:

$A_{eff}$  is the shear area.

If the shear stiffness is very large, shear deformation is negligible.

## 4.2 Properties of equivalent beams

In order to evaluate the properties of the equivalent beams it is important to note that the section of an upright frame does not remain perpendicular to the neutral axis (Figure 4-4), so the Timoshenko beam theory must be used for the definition of the stiffness matrix of the equivalent upright. The following parameters should be evaluated to define the stiffness matrix of a 2D prismatic homogeneous isotropic beam element:

- E: Young's modulus;
- G: shear modulus;
- L: length;
- A: cross-section area;
- I: moment of inertia;
- $A_{eff}$ : shear area.

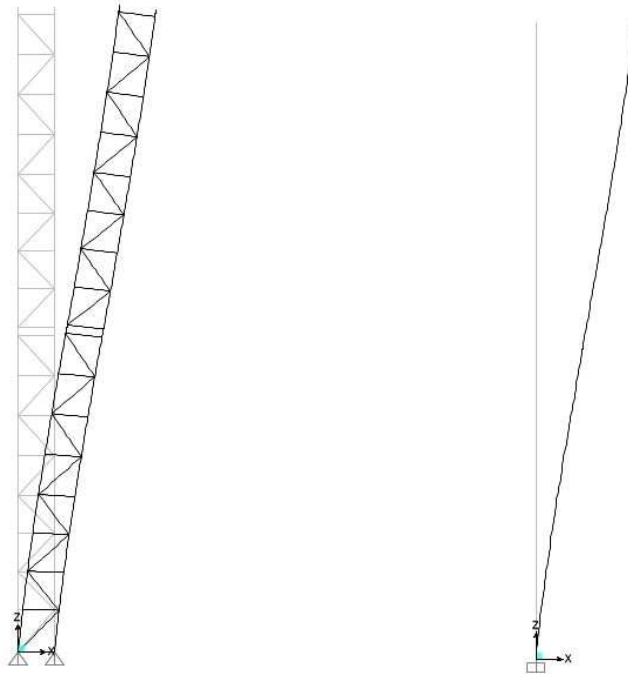


**Figure 4-4:** In built-up columns (left), "cross sections" do not remain perpendicular to the neutral axis. This effect must be considered when assigning element's properties to the equivalent upright (right)

### 4.2.1 Material properties

No changes occur in the definition of these properties because the same materials are used to perform the reduced-order model.

- $E_{eq} = E$  Eq. (4.7)

- $G_{eq} = G$  Eq. (4.8)

### 4.2.2 Frame length

The upright frames have been transformed in single frames placed in correspondence of the central axis of each upright frame. Therefore, the length of elements such us z-section pallet profiles and supporting shuttle beams became longer than their length in the detailed model (see Figure 4-5). Also, the roof truss has been translated into a simple frame placed in correspondence of the average height of each roof truss verticals and each single upright became longer as well to be connected directly with the equivalent roof frames.

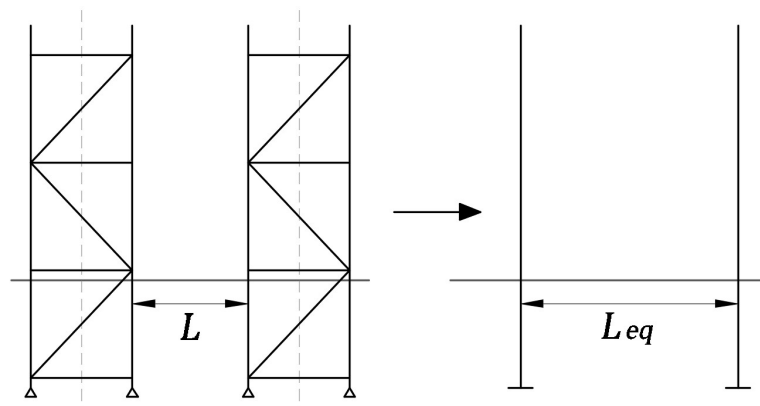


**Figure 4-5:** example of how the length of a z-pallet profile change in the reduced-order model

### 4.2.3 Cross-section Area

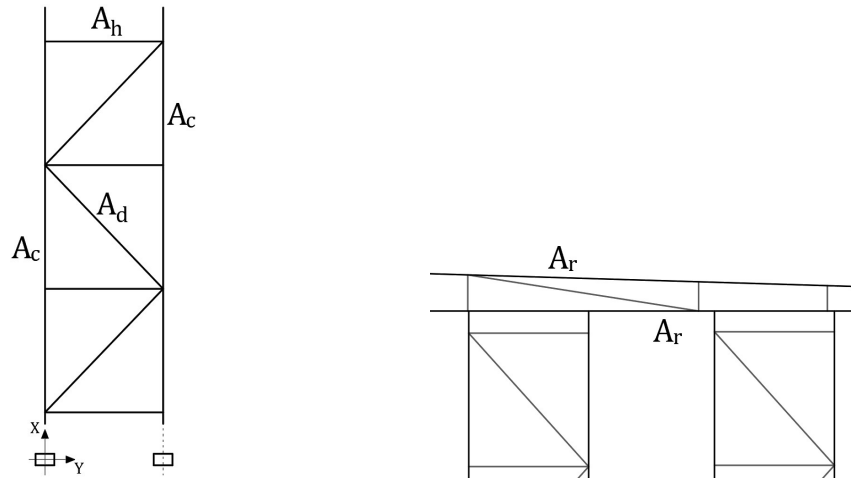


**Figure 4-6:** Scheme for the evaluation of  $A_{eq}$ . **a)**  $A_{eq}$  of an upright frame, **b)**  $A_{eq}$  of the equivalent roof

The cross-section area of an equivalent frame is equal to the sum of the area of each member, which gives the same contribution. For example, in the case study, the area of each equivalent upright is the sum of the area of two braced uprights while the roof has been evaluated as the sum of the area of the upper and top chords, using the following equation:

$$A_{eq} = \sum_{i=1}^N A_i \quad \text{Eq. (4.9)}$$

where:

- $A_i$  is the cross-section area of each member
- $N$  is the total number of members.

The equivalent area for the upright frames is  $A_{eq} = 2A_c$  and for the equivalent roof  $A_{eq} = 2A_r$  as shown in Figure 4-6.

### 4.2.4 Moment of Inertia

Defining  $h_0$  the width of an upright frame, and considering that the equivalent upright takes place at a distance equal to  $h_0/2$  from each upright, the equivalent moment of inertia has been evaluated using the following equation:

$$I_{eq} = A_c \left(-\frac{h_0}{2}\right)^2 + A_c \left(\frac{h_0}{2}\right)^2 = A_c \frac{h_0^2}{2} \quad \text{Eq. (4.10)}$$

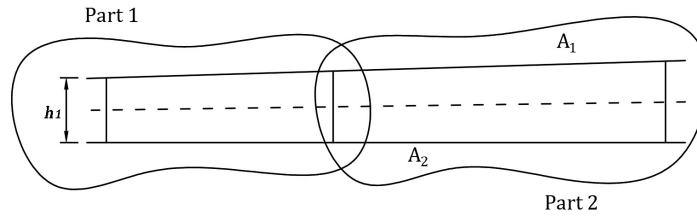


**Figure 4-7:** Scheme used to have a more accurate evaluation of the equivalent roof

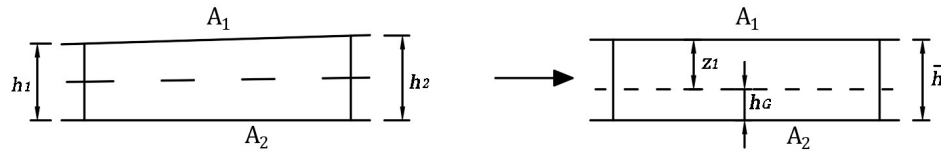


**Figure 4-8:** Evaluation of the average height and position of the centre of gravity

To evaluate the moment of inertia of the equivalent roof, the same equation could be used as long as we consider the slope of the top chord (the upper chords are built on a slant and for this reason the distance between the roof chords is variable from the border to the middle in the cross-aisle direction). In order to be more accurate, the idea was to divide the roof truss into more parts, each one defined by two consecutive “roof truss verticals” (schematically shown in Figure 4-7), to evaluate an average height ( $\bar{h}$ ) for each part in order to translate the inclined “top chord” into a plane one (Figure 4-8), and to finally find the height of the centre of gravity  $h_G$  with the following equation:

$$h_G = \frac{A_1 \bar{h}}{A_1 + A_2} \quad \text{Eq. (4.11)}$$

The  $h_G$  could be used to define the moment of inertia of each single frame of the equivalent roof using the following equation:

$$I_{eq} = 2I_c + A_2(-h_G)^2 + A_1(z_1)^2 \quad \text{Eq. (4.12)}$$

#### 4.2.5 Shear Area

The shear area is usually neglected for beams due to its irrelevant contribution. However, for the upright frames the section does not remain perpendicular to the neutral axis, so shear contribution ( $A_{eff}$ ) must be considered, otherwise the equivalent members may be 10 to 30 % stiffer than the detailed model uprights [1]. However, the assessment of the shear area depends on the geometry and on the type of upright frames. In the case study, a “K-braced frame” configuration has been used and the shear deformation depends only on the contribution of the

diagonals, while the horizontal frames remain unstressed. The  $A_{eff}$  has been evaluated with the following equation:

$$A_{eff} = \frac{EA_d h_0^2 a}{G d^3} \quad \text{Eq. (4.13)}$$

Also, it must be considered that the value of  $A_d$  is strongly dependent on the axial spring used to take into account the shear stiffness (see the paragraph 2.2.4.1). For the evaluation of the diagonals area, the procedure below has been followed. Considering the scheme of the diagonal's axial stiffness shown in Figure 4-9, the  $K_{tot}$  has been derived from the following equation:

$$\frac{1}{K_{tot}} = \frac{1}{K_d} + \frac{1}{K_s} \quad \text{Eq. (4.14)}$$

where

$$K_d \text{ is the stiffness of the diagonals equal to } \frac{EA_d}{L}; \quad \text{Eq. (4.15)}$$

$K_s$  is the axial spring's stiffness evaluated in paragraph 2.2.4.1;

$$K_{tot} \text{ is the effective stiffness of the diagonal equal to } \frac{EA_d^I}{L}. \quad \text{Eq. (4.16)}$$

So, the value of  $A_{eff}$  is given by the formula:

$$A_d^I = \frac{EK_{tot}}{L} \quad \text{Eq. (4.17)}$$

In Table 4-1, the properties of the equivalent frames are detailed, and the position where they are located is shown in Figure 4-10.

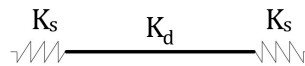


**Figure 4-9:** Scheme of the real stiffness of diagonals

**Table 4-1:** Section properties of equivalent beams

Equivalent Frame	$A_{g,eq}$ [mm <sup>2</sup> ]	$I_{y,eq}$ [mm <sup>4</sup> ]	$I_{z,eq}$ [mm <sup>4</sup> ]	$A_{eff,y}$ [mm <sup>2</sup> ]	$A_{eff,z}$ [mm <sup>2</sup> ]
U 1	6886	3,14E+09	1,81E+07	2,71E+01	5,97E+03
U 2	3440	1,57E+09	7,86E+06	2,87E+01	2,91E+03
U 3	2140	9,75E+08	4,98E+06	2,87E+01	1,43E+03
U 4	2580	1,18E+09	5,97E+06	2,71E+01	2,26E+03
U 5	1720	7,84E+08	4,02E+06	2,71E+01	0,00E+00
R1	2320	1,83E+06	6,31E+07	2320	2320
R2	2320	1,83E+06	9,37E+07	2320	2320
R3	2320	1,83E+06	1,31E+08	2320	2320
R4	2320	1,83E+06	1,74E+08	2320	2320
R5	2320	1,83E+06	2,25E+08	2320	2320
R6	2320	1,83E+06	2,86E+08	2320	2320
R7	2320	1,83E+06	3,55E+08	2320	2320
R8	2320	1,83E+06	4,26E+08	2320	2320
R9	2320	1,83E+06	5,03E+08	2320	2320
R10	2320	1,83E+06	5,87E+08	2320	2320
R11	2320	1,83E+06	6,78E+08	2320	2320
R12	2320	1,83E+06	7,25E+08	2320	2320

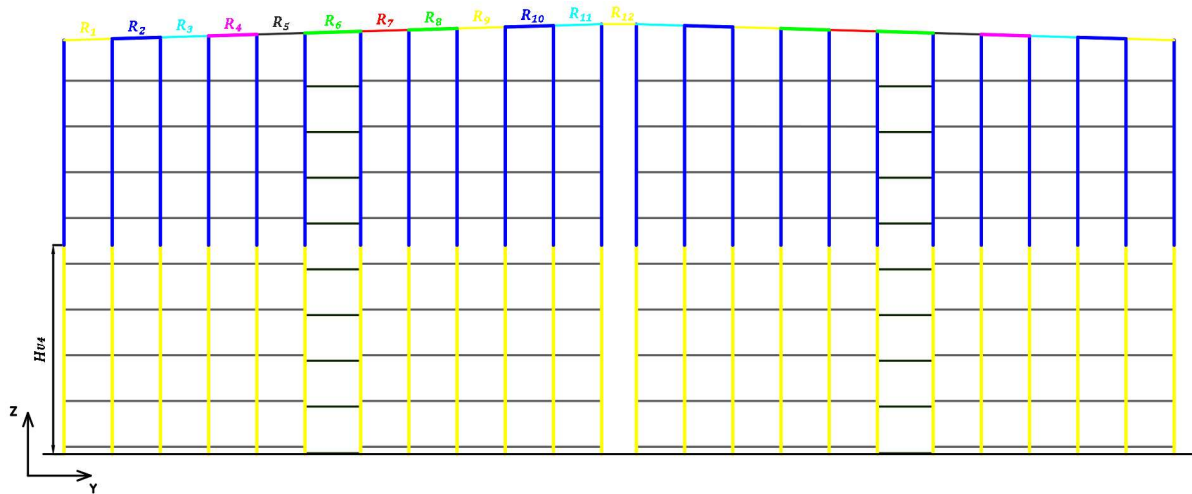


**Figure 4-10:** Location of each section in Cross-aisle direction (Reduced-order model)

### 4.3 2D Model Finite Element Analysis

After the definition of the properties of the reduced-order model, we must evaluate the behaviour of the structure in the elastic and anelastic region, to compare the results with the detailed model in cross-aisle direction, in order to check if the reduced-order model is well calibrated. As we already mentioned, no gain in terms of reduction of the elements number and of computational analysis as well, could be reached performing the model also in the down-aisle direction, because the number of elements and nodes remains exactly the same; we just need to

double the down-aisle section and the relative properties (see Figure 5-1, to a better compression). This is the reason why only in the cross-aisle direction a modal and a push-over analysis have been performed. Performing the analyses, the same parameters considered for the detailed model, unless otherwise specified, have been set on SAP2000 for the reduced-order model. A speech deserves the definition of the geometric properties of the reduced-order model and the way the loads have been applied. In order to provide for the lack of the bracing members, avoiding therefore a mechanism of the structure, each equivalent frame must be fixed to the floor, in the reduced-order model. At the top of the uprights, the equivalent frames are fixed to the roof as well. Concerning the loads considered for the analysis in the model, the following loads have been applied as well as in the detailed model:

▪ **Dead loads:**

The “dead loads” of the elements drawn in the model, are automatically taken into account by the finite element software, it is worthy to note the importance of adding the mass of all of the elements that are not represented in the reduced-order model, like the bracing members of each upright frames. The procedure followed in order to take into account the contribution of these elements consisted of applying concentrated masses in correspondence to the bracing-to-upright connection level, schematically shown in Figure 4-11

where:

- $M_d$  is the mass of each diagonal given by  $M_d = \gamma \cdot A_d d$  Eq. (4-18)
- $m_d$  is half of the diagonal’s mass  $M_d$  applied in correspondence of the end of each bracing member.

with:

- $\gamma$  is the weight per unit volume
- $d$  is the length of the diagonal
- $A_d$  the cross-section area of diagonals

The same procedure has been followed to consider the dead load for the upright horizontals, the diagonal and vertical members of the roof truss as well and of all the members which are not explicitly drawn in the reduced-order model.

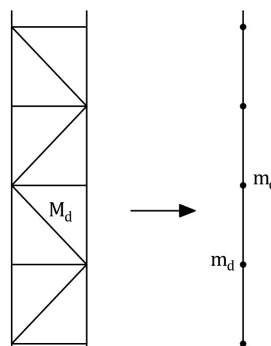


**Figure 4-11:** Schematic figure to show how the dead loads have been taken into account in the reduced-order model

▪ **Pallet loads:**

In order to take into account the contribution of the Pallet loads, considered uniformly distributed along the Z-pallet profile in the detailed model (see §2.2.5), in the reduced-order model, concentrated loads have been applied along the “equivalent” uprights in correspondence to the connection between the uprights with the Z-pallet profiles, considering the area of influence of the pallet loads competing on each upright (see Figure 4-12).

▪ **Additional masses G2:**

The contribution of the additional masses has been taken into account as well, as we did in the detailed model applying a distributed load along each element of the equivalent roof.

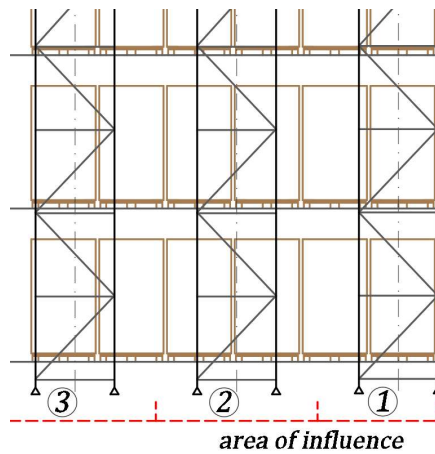


**Figure 4-12:** Area of influence of the pallet loads competing on each upright frame

### 4.3.1 Modal Analysis

After all the properties concerning the reduced-order model have been given, a linear dynamic analysis, is executed in order to evaluate the elastic behaviour and the free vibration modes of the case study, and to compare the response with the detailed model as well. The same condition that we applied to the detailed model, has been considered for the reduced-order model as well, i.e.:

- the analysis starts from an unstressed condition;
- a maximum and minimum number of vibration modes equal to 12 has been taken into account by default;
- the mass for the evaluation of the inertia to be considered in the modal analysis, has been evaluated as defined in paragraph 3.2.1;
- a multiplier of 0,8 has been assigned to the pallet loads in order to consider the possibility that in serviceability condition not all of the shelves would be filled.

In the table below, the periods of the first free vibration modes, of the two models, with the same modal shapes, are shown, and the results are satisfying, having differences less than 10% (Table 4-2). The test case analyzed demonstrates that the reduced-order model is well calibrated in linear analysis. In Figures 4-13, the modal shapes of the two models with the relative periods are also compared. It is worth noting that a reduction of 55% of the degrees of freedom can be gained with the reduced-order model. One step further was to include nonlinear properties in order to achieve adequate accuracy for push-over analysis.

**Table 4-2:** Comparison of modal periods between the detailed and the reduced-order model

Mode	Detailed model - T (s)	Reduced-order model - T (s)	Differ. %
1	1,703	1,706	0,15%
2	0,843	0,866	2,83%
3	0,565	0,573	1,47%
4	0,409	0,425	3,92%
5	0,304	0,319	4,99%
6	0,263	0,283	7,71%
7	0,215	0,231	7,42%
8	0,194	0,213	9,71%

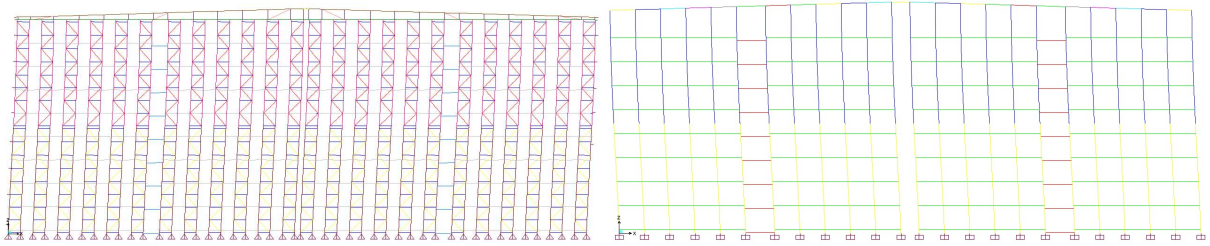
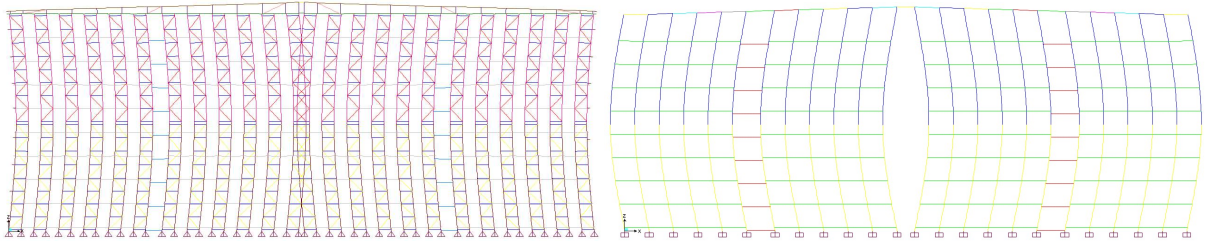
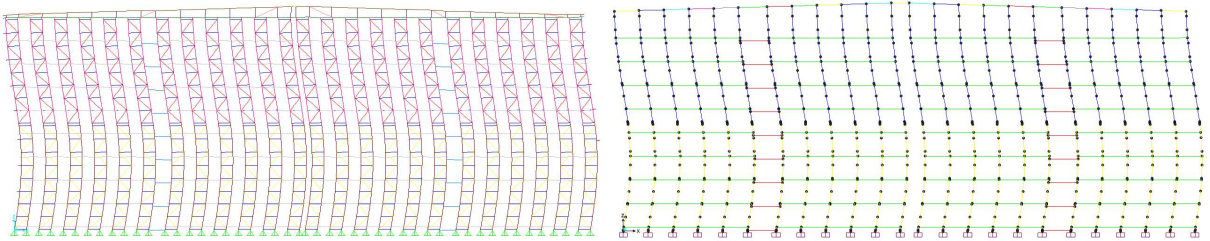


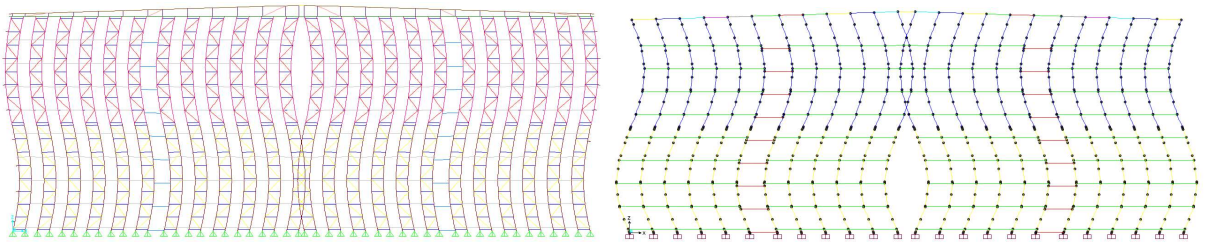
**Figure 4-13 (a):** 1<sup>st</sup> Eigenmode (translational) of 2D Detailed model ( $T_{1,1}=1.703$  sec) and 2D Reduced-order model ( $T_{1,2}=1.706$  sec)



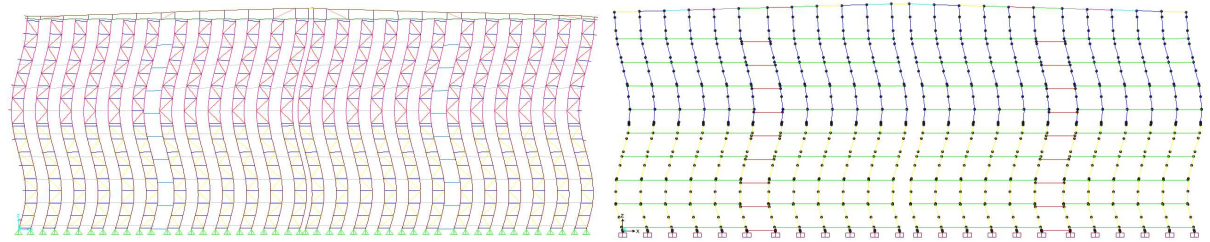
**(b):** 2<sup>nd</sup> vibration mode (sine shape) of 2D Detailed Model ( $T_{2,1}=0.843$  sec) and Reduced-order Model ( $T_{2,2}=0.866$  sec)



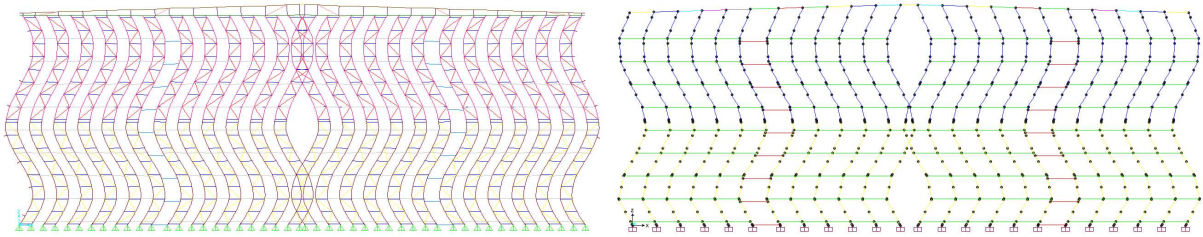
**(c):** 3<sup>rd</sup> vibration mode (sine shape) of 2D Detailed Model ( $T_{3,1}=0.565$  sec) and Reduced-order Model ( $T_{3,2}=0.573$  sec)



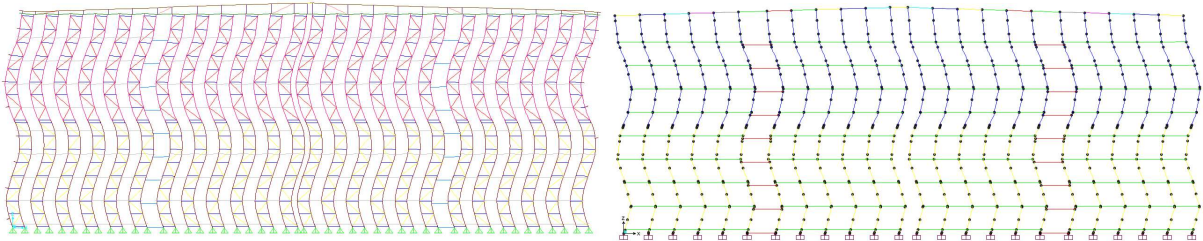
**(d):** 4<sup>th</sup> vibration mode (sine shape) of 2D Detailed Model ( $T_{4,1}=0.409$  sec) and Reduced-order Model ( $T_{4,2}=0.425$  sec)



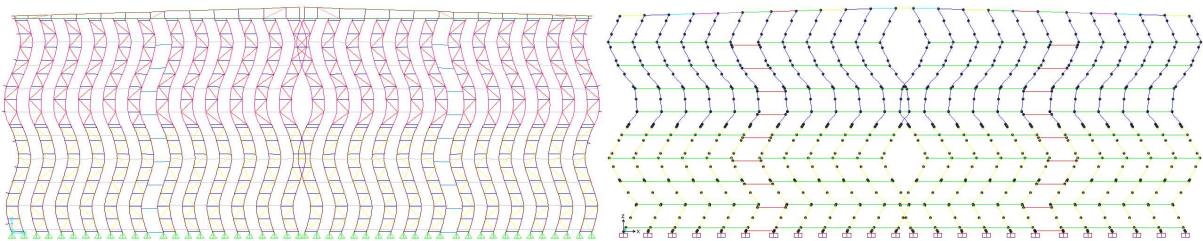
**(e):** 5<sup>th</sup> vibration mode (sine shape) of 2D Detailed Model ( $T_{5,1}=0.304$  sec) and Reduced-order Model ( $T_{5,2}=0.319$  sec)



**(f):** 6<sup>th</sup> vibration mode (sine shape) of 2D Detailed Model ( $T_{6,1}=0.263$  sec) and Reduced-order Model ( $T_{6,2}=0.283$  sec)



**(g):** 7<sup>th</sup> vibration mode (sine shape) of 2D Detailed Model ( $T_{7,1}=0.215$  sec) and Reduced-order Model ( $T_{7,2}=0.231$  sec)



**(h):** 8<sup>th</sup> vibration mode (sine shape) of 2D Detailed Model ( $T_{8,1}=0.194$  sec) and Reduced-order Model ( $T_{8,2}=0.213$  sec)

### 4.3.2 Reliability of the Reduced-order model

Before comparing the results of the push-over analysis, one more step was to evaluate the reliability of the reduced-order model in order to check its accuracy. The scope of this analysis was to ensure that managing a computationally simpler model, we are able to predict the response of a built-up column extremely accurately, i.e. stresses on the elements and their deformation capacity of the detailed model, having acceptable errors. In particular, the following analysis has been done. In order to do these evaluations, the behaviour under “gravity” loads and under the seismic action (defined in paragraph 2.2.5) has been considered. The errors, for each analysis are detailed below.

First of all, the differences concerning the displacements of the structure under horizontal actions has been checked. For the assessment of the displacements, the two models have been subjected to the seismic hazard and the differences have been evaluated on different levels, in correspondence to each diagonal bracings (see Figure 4-14 b); the results, quite satisfying, are reported in Table 4-3.

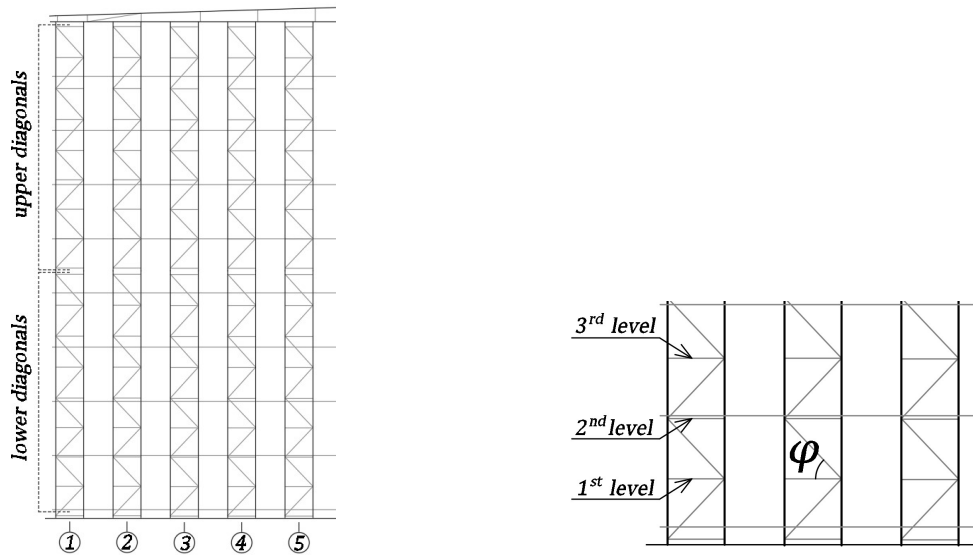


**Figure 4-14:** a) Lower and upper diagonals of the structure, b) Levels for the evaluation of the displacements

**Table 4-3:** Differences between the displacements of Detailed ( $\delta_D$ ) and Reduced-order model ( $\delta_{RO}$ ) concerning: a) absolute displacement, b) relative displacement

Total displacement				
Level	h [m]	$\delta_D$ [m]	$\delta_{RO}$ [m]	diff %
1 <sup>st</sup>	1,55	0,038	0,035	7%
2 <sup>nd</sup>	2,98	0,071	0,070	1%
3 <sup>rd</sup>	4,41	0,105	0,105	0%
4 <sup>th</sup>	5,83	0,139	0,141	1%
5 <sup>th</sup>	7,33	0,176	0,179	1%
6 <sup>th</sup>	8,83	0,213	0,216	2%
7 <sup>th</sup>	10,33	0,249	0,253	2%
8 <sup>th</sup>	11,83	0,286	0,289	1%
9 <sup>th</sup>	13,56	0,328	0,328	0%
10 <sup>th</sup>	14,98	0,359	0,359	0%
11 <sup>th</sup>	16,41	0,388	0,388	0%
12 <sup>th</sup>	17,83	0,414	0,414	0%
13 <sup>th</sup>	19,33	0,440	0,439	0%
14 <sup>th</sup>	20,83	0,461	0,460	0%
15 <sup>th</sup>	22,33	0,478	0,476	0%
16 <sup>th</sup>	23,83	0,492	0,490	0%

Relative displacement				
Level	h [m]	$\delta_D$ [m]	$\delta_{RO}$ [m]	diff %
1 <sup>st</sup>	1,55	0,038	0,035	7%
2 <sup>nd</sup>	2,98	0,033	0,035	6%
3 <sup>rd</sup>	4,41	0,034	0,035	2%
4 <sup>th</sup>	5,83	0,035	0,036	5%
5 <sup>th</sup>	7,33	0,037	0,037	2%
6 <sup>th</sup>	8,83	0,037	0,038	3%
7 <sup>th</sup>	10,33	0,036	0,037	2%
8 <sup>th</sup>	11,83	0,037	0,035	4%
9 <sup>th</sup>	13,56	0,042	0,040	5%
10 <sup>th</sup>	14,98	0,031	0,030	2%
11 <sup>th</sup>	16,41	0,029	0,030	1%
12 <sup>th</sup>	17,83	0,027	0,026	2%
13 <sup>th</sup>	19,33	0,025	0,025	1%
14 <sup>th</sup>	20,83	0,021	0,021	3%
15 <sup>th</sup>	22,33	0,017	0,017	4%
16 <sup>th</sup>	23,83	0,014	0,013	2%

The next evaluation was to estimate the stresses on the diagonal bracings (the horizontal bracings are mostly unstressed), starting from the shear force  $V_{eq,SAP}$  that each equivalent upright is subjected. The value of  $V_{eq,SAP}$  has been compared with  $N_{SAP}$ . In order to do this, the shear force of the equivalent uprights  $V_{eq,SAP}$  was measured directly from the reduced-order model in SAP and  $V_{eq}^*$  was evaluated from the detailed model with the following equation:

$$V_{eq}^* = N_{SAP} \cdot \cos \varphi \quad \text{Eq. (4.22)}$$

where:

$N_{SAP}$  is the axial forces measured on the diagonal bracings of the detailed model;

$\varphi$  is the angle of inclination of the diagonal bracings (see Figure 4-14 b).

The relative error has been estimated with the following relation:

$$diff. \% = \frac{V_{eq,SAP} - V^*_{eq}}{V^*_{eq}} \quad \text{Eq. (4.23)}$$

In the Table 4-4, the differences are shown and the results are quite satisfying. The errors concerning the highest diagonals (upper diagonals, see Figure 4-14 a) are much bigger than the other ones but stresses on them are so small that they can be ignored.

**Table 4-4:** Differences for the assessment of the axial forces on the diagonal bracings between the Detailed and the Reduced-order model

<b>1° lower diagonals</b>		<b>Upright 1</b>			<b>Upright 2</b>			<b>Upright 3</b>		
h [m]	cosφ	V <sub>eq,SAP</sub>	V* <sub>eq</sub>	N <sub>SAP</sub>	V <sub>eq,SAP</sub>	V* <sub>eq</sub>	N <sub>SAP</sub>	V <sub>eq,SAP</sub>	V* <sub>eq</sub>	N <sub>SAP</sub>
1,55	0,688	44,28	49,66	72,21	44,37	49,63	72,16	44,39	49,59	72,11
diff. %		10,84%			10,60%			10,49%		
<b>2° lower diagonals</b>		<b>Upright 1</b>			<b>Upright 2</b>			<b>Upright 3</b>		
h [m]	cosφ	V <sub>eq,SAP</sub>	V* <sub>eq</sub>	N <sub>SAP</sub>	V <sub>eq,SAP</sub>	V* <sub>eq</sub>	N <sub>SAP</sub>	V <sub>eq,SAP</sub>	V* <sub>eq</sub>	N <sub>SAP</sub>
2,98	0,688	44,23	43,51	63,27	44,32	43,84	63,75	44,34	43,90	63,83
diff. %		1,64%			1,08%			1,00%		
<b>3° lower diagonals</b>		<b>Upright 1</b>			<b>Upright 2</b>			<b>Upright 3</b>		
h [m]	cosφ	V <sub>eq,SAP</sub>	V* <sub>eq</sub>	N <sub>SAP</sub>	V <sub>eq,SAP</sub>	V* <sub>eq</sub>	N <sub>SAP</sub>	V <sub>eq,SAP</sub>	V* <sub>eq</sub>	N <sub>SAP</sub>
4,405	0,688	39,72	40,46	58,83	39,96	40,71	59,19	40,00	40,70	59,18
diff. %		1,83%			1,84%			1,72%		
<b>4° lower diagonals</b>		<b>Upright 1</b>			<b>Upright 2</b>			<b>Upright 3</b>		
h [m]	cosφ	V <sub>eq,SAP</sub>	V* <sub>eq</sub>	N <sub>SAP</sub>	V <sub>eq,SAP</sub>	V* <sub>eq</sub>	N <sub>SAP</sub>	V <sub>eq,SAP</sub>	V* <sub>eq</sub>	N <sub>SAP</sub>
5,83	0,688	39,62	38,21	55,56	39,86	38,76	56,35	39,91	38,75	56,34
diff. %		3,69%			2,85%			3,00%		
<b>5° lower diagonals</b>		<b>Upright 1</b>			<b>Upright 2</b>			<b>Upright 3</b>		
h [m]	cosφ	V <sub>eq,SAP</sub>	V* <sub>eq</sub>	N <sub>SAP</sub>	V <sub>eq,SAP</sub>	V* <sub>eq</sub>	N <sub>SAP</sub>	V <sub>eq,SAP</sub>	V* <sub>eq</sub>	N <sub>SAP</sub>
7,33	0,669	35,28	35,46	53,01	35,73	36,02	53,84	35,83	35,98	53,79
diff. %		0,51%			0,80%			0,43%		
<b>6° lower diagonals</b>		<b>Upright 1</b>			<b>Upright 2</b>			<b>Upright 3</b>		
h [m]	cosφ	V <sub>eq,SAP</sub>	V* <sub>eq</sub>	N <sub>SAP</sub>	V <sub>eq,SAP</sub>	V* <sub>eq</sub>	N <sub>SAP</sub>	V <sub>eq,SAP</sub>	V* <sub>eq</sub>	N <sub>SAP</sub>
8,83	0,669	33,01	32,74	48,94	33,59	33,74	50,44	35,72	33,72	50,40
diff. %		0,81%			0,47%			5,94%		
<b>7° lower diagonals</b>		<b>Upright 1</b>			<b>Upright 2</b>			<b>Upright 3</b>		
h [m]	cosφ	V <sub>eq,SAP</sub>	V* <sub>eq</sub>	N <sub>SAP</sub>	V <sub>eq,SAP</sub>	V* <sub>eq</sub>	N <sub>SAP</sub>	V <sub>eq,SAP</sub>	V* <sub>eq</sub>	N <sub>SAP</sub>
10,33	0,669	30,75	30,63	45,79	31,47	31,68	47,36	31,62	31,64	47,29
diff. %		0,38%			0,67%			0,05%		
<b>8° lower diagonals</b>		<b>Upright 1</b>			<b>Upright 2</b>			<b>Upright 3</b>		
h [m]	cosφ	V <sub>eq,SAP</sub>	V* <sub>eq</sub>	N <sub>SAP</sub>	V <sub>eq,SAP</sub>	V* <sub>eq</sub>	N <sub>SAP</sub>	V <sub>eq,SAP</sub>	V* <sub>eq</sub>	N <sub>SAP</sub>
11,83	0,669	30,66	30,49	45,58	31,37	31,86	47,63	31,52	31,96	47,78
diff. %		0,55%			1,55%			1,39%		

1°_upper diagonals		Upright 1			Upright 2			Upright 3		
h [m]	cosφ	V <sub>eq,SAP</sub>	V* <sub>eq</sub>	N <sub>SAP</sub>	V <sub>eq,SAP</sub>	V* <sub>eq</sub>	N <sub>SAP</sub>	V <sub>eq,SAP</sub>	V* <sub>eq</sub>	N <sub>SAP</sub>
13,56	0,688	26,38	28,32	41,18	27,43	29,11	42,33	27,65	29,75	43,25
diff. %		6,86%			5,78%			7,04%		
2°_upper diagonals		Upright 1			Upright 2			Upright 3		
h [m]	cosφ	V <sub>eq,SAP</sub>	V* <sub>eq</sub>	N <sub>SAP</sub>	V <sub>eq,SAP</sub>	V* <sub>eq</sub>	N <sub>SAP</sub>	V <sub>eq,SAP</sub>	V* <sub>eq</sub>	N <sub>SAP</sub>
14,98	0,688	22,41	22,49	32,70	23,96	24,96	36,29	24,27	24,91	36,22
diff. %		0,35%			4,00%			2,57%		
3°_upper diagonals		Upright 1			Upright 2			Upright 3		
h [m]	cosφ	V <sub>eq,SAP</sub>	V* <sub>eq</sub>	N <sub>SAP</sub>	V <sub>eq,SAP</sub>	V* <sub>eq</sub>	N <sub>SAP</sub>	V <sub>eq,SAP</sub>	V* <sub>eq</sub>	N <sub>SAP</sub>
16,41	0,688	19,63	20,52	29,83	23,86	23,01	33,45	24,18	23,01	33,45
diff. %		4,34%			3,71%			5,11%		
4°_upper diagonals		Upright 1			Upright 2			Upright 3		
h [m]	cosφ	V <sub>eq,SAP</sub>	V* <sub>eq</sub>	N <sub>SAP</sub>	V <sub>eq,SAP</sub>	V* <sub>eq</sub>	N <sub>SAP</sub>	V <sub>eq,SAP</sub>	V* <sub>eq</sub>	N <sub>SAP</sub>
17,83	0,688	16,86	16,58	24,11	18,94	19,90	28,94	19,37	19,90	28,93
diff. %		1,68%			4,84%			2,65%		
5°_upper diagonals		Upright 1			Upright 2			Upright 3		
h [m]	cosφ	V <sub>eq,SAP</sub>	V* <sub>eq</sub>	N <sub>SAP</sub>	V <sub>eq,SAP</sub>	V* <sub>eq</sub>	N <sub>SAP</sub>	V <sub>eq,SAP</sub>	V* <sub>eq</sub>	N <sub>SAP</sub>
19,33	0,669	12,93	13,09	19,57	15,27	16,58	24,78	15,76	16,55	24,74
diff. %		1,24%			7,89%			4,81%		
6°_upper diagonals		Upright 1			Upright 2			Upright 3		
h [m]	cosφ	V <sub>eq,SAP</sub>	V* <sub>eq</sub>	N <sub>SAP</sub>	V <sub>eq,SAP</sub>	V* <sub>eq</sub>	N <sub>SAP</sub>	V <sub>eq,SAP</sub>	V* <sub>eq</sub>	N <sub>SAP</sub>
20,83	0,669	8,99	8,05	12,03	11,58	12,14	18,15	12,13	12,15	18,16
diff. %		11,71%			4,63%			0,15%		
7°_upper diagonals		Upright 1			Upright 2			Upright 3		
h [m]	cosφ	V <sub>eq,SAP</sub>	V* <sub>eq</sub>	N <sub>SAP</sub>	V <sub>eq,SAP</sub>	V* <sub>eq</sub>	N <sub>SAP</sub>	V <sub>eq,SAP</sub>	V* <sub>eq</sub>	N <sub>SAP</sub>
22,33	0,669	2,21	3,03	4,53	6,82	6,21	9,29	7,29	6,24	9,33
diff. %		27,07%			9,66%			16,72%		
8°_upper diagonals		Upright 1			Upright 2			Upright 3		
h [m]	cosφ	V <sub>eq,SAP</sub>	V* <sub>eq</sub>	N <sub>SAP</sub>	V <sub>eq,SAP</sub>	V* <sub>eq</sub>	N <sub>SAP</sub>	V <sub>eq,SAP</sub>	V* <sub>eq</sub>	N <sub>SAP</sub>
23,83	0,669	2,35	4,91	7,34	2,00	2,47	3,69	2,40	2,55	3,81
diff. %		52,14%			18,98%			5,84%		

<b>1°_lower diagonals</b>		<b>Upright 4</b>			<b>Upright 5</b>			<b>Upright 6</b>		
h [m]	cosφ	V <sub>eq,SAP</sub>	V* <sub>eq</sub>	N <sub>SAP</sub>	V <sub>eq,SAP</sub>	V* <sub>eq</sub>	N <sub>SAP</sub>	V <sub>eq,SAP</sub>	V* <sub>eq</sub>	N <sub>SAP</sub>
1,55	0,688	44,40	49,56	72,07	44,40	49,53	72,01	44,42	49,48	71,95
diff. %		10,42%			10,35%			10,23%		
<b>2°_lower diagonals</b>		<b>Upright 4</b>			<b>Upright 5</b>			<b>Upright 6</b>		
h [m]	cosφ	V <sub>eq,SAP</sub>	V* <sub>eq</sub>	N <sub>SAP</sub>	V <sub>eq,SAP</sub>	V* <sub>eq</sub>	N <sub>SAP</sub>	V <sub>eq,SAP</sub>	V* <sub>eq</sub>	N <sub>SAP</sub>
2,98	0,688	44,35	43,95	63,90	44,35	44,00	63,98	44,37	44,05	64,05
diff. %		0,92%			0,79%			0,72%		
<b>3°_lower diagonals</b>		<b>Upright 4</b>			<b>Upright 5</b>			<b>Upright 6</b>		
h [m]	cosφ	V <sub>eq,SAP</sub>	V* <sub>eq</sub>	N <sub>SAP</sub>	V <sub>eq,SAP</sub>	V* <sub>eq</sub>	N <sub>SAP</sub>	V <sub>eq,SAP</sub>	V* <sub>eq</sub>	N <sub>SAP</sub>
4,405	0,688	40,03	40,71	59,19	40,04	40,72	59,20	40,08	40,73	59,22
diff. %		1,67%			1,66%			1,59%		
<b>4°_lower diagonals</b>		<b>Upright 4</b>			<b>Upright 5</b>			<b>Upright 6</b>		
h [m]	cosφ	V <sub>eq,SAP</sub>	V* <sub>eq</sub>	N <sub>SAP</sub>	V <sub>eq,SAP</sub>	V* <sub>eq</sub>	N <sub>SAP</sub>	V <sub>eq,SAP</sub>	V* <sub>eq</sub>	N <sub>SAP</sub>
5,83	0,688	39,93	38,74	56,33	39,94	38,74	56,33	40,00	38,70	56,27
diff. %		3,07%			3,09%			3,36%		
<b>5°_lower diagonals</b>		<b>Upright 4</b>			<b>Upright 5</b>			<b>Upright 6</b>		
h [m]	cosφ	V <sub>eq,SAP</sub>	V* <sub>eq</sub>	N <sub>SAP</sub>	V <sub>eq,SAP</sub>	V* <sub>eq</sub>	N <sub>SAP</sub>	V <sub>eq,SAP</sub>	V* <sub>eq</sub>	N <sub>SAP</sub>
7,33	0,669	35,86	35,98	53,79	35,89	35,97	53,77	35,96	35,96	53,75
diff. %		0,35%			0,23%			0,01%		
<b>6°_lower diagonals</b>		<b>Upright 4</b>			<b>Upright 5</b>			<b>Upright 6</b>		
h [m]	cosφ	V <sub>eq,SAP</sub>	V* <sub>eq</sub>	N <sub>SAP</sub>	V <sub>eq,SAP</sub>	V* <sub>eq</sub>	N <sub>SAP</sub>	V <sub>eq,SAP</sub>	V* <sub>eq</sub>	N <sub>SAP</sub>
8,83	0,669	33,75	33,73	50,42	33,77	33,73	50,42	33,88	33,70	50,37
diff. %		0,06%			0,10%			0,53%		
<b>7°_lower diagonals</b>		<b>Upright 4</b>			<b>Upright 5</b>			<b>Upright 6</b>		
h [m]	cosφ	V <sub>eq,SAP</sub>	V* <sub>eq</sub>	N <sub>SAP</sub>	V <sub>eq,SAP</sub>	V* <sub>eq</sub>	N <sub>SAP</sub>	V <sub>eq,SAP</sub>	V* <sub>eq</sub>	N <sub>SAP</sub>
10,33	0,669	31,67	31,65	47,31	31,72	31,66	47,32	31,82	31,67	47,34
diff. %		0,07%			0,20%			0,48%		
<b>8°_lower diagonals</b>		<b>Upright 4</b>			<b>Upright 5</b>			<b>Upright 6</b>		
h [m]	cosφ	V <sub>eq,SAP</sub>	V* <sub>eq</sub>	N <sub>SAP</sub>	V <sub>eq,SAP</sub>	V* <sub>eq</sub>	N <sub>SAP</sub>	V <sub>eq,SAP</sub>	V* <sub>eq</sub>	N <sub>SAP</sub>
11,83	0,669	31,58	31,96	47,77	31,62	31,94	47,74	31,34	31,86	47,62
diff. %		1,18%			0,99%			1,62%		

1°_upper diagonals		Upright 4			Upright 5			Upright 6		
h [m]	cosφ	V <sub>eq,SAP</sub>	V* <sub>eq</sub>	N <sub>SAP</sub>	V <sub>eq,SAP</sub>	V* <sub>eq</sub>	N <sub>SAP</sub>	V <sub>eq,SAP</sub>	V* <sub>eq</sub>	N <sub>SAP</sub>
13,56	0,688	27,73	29,72	43,21	27,79	29,67	43,14	27,95	29,59	43,03
diff. %		6,69%			6,34%			5,56%		
2°_upper diagonals		Upright 4			Upright 5			Upright 6		
h [m]	cosφ	V <sub>eq,SAP</sub>	V* <sub>eq</sub>	N <sub>SAP</sub>	V <sub>eq,SAP</sub>	V* <sub>eq</sub>	N <sub>SAP</sub>	V <sub>eq,SAP</sub>	V* <sub>eq</sub>	N <sub>SAP</sub>
14,98	0,688	24,39	24,92	36,24	24,48	24,92	36,24	24,67	24,87	36,16
diff. %		2,14%			1,78%			0,80%		
3°_upper diagonals		Upright 4			Upright 5			Upright 6		
h [m]	cosφ	V <sub>eq,SAP</sub>	V* <sub>eq</sub>	N <sub>SAP</sub>	V <sub>eq,SAP</sub>	V* <sub>eq</sub>	N <sub>SAP</sub>	V <sub>eq,SAP</sub>	V* <sub>eq</sub>	N <sub>SAP</sub>
16,41	0,688	24,30	23,02	33,47	24,39	23,01	33,46	24,58	22,94	33,35
diff. %		5,56%			5,99%			7,16%		
4°_upper diagonals		Upright 4			Upright 5			Upright 6		
h [m]	cosφ	V <sub>eq,SAP</sub>	V* <sub>eq</sub>	N <sub>SAP</sub>	V <sub>eq,SAP</sub>	V* <sub>eq</sub>	N <sub>SAP</sub>	V <sub>eq,SAP</sub>	V* <sub>eq</sub>	N <sub>SAP</sub>
17,83	0,688	19,53	19,92	28,96	19,65	19,90	28,94	19,81	19,83	28,84
diff. %		1,95%			1,27%			0,13%		
5°_upper diagonals		Upright 4			Upright 5			Upright 6		
h [m]	cosφ	V <sub>eq,SAP</sub>	V* <sub>eq</sub>	N <sub>SAP</sub>	V <sub>eq,SAP</sub>	V* <sub>eq</sub>	N <sub>SAP</sub>	V <sub>eq,SAP</sub>	V* <sub>eq</sub>	N <sub>SAP</sub>
19,33	0,669	15,94	16,56	24,75	16,06	16,53	24,71	16,13	16,40	24,52
diff. %		3,76%			2,88%			1,67%		
6°_upper diagonals		Upright 4			Upright 5			Upright 6		
h [m]	cosφ	V <sub>eq,SAP</sub>	V* <sub>eq</sub>	N <sub>SAP</sub>	V <sub>eq,SAP</sub>	V* <sub>eq</sub>	N <sub>SAP</sub>	V <sub>eq,SAP</sub>	V* <sub>eq</sub>	N <sub>SAP</sub>
20,83	0,669	12,32	12,16	18,17	12,45	12,14	18,14	12,43	12,02	17,97
diff. %		1,35%			2,59%			3,40%		
7°_upper diagonals		Upright 4			Upright 5			Upright 6		
h [m]	cosφ	V <sub>eq,SAP</sub>	V* <sub>eq</sub>	N <sub>SAP</sub>	V <sub>eq,SAP</sub>	V* <sub>eq</sub>	N <sub>SAP</sub>	V <sub>eq,SAP</sub>	V* <sub>eq</sub>	N <sub>SAP</sub>
22,33	0,669	7,35	6,29	9,40	7,37	6,32	9,44	7,39	6,21	9,29
diff. %		16,88%			16,62%			18,83%		
8°_upper diagonals		Upright 4			Upright 5			Upright 6		
h [m]	cosφ	V <sub>eq,SAP</sub>	V* <sub>eq</sub>	N <sub>SAP</sub>	V <sub>eq,SAP</sub>	V* <sub>eq</sub>	N <sub>SAP</sub>	V <sub>eq,SAP</sub>	V* <sub>eq</sub>	N <sub>SAP</sub>
23,83	0,669	2,57	2,66	3,97	2,47	2,73	4,08	2,51	2,68	4,00
diff. %		3,23%			9,51%			6,20%		

The upright frames are mostly susceptible to the axial forces, and to the base shear under horizontal actions as well. An evaluation considering both load conditions has been done. In order to estimate the axial forces that the upright frames should bear (in the detailed model), two different load cases have been taken into account. First of all, considering the gravity load condition,  $N_{eq,SAP}$  of the equivalent uprights has been measured (from the reduced-order model) and the value of  $N^*$  has been estimated with the following equation:

$$N^* = \frac{N_{eq,SAP}}{2} \quad \text{Eq. (4.24)}$$

where:

- $N_{eq,SAP}$  is the axial force, under gravity load condition, of the equivalent upright, measured directly from the reduced-order model;

- $N^*$  in the axial force that each upright in the detailed model should be subjected, estimated from the reduced order model and to be compared with  $N_{sx,SAP}$  and  $N_{dx,SAP}$ ;
- $N_{sx,SAP}$  and  $N_{dx,SAP}$  are the axial forces of each upright, of a single upright frame, in the detailed model, measured under the same gravity load condition. The results are shown only for half of the structure because of the symmetry. In the Table 4-5, the differences evaluated for each upright are shown and the results are quite satisfying.

**Table 4-5:** Results for the estimation of the axial force of each Upright frame under gravity load condition

Upright frame	$N_{eq,SAP}$	$N^*$	$N_{sx,SAP}$	diff. %	$N_{dx,SAP}$	diff. %
1°	109,23	54,61	48,96	10%	61,16	12%
2°	133,59	66,79	67,23	1%	66,91	0%
3°	134,40	67,20	67,35	0%	66,93	0%
4°	134,37	67,18	67,36	0%	66,92	0%
5°	133,50	66,75	67,34	1%	66,80	0%
6°	111,29	55,65	61,57	11%	48,86	12%
7°	111,34	55,67	48,82	12%	61,55	11%
8°	133,52	66,76	66,80	0%	67,35	1%
9°	134,40	67,20	66,92	0%	67,37	0%
10°	134,37	67,19	66,91	0%	67,34	0%
11°	133,42	66,71	66,58	0%	67,05	1%
12°	110,16	55,08	61,36	11%	49,05	11%

**Table 4-6:** Results for the estimation of the axial force of each Upright frame under seismic load

Upright frame	$M_{eq,SAP}$	$N^*$	$N_{sx,SAP}$	diff. %	$N_{dx,SAP}$	diff. %
1°	468,15	346,78	371,14	7%	334,07	4%
2°	460,87	341,39	345,90	1%	342,72	0%
3°	459,41	340,30	344,76	1%	344,45	1%
4°	458,86	339,90	344,64	1%	344,56	1%
5°	458,44	339,59	344,41	1%	344,90	2%
6°	457,83	339,13	346,34	2%	343,49	1%
7°	457,71	339,04	344,16	2%	346,08	2%
8°	457,95	339,22	344,94	2%	344,44	2%
9°	457,99	339,25	344,59	2%	344,70	2%
10°	458,03	339,28	344,46	2%	344,87	2%
11°	458,21	339,41	342,22	1%	346,06	2%
12°	458,67	339,76	365,05	7%	317,71	7%

Afterwards, regarding the analysis under the seismic action, the bending moment  $M_{eq,SAP}$  to which the equivalent uprights are subjected, has been measured from the reduced-order model in SAP, and the  $N^*$  that each upright of the detailed models should be subjected to, under the same load condition, has been evaluated with the following equation:

$$N^* = \frac{M_{eq,SAP}}{h_0} \quad \text{Eq. (4.24)}$$

where:

$h_0$  is the distance between two uprights for each upright frame.

It is worth noting that considering the gravity load condition, the errors evaluated for some uprights, are much bigger than the errors evaluated under the seismic action (see Table 4-6). We should consider that the stresses that the upright frames are subjected to under the seismic load are more significant than the gravity load condition, and for this reason are taken more into consideration.

Also, concerning the force of the base plate connections, the error between the value obtained estimating that force from the reduced-order model and the value measured from the detailed model, have been evaluated considering the seismic load condition. Therefore, the value of  $V_{eq,SAP}$  has been measured and compared with  $\sum V_{SAP}$ ,

where:

- $V_{eq,SAP}$  is the shear force at the base of each equivalent upright, measured from the reduced-order model;
- $\sum V_{SAP}$  is the sum of the base shear force of each upright ( $V_{sx,SAP}$  and  $V_{dx,SAP}$ ) of an upright frame measured from the detailed model;
- $V_{sx,SAP}$  and  $V_{dx,SAP}$  are the shear force of the left and the right upright of each upright frame in the detailed model.

**Table 4-7:** Comparison between the base shear force of the two models under seismic action

Upright frame	$V_{eq,SAP}$ [kN]	$V_{sx,SAP}$	$V_{dx,SAP}$	$\sum V_{SAP}$ [kN]	diff. %
1°	45,09	36,56	10,085	46,65	3%
2°	45,11	36,269	9,76	46,03	2%
3°	45,13	36,094	9,59	45,68	1%
4°	45,13	35,932	9,44	45,38	1%
5°	45,13	35,733	9,28	45,01	0%
6°	45,14	35,454	9,10	44,55	1%
7°	45,15	9,049	35,48	44,53	1%
8°	45,17	9,299	35,76	45,06	0%
9°	45,17	9,469	35,96	45,43	1%
10°	45,17	9,629	36,14	45,77	1%
11°	45,17	9,823	36,34	46,16	2%
12°	45,16	9,985	36,43	46,42	3%

Table 4-7 shows the difference between the two values, assessed for half of the structure because of its symmetry. The errors, less than 3%, highlight that the reduced-order model is well calibrated.

Therefore, evaluating the results of the previous analyses, we can conclude that the reduced-order model demonstrates the capability to predict the response of the detailed model in linear analysis extremely well.

### 4.3.3 Push-over Analysis

One step further was to include nonlinear properties in order to check if the reduced-order model has the same accuracy in the nonlinear region. Therefore, a push-over analysis has been carried out for the reduced-order mode, the response has been compared with the behaviour of the detailed model (cross-aisle direction). The same parameters of the detailed model have been set in the FEM analysis in SAP2000:

- a displacement control method, monitoring a specified node at the top of the structure has been considered;
- a modal load distribution has been applied;
- the push-over analysis starts from the end of a nonlinear gravity load case (considering the vertical loads);
- a lumped plasticity model has been used;
- P- Δ effects have been taken into account.

The structural and geometric properties and the distribution of loads have been defined as well in the previous paragraphs. However, in order to define the nonlinear behaviour of the plastic hinges, it is important to note that even if the structural scheme of the equivalent elements in the reduced-order model is different from the detailed model, each equivalent elements should be able to provide all the failures that the detailed model is interested in. In the detailed model, loads are not primarily carried by bending mechanisms, as bracings are considered to be pinned and uprights are usually supported to the foundations. However, the bending moment could be absorbed by each upright frame, producing in each upright a couple of axial forces  $N_u$  acting in the opposite direction. Considering that, the value of  $M_{eq}$  that each equivalent upright must be able to bear is given by the following equation (Figure 4-15):

$$M_{eq} = N_u \cdot h_0 \quad \text{Eq. (4.19)}$$

On the other hand, each equivalent upright, must be able to bear an equivalent axial force  $N_{eq}$ , as well as each upright frame in the detailed model, that could be given considering the

contribution of two axial forces acting on the uprights in the same direction, by the following equation:

$$N_{eq} = 2N_u \tag{4.20}$$

Considering the interaction between  $N_{eq}$  and  $M_{eq}$ , the equivalent upright's resistance in compression could be expressed by the following equation:

$$N_{Rd,eq.upright} = \frac{N_{eq}}{2} + \frac{M_{eq}}{h_0} \tag{4.21}$$

Therefore, the hinges used, in the FEM software, for each equivalent upright, are type “interacting P-M”, in order to reproduce the same nonlinear behaviour of each upright frame in the detailed model. The relative diagram, considering the different behaviour in tension and compression, is given defining three point as shown in Figure 4-16.

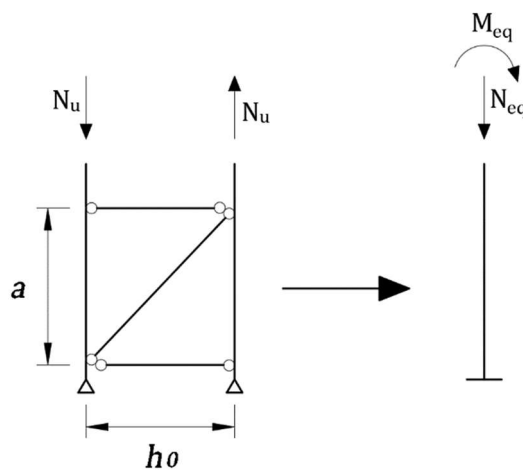


**Figure 4-15:** Relation between axial forces and bending moment of the two models

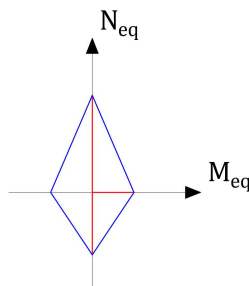


**Figure 4-16:** M-N interaction diagram of type “interacting P-M” hinges in the reduced-order model

However, it's important to note that using nonlinear rotational hinges, it is not possible to predict shear failure of the system, which is related to bracings' buckling. However, the choice to not take into account the shear failure, is due to the results given by the detailed model where no diagonals are failing. In addition, comparing the results of the push-over analysis of the two models, it is clear that the results are similar; i.e. when both models reach the complete failure, plastic hinges are produced at the base of all uprights in both models (see Figure 4-17). The colours represent the achievement of different limit states, detailed in paragraph 3.2.2. In Figure 4-18 the push-over curves of the two models are presented and the results, even though the shear failure is not directly considered, are quite satisfying. Comparing the base shear and the displacements of the two models when the yield and the collapse point are reached, the differences (see the Table 4-3) are less than 6%. The push-over curves are compared in Figure 4-15.

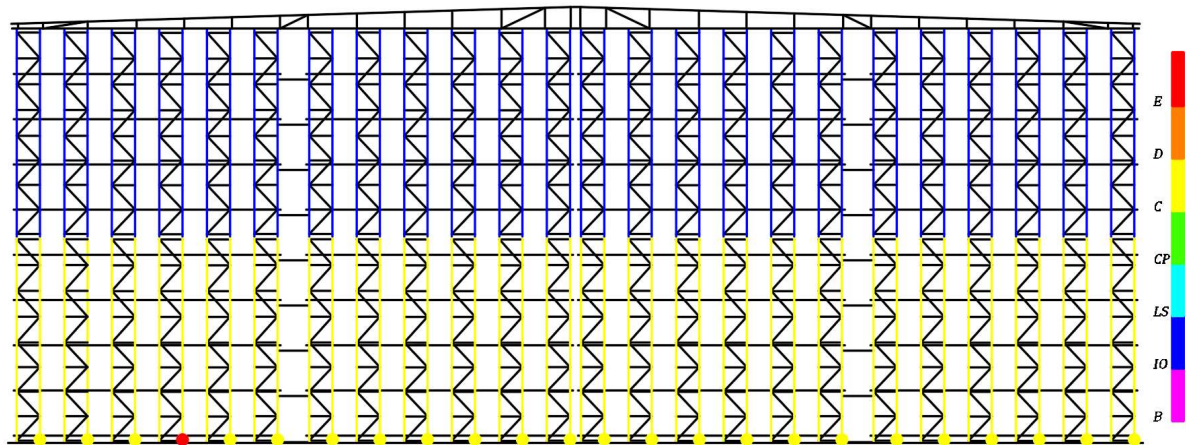
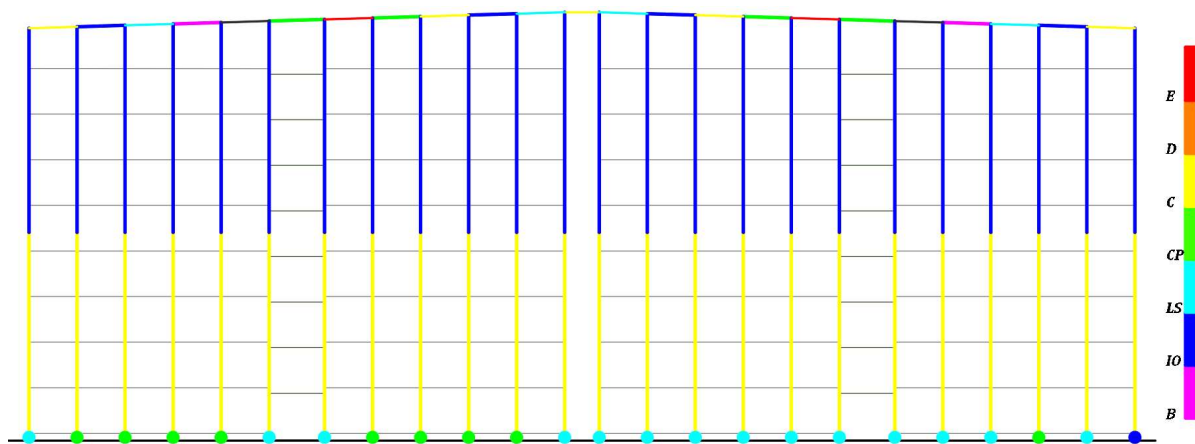


**Figure 4-17 (a):** Achievement of different limit states in correspondence of the last step of the analysis (about 42 cm of displacement). Detailed 2D model (Cross-aisle direction)



**(b)** Achievement of different limit states in correspondence of the last step of the analysis (about 46 cm of displacement). Reduced-order 2D model (Cross-aisle direction)

**Table 4-8:** Differences between the Yield and the Collapse point of the two models

Detailed model			
Yield		Collapse	
Shear Base [kN]	Displacement [m]	Shear Base [kN]	Displacement [m]
501,29	0,272	528,56	0,301
Reduced-order model			
Yield		Collapse	
Shear Base [kN]	Displacement [m]	Shear Base [kN]	Displacement [m]
530,26	0,288	545,24	0,311
Differences			
Yield		Collapse	
Shear Base [kN]	Displacement [m]	Shear Base [kN]	Displacement [m]
5,78%	5,95%	3,15%	3,34%

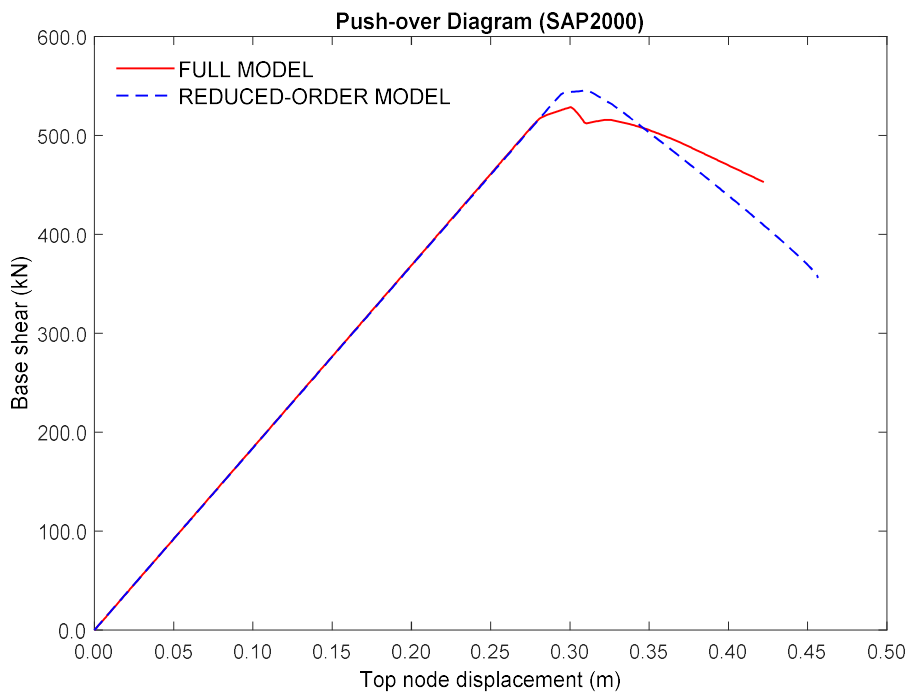


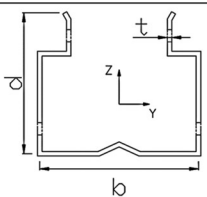
**Figure 4-18:** Comparison between the capacity curves of the two models designed for a distribution of load proportional to the product of modal shapes

## 5 Consideration about the 3D reduced-order model

Some consideration, still a work in progress, would be shown concerning the reduced-order model performed in three dimensions. All of the properties of each equivalent element, as well as all the parameters set in order to perform the model on the FEM software, SAP2000, will not be mentioned again, given that they have been well detailed in the previous paragraphs. It is worth mentioning that, as we did for the previous models, the contribution, on the bracing tower, of the spine bracings in compression, has been not considered for the global analysis. In Tables 5-1 (a) and (b), the properties of the cross-sections of some elements added in the 3D model are detailed; those elements, i.e. the “roof purlins” and the “roof truss vertical bracings” (included to avoid forming a mechanism on the roof level), were no included in the previous models in two dimensions, because they didn’t offer any contribution.

It could be noted, as already mentioned, that in the down-aisle direction, the properties of each element, must be simply doubled in order to consider the contribution of the two down-aisle sections for each upright frame; any reduction, in terms of numbers of elements, has been done in the down-aisle direction, so no further consideration needs to be done concerning those element properties. For a better comprehension, see Figure 5-1. The next step was to carry out a modal analysis in the 3D reduced-order model, in order to compare the response with the results of the modal analysis of the detailed model in 3D. A desirable future work, would be the evaluation of the response of the 3D model, performing a nonlinear analysis.

**Table 5-1: (a)** Section properties of the additional members considered in the 3D model

3D_Cold formed profiles						
	R 4	Roof purlins	1020	9,37E+05	2,05E+06	S350GD
<b>L section</b>	R 3	Roof truss vertical bracings	165	1,41E+04	1,41E+04	S355JR

**(b)** Section properties of the additional members considered in the 3D model

3D_Hot rolled profiles						
<b>R section</b>	S 2	Shuttle beam	2100	4,42E+06	3,32E+06	S275JR
<b>U section</b>	BP 2	Pallet beams	1350	2,05E+06	2,91E+05	S275JR

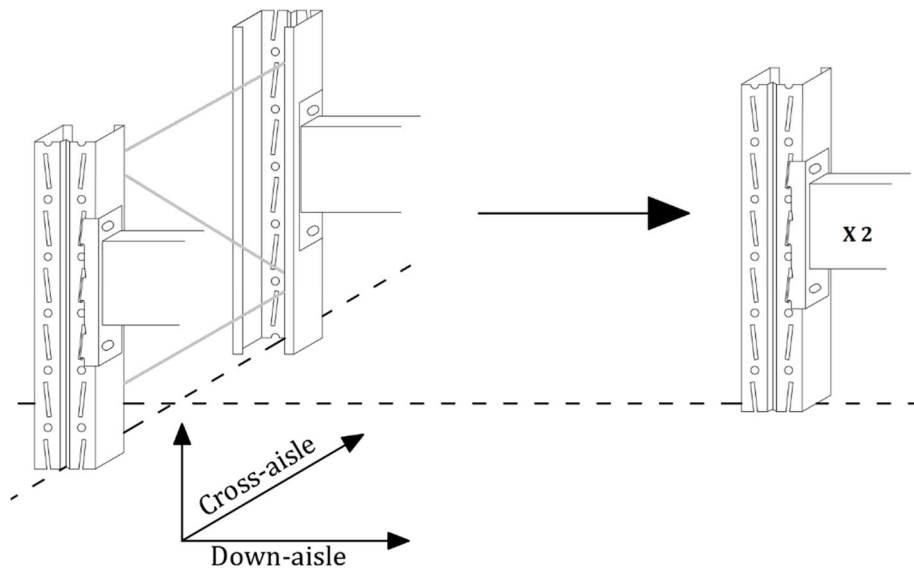


**Figure 5-1:** Reduction of the 3D model

### 5.1.1 Modal Analysis

A linear dynamic analysis has been carried out in 3D for the reduced-order model in order to evaluate the accuracy of the model, and to compare the results with the detailed model (3D) as well. In Table 5-1, the differences in percentage of the periods of the first five eigenmodes, having the same shape, between the two models are shown. As with the 2D models, the results are quite satisfying, less than 4%. It can be concluded, that the reduced-order model predicts the response of the detailed model very well, it is expected to give accurate results in the nonlinear analysis as well. In Figure 5-2 the modal shapes of both models, in 3D, are compared with the relative periods.

**Table 5-2:** Results of the modal analysis of the detailed and reduced-order 3D models and comparison

Mode	3D Full model - T (s)	3D Equivalent model - T (s)	Differ. %
1	1,526	1,489	2,45%
2	1,499	1,473	1,73%
3	1,330	1,323	0,50%
4	1,329	1,321	0,62%
5	1,304	1,355	3,92%

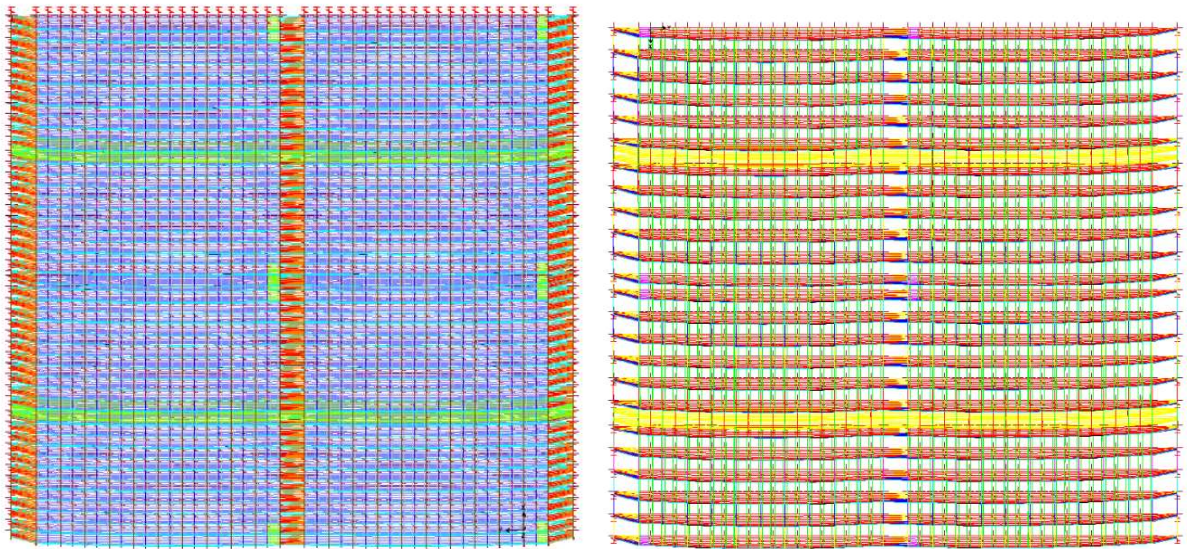
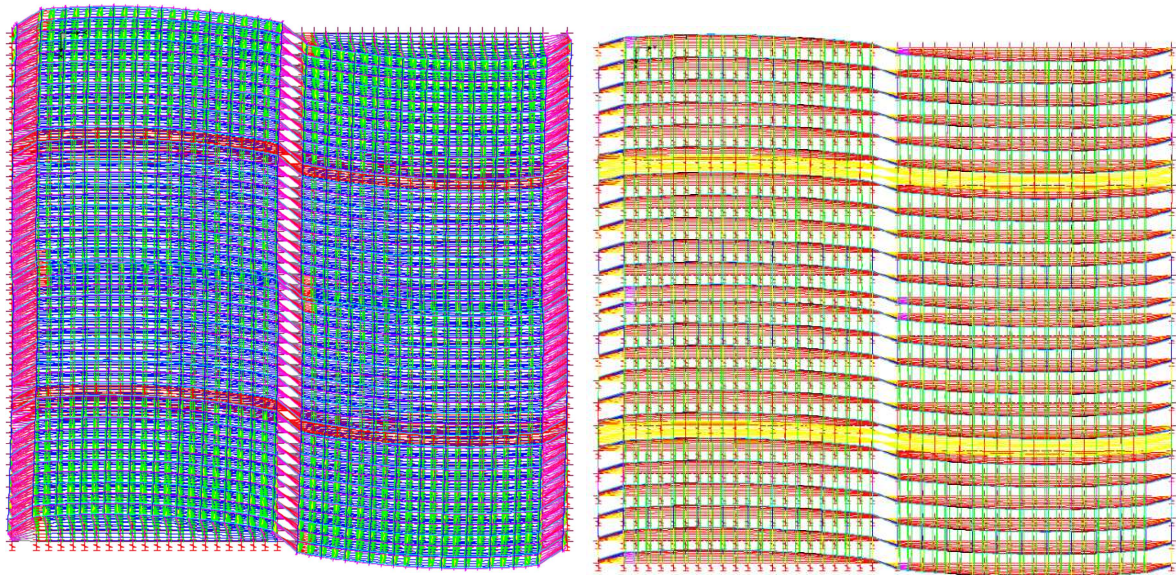
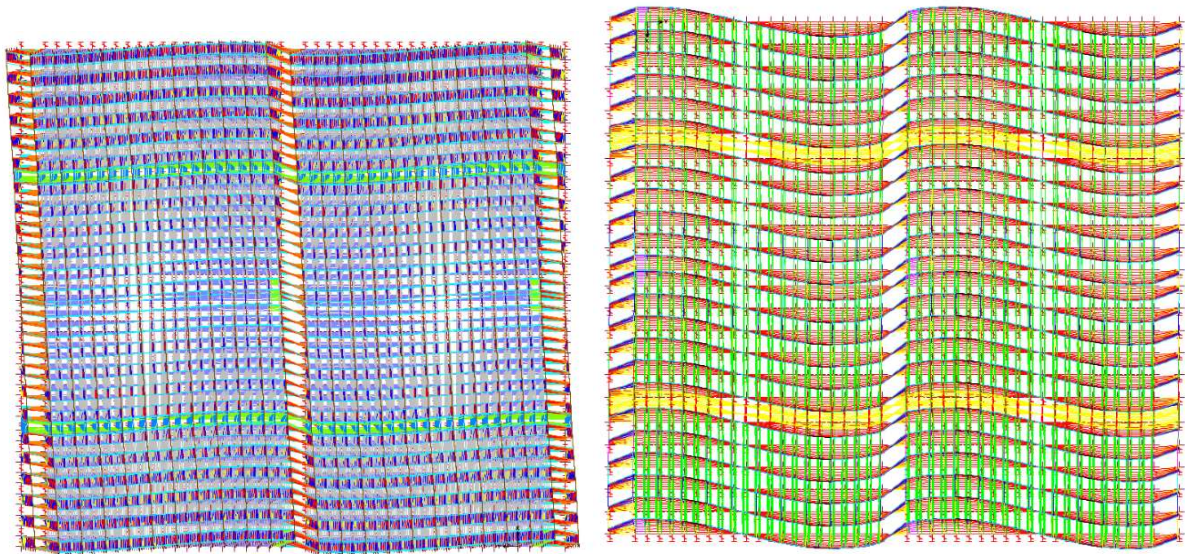


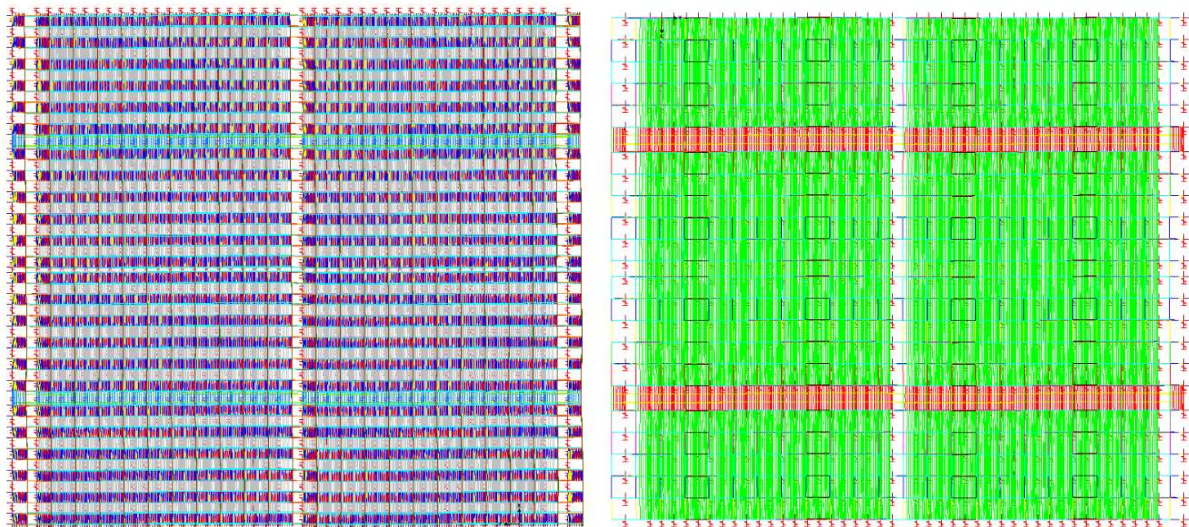
**Figure 5-2:** 1<sup>st</sup> Eigenmode of the 3D detailed model ( $T_{1,1}=1.526$  sec) and the 3D reduced-order model ( $T_{1,2}=1.489$  sec). Translational in the Cross-aisle direction



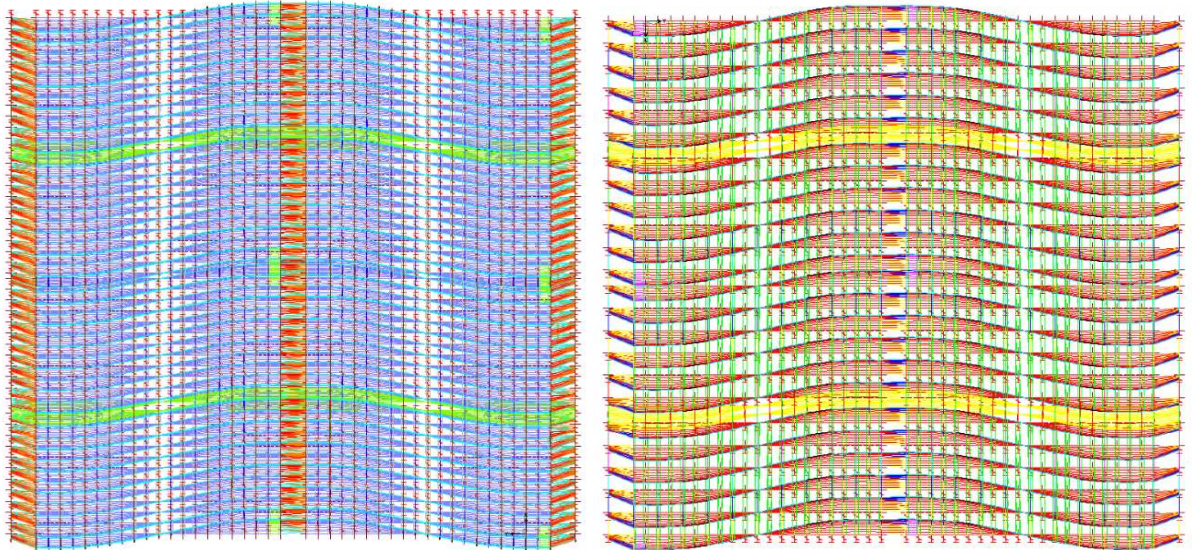
**(b):** 2<sup>nd</sup> vibration mode of the 3D detailed model ( $T_{2,1}=1.499$  sec) and the 3D reduced-order model ( $T_{2,2}=1.473$  sec). Sine shape in the Cross-aisle direction



**(c):** 3<sup>rd</sup> vibration mode of the 3D detailed model ( $T_{3,1}=1.330$  sec) and the 3D reduced-order model ( $T_{3,2}=1.323$  sec). Multi-sine shape in the Cross-aisle direction



**(d):** 4<sup>th</sup> vibration mode of the 3D detailed model ( $T_{4,1}=1.329$  sec) and the 3D reduced-order model ( $T_{4,2}=1.321$  sec). Translational in the down-aisle direction



**(e):** 5<sup>th</sup> vibration mode of the 3D detailed model ( $T_{5,1}=1.304$  sec) and the 3D reduced-order model ( $T_{5,2}=1.355$  sec). Multi-sine shape in the Cross-aisle direction

## **6 Conclusion and future work**

The main purpose of this research was the implementation of a reduced-order model able to predict accurately, in particular, the nonlinear behaviour of the structure. The test case analysed, was a multi-depth Automated Rack Supported Warehouse, designed to support a medium/high level of seismic hazard. Such a structure, modelled on finite element software (SAP2000, CSI), is made of hundreds of thousands of elements, making the analysis cost in terms of time and CPU prohibitive. In particular, when the nonlinear phenomena has to be included. The implementation of such a reduced-order model, made it easier for us to manage and analyse the model compared to the detailed one. A reduction of 55% in terms of degrees of freedom has been reached operating the reduction in the 2D model. A bigger reduction can be noted examining the reduced-order model in 3D. In addition, examining the satisfying results concerning the validation of the reduced-order model, we can note the capability, of the reduced-order model, to predict the response of the detailed model in linear analysis extremely well. However, concerning nonlinear analysis, a question remains about the local buckling of the bracing members that has not be considered, even if the choice for this case study was motivated by the nonlinear response of the detailed model where, no diagonals failed.

Moreover, the following questions, and desirable future work as well, still remain unanswered:

- Including the shear failure in the definition of plastic hinges, combined with the axial and bending failure, allows us to take into account the nonlinear behaviour of the bracing members for a more accurate evaluation of the response structure, which is useful to be implemented for other and different case studies.
- Extending the analyses, performed in the 2D models to the 3D model, it would be useful to have more information about the ARSWs behaviour, quantifying as well, in the same way we did for the 2D model, the reduction of the costs we can reach in terms of time and CPU.

## **7 References**

- [1] Tsarpalis, D., 2018, "Analysis of Pallet Racking Systems with Equivalent Beam Elements", National Technical University of Athens, School of Civil Engineering
- [2] Kanyilmaz A., Brambilla G., Chiarelli G. P., Castiglioni C. A., 2016. "Assessment of the seismic behaviour of braced steel storage racking systems by means of full scale push over tests", *Thin-Walled Structures*, ELSEVIER, pp. 138-155  
[<http://www.elsevier.com/locate/tws>]
- [3] Bernuzzi, C., Gabbianelli, G., Gobetti, A., Rosti, A., 2015, "Beam design for steel storage racks", *Journal of Constructional Steel Research*
- [4] T.Pekoz, G.Winter, "Cold-formed steel rack structures", 1973, Proc., *2<sup>nd</sup> Specialty Conference on Cold-Formed Steel Structures*, 603-615
- [5] Caprili S., Morelli F., Salvatore W., Natali A., Lippi F., Falleni V., 2017 "Seismic Design of Automated Rack Supported Warehouses", ANIDIS, Pistoia
- [6] Caprili, S., Morelli, F., Salvatore, W., Natali, A., 2018, "Design and Analysis of Automated Rack Supported Warehouses", *The Open Civil Engineering Journal*, pp. 150-166
- [7] Castiglioni C. A., Drei A., Kanyilmaz, A., 2018, "Continuous Monitoring of Service Conditions of a Steel Storage Racking System". *JOURNAL OF EARTHQUAKE ENGINEERING*
- [8] European Standard EN 15512:2009, (n.d.), *Steel static storage systems - Adjustable pallet racking systems - Principles for structural design*. European Committee for Standardization, Brussels
- [9] EU-RFCS Steel RTD Programme RFSR-CT-2004-00045, "SEISRACKS: Storage Racks in Seismic Areas", 01.12.2004 – 31.05.2007
- [10] EU-RFCS Steel RTD Programme RFSR-CT-2011-00031, "SEISRACKS2: Seismic Behavior of Steel Storage Pallet Racking Systems", 01.07.2011 - 30.06.2014
- [11] European Standard EN 16681:2016, (n.d.), *Steel static storage systems - Adjustable pallet racking systems - Principles for seismic design*. European Committee for Standardization, Brussels

- [12] FEM 10.2.08 “Recommendations for the design of static steel pallet racks in seismic conditions”, Version 1.04, May 2011
- [13] RMI MH 16.1, “Specification for the Design, Testing and Utilization of Industrial Steel Storage Racks”, Racks Manufacturers Institute, 2012, p. 59
- [14] AISI, “North American Specification for the Design of Cold-formed Steel Structural Members”, American Iron and Steel Institute, Washington, 2010
- [15] FEMA 460 – “Seismic Considerations for Steel Storage racks Located in Areas Accessible to the Public” - Prepared by the Building Seismic Safety Council of the National Institute of Building Sciences for the Federal Emergency Management Agency, Washington D.C., September 2005
- [16] EUR 25893 EN, 2013, “Optimising the seismic - performance of steel and steel-concrete structures by standardising material quality control (OPUS)”, European Commission
- [17] Markazi F. D., Beale R. G., & Godley M. H., 1997, “Experimental Analysis of Semi-Rigid Boltless Connectors”, *Thin-Walled Structures*, Vol. 28, No. 1, ELSEVIER, pp. 57-87
- [18] Avgerinou, S., “Seismic performance of steel pallet racks”, 2012, Post graduate Diploma Thesis, Athens
- [19] European Committee for Standardization, CEN, May 2005, Eurocode 3 – “Design of Steel Structures – Part 1-1”, De, CEN, Brussels
- [20] K. J. Bathe, "Finite Element Procedures", 1<sup>st</sup> Edition, Prentice Hall, 1996; 2<sup>nd</sup> Edition, Water-town, MA: Klaus-Jürgen Bathe, 2014
- [21] McGraw-Hill, “Fundamentals of Finite Element Analysis”, 1 edition (June 27, 2003)
- [22] G. Thomas Mase, George E. Mase “Continuum Mechanics for Engineers”, CRC-Press, 1999
- [23] Thomas J. R. Hughes, “The Finite Element Method: Linear Static and Dynamic Finite Element Analysis”, *Dover Publications*, 1 edition (August 16, 2000)
- [24] Henri P. Gavin, “Structural Element Stiffness, Mass, and Damping Matrices”, online courses, Department of Civil and Environmental Engineering Duke University (Fall 2018)
- [25] J. N. Reddy, “An Introduction to Continuum Mechanics”, Cambridge University Press, 2007